CHLOROPLAST LIPID METABOLISM IN THE CONTEXT OF PLANT GROWTH AND DEVELOPMENT

By

Ron Cook

A DISSERTATION

Submitted to
Michigan State University
in partial fulfillment of the requirements
for the degree of

Biochemistry and Molecular Biology – Doctor of Philosophy

2023

ABSTRACT

For over two billion years, most life on earth has depended on oxygenic photosynthesis for fuel and sustenance. In plants, the descendants of ancient cyanobacteria operate as subcellular photosynthetic organelles, the chloroplasts, where an extensive membrane infrastructure converts light into high-energy chemical bonds. Chloroplast membranes are distinctive in that their lipid components primarily rely on sugars as head groups, as opposed to phosphate-based moieties. Plant membrane metabolism is therefore highly geared towards the conversion of *de novo*-synthesized phospholipids into chloroplast galactolipids, and in *Arabidopsis thaliana*, portions of these pathways operate in parallel at the chloroplast and the endoplasmic reticulum (ER). Here, I present novel insights into the roles of chloroplast-associated lipid phosphate phosphatases LPPγ, LPPε1, and LPPε2, which dephosphorylate phosphatidic acid (PA) to make diacylglycerol (DAG), the substrate for galactosylation reactions. LPPγ and LPPε1 were determined to act on ER-assembled PA, with their catalytic activity at the chloroplast outer envelope membrane. All three chloroplast LPPs appeared uninvolved in the dephosphorylation of chloroplast-derived PA, despite localization of LPPε2 to the interior chloroplast membranes. Growth inhibition in *lppγ lppε1* double mutant plants implicated PA pools at the outer envelope membrane as affecting developmental regulation, thus linking LPPγ or LPPε1 to plant growth and development.

The connection between chloroplast lipid metabolism and plant growth regulation was also exploited in a suppressor screen using a transgenic Arabidopsis line, in which overexpression of the plastid lipase-encoding gene *PLIP3* leads to accumulation of the defense hormone jasmonic acid (JA). These *PLIP3*-OX lines exhibit unique JA-induced morphological phenotypes, and suppression of these phenotypes was targeted in the screen. One mutant, *sup72*, had a point mutation in *KEEP ON GOING* (*KEG*) which co-segregated with the suppression phenotype. KEG is known to have a repressive role in abscisic acid (ABA) signaling, and its apparent effects on JA signaling in *sup72* indicate it may also facilitate coordination of the ABA and JA pathways. In another mutant, *sup11*, *PLIP3*-OX suppression was caused by a nonsense mutation in *CDK8*, linking the gene product to activation of JA-responsive transcription. Overall, these Arabidopsis lines with distorted chloroplast lipid pathways provide greater insight into the nuances of

metabolism and lipid trafficking, as well as connections to broader elements of plant growth and development.

ACKNOWLEDGEMENTS

The work presented here was possible thanks to the support of many peers, coworkers, staff, family, and friends. As my degree-granting program, the Biochemistry and Molecular Biology (BMB) department provided a helpful framework for courses, teaching, and research, as well as administrative support, particularly from Jessica Lawrence. As the BMB graduate program director, David Arnosti was very accommodating, and also a pleasure to interact with. As a student at the MSU-DOE Plant Research Laboratory (PRL), the communication and responsiveness of the PRL staff to any of my needs was always superb, whether it was from the administrative staff, growth chamber facility, plant transformation facility, instrument repairs, or computer support. I am also grateful to PRL funding for financial support, in addition to that of the BioMolecular Science Gateway program, the MSU Plant Science Fellowship, and Plant Biotechnology for Health and Sustainability fellowship, which also partially funded a valuable 8-week industry internship. The collaborative environment of the PRL facilitated discussion with researchers in other labs, and such interactions with Deepak Bhandari and Nate Havko were particularly useful in the context of this work. Leah Johnson from the Gregg Howe lab walked me through the preparation of genomic sequencing samples, and the analysis of the resulting data. I also collaborated with the David Kramer lab to obtain the photosynthetic data presented here, which was generated by Jeff Cruz. Contributions by John Froehlich were absolutely instrumental, not just thanks to his execution of the chloroplast import experiments, but also because of his continuous guidance on my work with chloroplasts and protein biochemistry. Naturally, I have to thank all of the Benning lab members with whom I've worked over the past six years, and who are too numerous to mention all by name. In particular, my technical training with lipid analysis mostly came from Patrick Horn and Anastasiya Lavell, and many of the other skills and ideas applied here were developed with help from Carrie Hiser, Yang-Tsung Lin, and Yang Xu. Of the undergraduate students, Yash Manne was an exceptional peer who had an essential role in helping us to analyze genomic sequencing results, applying skills that he had developed as part of his data science degree. Likewise, undergraduate Ilayda Korkmaz was very quick to learn and operate independently in her ongoing pursuit to measure lipid phosphatase activity. Lab work in the Benning lab was efficient, and entertaining, thanks to Linda Danhof, who assisted with

Arabidopsis crossing, mutagenesis, and transformation, as well as innumerable aspects of lab management. I also appreciate the oversight and input from my guidance committee members Gregg Howe, Hideki Takahashi, Tom Sharkey, and Yair Shachar-Hill. Personal friends and family provided fresh perspectives and suggestions throughout, with my parents, Orna and Boaz, always curious about research developments. Finally, I would like to thank Christoph Benning for his mentorship, patience, generosity, and genuine devotion to the success and well-being of his students.

TABLE OF CONTENTS

CHAPTER 1:

Chloroplast membrane lipid metabolism and connections to signaling

---

Major components of this chapter, including Figures 1.1 and 1.2, have been published in Cook et al. 2021 [1]. I wrote part 2 of the review, with some contribution to parts 1 and 4.

Introduction

Plants are the basis for much of Earth's multicellular life, owing to their capacity for using light energy and water to reduce CO_2 into various organic molecules. While chloroplasts are primarily associated with photosynthesis in plants, these organelles host additional metabolic networks that are essential for robust cellular constitution and physiology. In particular, chloroplasts have a central role in glycerolipid metabolism, which serves both to maintain functional membranes in fluctuating environments, and as a chassis for broader sensing, signaling, and response mechanisms to external stimuli.

Chloroplast membrane lipid metabolism

Chloroplast membranes have evolved to accommodate an extensive photosynthetic apparatus, while maintaining minimal dependence on limiting nutrients. While phosphorus is a component of most lipids in virtually all other biological membranes, within chloroplasts it exists in less than half of envelope membrane lipids and less than 15% of thylakoid membrane lipids [2, 3]. Instead, these membranes are primarily composed of galactolipids, which are entirely derived from photosynthetic products made of carbon, oxygen, and hydrogen. In addition, sulfolipids are present as an alternative to phosphorus-based anionic membrane lipids. Plant chloroplast lipid metabolism is also closely linked to that of the ER, as the acyl components of ER-assembled lipids are synthesized and exported by chloroplasts, and ER-assembled lipids are often imported back into chloroplasts.

Glycerolipid precursors and chloroplast fatty acid export

Nearly all plant lipid biosynthesis begins with fatty acid (FA) biosynthesis in the chloroplast stroma by a Type II FA synthase similar to that of prokaryotes [4]. These FAs have various metabolic fates, including cuticular hydrocarbons, sphingolipids, and hormones, but the majority of FAs are esterified to glycerol to form glycerolipids. In the plastid pathway of glycerolipid biosynthesis, the acyltransferase ATS1 transfers 18:1 acyl groups from acyl-acyl carrier protein (acyl-ACP) to the *sn-1* position of glycerol 3-phosphate [5, 6]. ATS2 then transfers an additional acyl group from acyl-ACP to the *sn-2* position, producing phosphatidic acid (PA) at the inner leaflet of the chloroplast inner envelope membrane (IEM) [7]. Because ATS2 is specific to 16:0 acyl-ACP, lipids with a 16-

carbon moiety at the *sn-2* position can be identified as originating from plastid-synthesized PA [8]. The plastid pathway for membrane lipid biosynthesis is also referred to as the "prokaryotic" pathway, although its enzyme components actually have eukaryotic origins [9].

Fatty acids destined for the ER are released from ACP in the stroma by IEM-associated thioesterases, exported, and activated by acyl-CoA synthetases associated with the outer envelope membrane (OEM) [10, 11]. Acyl-CoAs are used for PA biosynthesis in the ER just as acyl-ACPs are used in plastid PA biosynthesis, with one key difference in substrate specificity: the ER acyltransferase which acylates the *sn-2* position is specific to 18-carbon substrates [12]. This allows for lipids with 18-carbon chains at the *sn-2* position to be identified as derivatives of ER-synthesized PA, or the "eukaryotic" pathway.

Chloroplast studies have determined that a dedicated FA export machinery is required to account for observed FA transport rates, but the proteins and mechanisms involved remain largely unknown [13]. One export component in the IEM, FAX1, has been shown to contribute to efficient FA transport [14]. However, null *fax1* mutants do maintain substantial FA export, indicating that supplementary or partially redundant export factors likely coexist with FAX1. Subsequent research led to the discovery of FAX2, FAX3, and FAX4, with FAX2/4 involved in plastid FA export in seeds, and FAX3 acting in partial redundancy with FAX1 in vegetative tissues [15-17]. While the FAX proteins may account for FA transport across the IEM, FA transfer across the intermembrane space would likely require mediation, as would FA flipping across the OEM for carboxyl exposure to cytosolic acyl-CoA synthetases. Discovery of novel FA export components was attempted through a suppressor screen, described in chapter 3.

Chloroplast galactolipids

The two primary glycerolipid constituents of chloroplast membranes are monogalactosyldiacylglycerol (MGDG) and digalactosyldiacylglycerol (DGDG) [3]. In some plants, including Arabidopsis, tomato, tobacco, and spinach, the *sn-2* position of MGDG may contain either 16:3 or 18:3 acyl moieties, meaning that both plastid- and ER-assembled PA is directed towards MGDG biosynthesis. Such plants are referred to as 16:3 plants. In contrast, 18:3 plants,

which include legumes and monocots, only have 18:3 acyl groups at the *sn-2* position of MGDG, indicating that MGDG is exclusively derived from ER-synthesized PA [18].

Due to the popularity of spinach and Arabidopsis in plant basic research, galactolipid metabolism is better characterized in 16:3 plants than in 18:3 plants. In 16:3 plants, bulk MGDG synthesis under nutrient replete conditions is observed at the IEM, and requires diacylglycerol (DAG) and UDP-galactose as substrates [19]. This reaction is catalyzed by the monogalactosyldiacylglycerol synthase (MGD1), which is associated with the outer leaflet of the chloroplast IEM in 16:3 plants [20-22]. 16:3 plants also exhibit PA phosphatase (PAP) activity primarily associated with the IEM, which presumably provides MGD1 with DAG substrate [19]. ER-derived MGDG is synthesized from precursors imported to the IEM by the TGD complex, although it is still unclear whether PA or DAG is the imported species [23]. On the other hand, pea chloroplasts exhibit substantial UDP:DAG galactosyltransferase activity in the OEM, which may explain the predominance of ER-derived galactolipids in 18:3 plants [24]. 18:3 plants also have far lower PAP activity in chloroplast envelopes, which is localized to the IEM [8, 25, 26]. Therefore, MGDG in 18:3 plants is possibly synthesized at the OEM from ER-derived DAG, while MGDG biosynthesis in 16:3 plants occurs at the IEM from a mixture of plastid-derived PA and ER-derived DAG or PA.

DGDG biosynthesis by a UDP-galactose:MGDG galactosyltransferase (DGD1) was initially identified in pea chloroplast envelopes [27]. The *dgd1* mutant was subsequently isolated in *Arabidopsis*, and the enzyme DGD1 was localized to the OEM and determined to require MGDG and UDP-galactose as substrates, likely at the cytosolic side of the membrane [28-31]. Despite equivalent concentrations of plastid-derived MGDG in the OEM and the IEM, DGDG has very low amounts of 16:3 acyl groups, indicating that DGD1 specifically galactosylates ER-derived MGDG [32]. This could be due to substrate preference, or to a low abundance of 16:3 MGDG at the outer leaflet of the OEM. DGD1 also contains an N-terminal domain that has been implicated in lipid transfer between the envelope membranes [32].

In 16:3 plants, MGD1 and DGD1 are the primary catalysts for galactolipid biosynthesis in the absence of environmental stress. However, in response to changing biotic and abiotic factors, other enzymes are synthesized or activated which redirect chloroplast lipid metabolism from this

baseline. In particular, phosphate depletion induces expression of genes encoding extraplastidic phospholipases and PAPs, as well as OEM-localized galactosyltransferases, which work together to convert extraplastidic phospholipids into galactolipids [1] (Fig. 1.1).

Chloroplast anionic lipids

In the chloroplast, the anionic membrane lipids phosphatidylglycerol (PG) and sulfoquinovosyldiacylglycerol (SQDG) are both synthesized at the IEM. PG is the only major phospholipid component of the IEM and thylakoid membranes, and its biosynthesis begins with the activation of plastid-synthesized PA to CDP-DAG [33]. PG phosphate synthase then exchanges the activated head group for glycerol 3-phosphate, producing PG phosphate [34-36], which is subsequently dephosphorylated by PG phosphate phosphatase, generating PG [37]. For SQDG biosynthesis, a UDP-sulfoquinovose precursor is produced from UDP-glucose and sulfite by SQD1 in the chloroplast stroma [38, 39]. SQD2 then synthesizes SQDG from the UDP-sulfoquinovose and DAG at the IEM [40, 41]. During phosphate deprivation, the SQDG biosynthetic pathways are upregulated, and the majority of chloroplast PG is replaced with SQDG [38, 40] (Fig. 1.1).

The roles of phosphatidic acid in the chloroplast

Although PA is the precursor for all other chloroplast glycerolipids, its low abundance means that quantification of chloroplast PA is difficult [42]. However, studies on PA-protein interactions and transgenic plants with alterations to PA metabolism do provide some preliminary insights into the role of PA, beyond its existence as a lipid precursor.

PA interactions with proteins of lipid metabolism

Several major proteins involved in chloroplast lipid metabolism are known to specifically bind PA (Fig. 1.2). MGD1 has been shown to require allosteric activation by PA and PG in order to synthesize MGDG from DAG and UDP-galactose [43]. Because DAG is itself an inhibitor of PAP activity [44], PA activation of MGD1 presumably maintains a consistent proportion in the activities of PAP and MGD1. This balance would prevent an excess accumulation of either PA or DAG in the IEM. Based on these discoveries, PA appears to have a typical role in allosteric activation of a metabolic pathway by the initial precursor. In addition, PA may promote MGDG export to the

OEM for subsequent DGDG biosynthesis: The N-terminal extension of DGD1 binds specifically to PA, potentially leading to PA-mediated membrane fusion that facilitates galactolipid transfer between the envelope membranes [32].

PA may also be a substrate or a regulator in the import of ER lipids to the IEM in 16:3 plants, a process that is mediated by the TGD complex [45]. The subunit TGD2 is anchored in the IEM by its N-terminus, while its C-terminus binds specifically to PA; however, the functional role of this interaction is unclear [46]. In addition, the OEM-localized TDG4 protein involved in the import of ER lipid precursors also specifically binds PA, and its PA binding site is required for activity [47-49].

Thylakoid membrane biosynthesis may also be regulated by PA. CHLOROPLAST SEC14-LIKE1 protein (CPSFL1), which is required for vesicle formation at the IEM and thylakoid membrane biogenesis, has a specific binding site for PA and traffics phosphoinositides to membranes enriched in PA [50, 51] (Fig. 1.2). While the specific roles of plastid phosphoinositides are not fully elucidated, they are known to be involved in development and signaling processes within chloroplasts through interactions with proteins such as WKS1, VIPP1 and VIPP2 [52].

Effects of modifying chloroplast PA metabolism

To better understand the potential regulatory and metabolic roles of PA, rerouting of lipid precursors to PA biosynthesis was carried out in 16:3 plants by targeting DAG Kinase (DAGK) to specific plastid compartments. In tobacco, introduction of a bacterial DAGK fused to the N-terminus of the small subunit of rubisco introduced DAGK activity to the chloroplast stroma-facing membranes, although the exact location was not determined. This resulted in accumulation of ER-derived PA, and subsequently ER-derived PG, in the chloroplast. These transgenic plants exhibited stunted growth, a substantial reduction in chloroplast lipids relative to ER lipids, and a smaller proportion of plastid-derived lipids within the chloroplast [53]. It remains puzzling as to why redirecting both plastid- and ER-derived DAG into PA synthesis at the stromal side of the chloroplast envelope would result in a disproportionate decrease of prokaryotic galactolipids.

A similar study in Arabidopsis targeted DAGK to chloroplast membrane leaflets facing the stroma, intermembrane space, or cytosol [54]. Surprisingly, DAGK targeted to stroma-facing membrane

leaflets did not result in the phenotype witnessed in tobacco, and plant growth and membrane lipid composition was largely unaffected. Further analysis revealed that the majority of DAGK-derived PA in this case was being degraded by phospholipase A activity, preventing a significant increase in PA accumulation. Therefore, excess PA at the IEM inner leaflet is likely responsible for the phenotypes of tobacco lines in which DAGK is targeted to this membrane. In the same Arabidopsis study [54], it was also discovered that DAGK targeted to the intermembrane space of the chloroplast resulted in an increased rate of PA accumulation and stunted plant growth. Taken together, these results suggest that excess PA in the IEM has a negative impact on the development of 16:3 plants.

Lipid phosphate phosphatases hypothesized to catalyze PAP activity in chloroplast lipid metabolism have been identified as LPPγ, LPPε1, and LPPε2 [55]. These were shown to associate specifically with chloroplasts and appeared to catalyze PA dephosphorylation when produced heterologously in yeast. However, null mutant analyses determined that *lppε1*, *lppε2*, and the *lppε1 lppε2* double mutant did not have any aberrant phenotypes, while the *lppγ* null mutation was presumed lethal in the respective study [55]. In addition, LPPε1 activity at the chloroplast OEM compensates for the *lppα2* null mutant, which lacks an ER PA phosphatase [56]. A deeper investigation into these chloroplast LPPs, their involvement in different aspects of PA metabolism, and implications for the potential roles of chloroplast PA are discussed in chapter 2. These include potential regulatory roles, as PA is known to be involved in various signaling pathways outside of the chloroplast [57].

Chloroplast lipids and jasmonic acid signaling

The broad regulatory effects of lipid metabolism in plants are not limited to PA, and other chloroplast membrane lipids are known to be involved in hormone pathways. In particular, synthesis of the defense hormone jasmonic acid (JA) utilizes chloroplast membrane lipid substrates, which allows for regulation of JA biosynthesis through changes in plastid lipid metabolism [1]. For example, the ratio of MGDG to DGDG has been shown to affect induction of JA biosynthesis, as was first witnessed in the stunted growth phenotype of the *dgd1* mutant [28,

58, 59]. While a mechanistic understanding of this phenomenon remains elusive, there are also lipase-mediated initiations of JA biosynthesis, some of which have been well-characterized.

JA biosynthesis begins in the chloroplast, with the conversion of 18:3 fatty acids to 12-oxo-phytodienoic acid (OPDA) in the stroma. OPDA is then exported from the chloroplast, and converted to JA through β-oxidation in the peroxisome and reduction in the cytosol or peroxisome [60]. Initiation of JA biosynthesis by chloroplast phospholipases A_1 has been demonstrated in overexpression lines of plastid lipase genes *PLIP1*, *PLIP2*, and *PLIP3* [61, 62]. The PLIP enzymes hydrolyze the *sn-1* linolenoyl moieties of chloroplast membrane lipids, and subsequent FA conversion to OPDA and JA results in plants with an elevated JA concentration and JA response phenotype [61, 62]. Under native regulation, PLIP2 and PLIP3 are involved in interaction between abscisic acid (ABA) and JA signaling, as *PLIP2/3* gene expression and subsequent JA production is induced by ABA, and *plip* triple mutants are hypersensitive to ABA during germination [62].

Because JA production requires OPDA export from chloroplasts, the JA-induced phenotypes of *PLIP*-overexpressing lines also relies on transport of this FA derivative. *PLIP*-overexpressing lines therefore provide an opportunity for suppression screening targeted at chloroplast FA export components, as a mutant deficient in OPDA export would be relieved of its JA-induced growth inhibition. A suppressor screen in the *PLIP3* overexpression background, and its results, are detailed in chapter 3.

Summary of research aims

Chapter 2 details the investigation of chloroplast lipid phosphate phosphatases LPPγ, LPPε1, and LPPε2, their activity, locations within the chloroplast, involvement in lipid metabolic pathways, and insights into potential roles of PA or DAG in plant development. The design and implementation of the *PLIP3*-OX suppressor screen are described in chapter 3, along with the subsequent mapping of suppressor mutations, genetic approaches for determining causal mutations, and the candidate genes themselves. One specific suppressor mutation in the gene *KEEP ON GOING* (*KEG*), and the deeper insight it may provide into JA-ABA interactions are also addressed in chapter 3. The broader implications of all these results, along with directions for future research, are discussed in chapter 4.

FIGURES

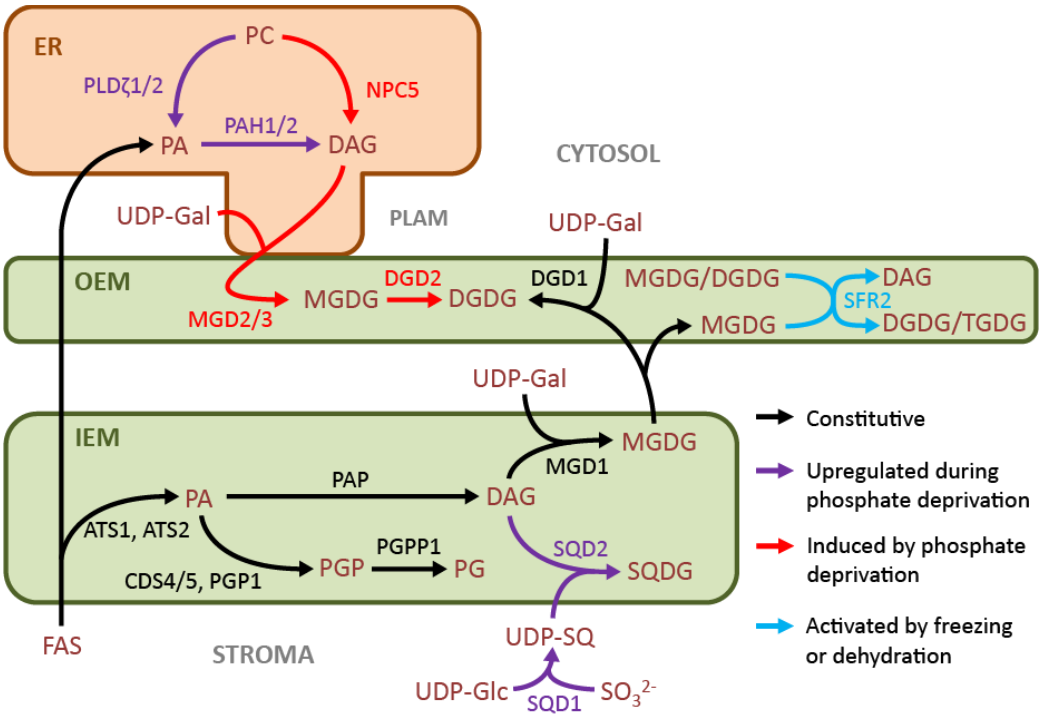

Figure 1.1. Chloroplast lipid metabolism as a scaffold for metabolic responses to environmental stress. In black, constitutive lipid metabolism in unstressed plants; In purple, constitutive pathways that are upregulated in response to phosphate deprivation; in red, non-constitutive pathways that are turned on during phosphate deprivation; in blue, pathways activated by freezing or dehydration stress. List of abbreviations in alphabetical order: ATS1/2, GLYCER-OL-3-PHOSPHATE ACYLTRANSFERASE 1/2; CDS4/5, CYTIDINE DIPHOSPHATE DIACYL-GLYCEROL SYNTHASE 4/5; DAG, diacylglycerol; DGD1, UDP-GALACTOSE:MGDG GALAC-TOSYLTRANSFERASE; DGD2, DIGALACTOSYLDIACYLGLYCEROL SYNTHASE 2; DGDG, digalactosyldiacylglycerol; ER, endoplasmic reticulum; MGDs, monogalactosyldiacylglycerol synthases; MGDG, monogalactosyldiacylglycerol; NPC5, NON-SPECIFIC PHOSPHOLIPASE C5; PA, phosphatidic acid; PAH1 and PAH2, PHOSPHATIDIC ACID PHOSPHOHYDROLASE1 and 2; PAP, PHOSPHATIDIC ACID PHOSPHATASE; PC, phosphatidylcholine; PG, phosphatidyl-glycerol; PGP, phosphatidylglycerol phosphate; PGPP1, PHOSPHATIDYLGLYCEROPHOS-PHATE PHOSPHATASE1; PLAM, plastid associated microsomes; PLDζ1/2, PHOSPHOLIPASES D ZETA1/2. SFR2, SENSITIVE TO FREEZING2; SQD1, UDP-sulfoquinovose synthase; SQD2, SQDG synthase; SQDG, sulfoquinovosyldiacylglycerol; TGDG, trigalactosyldiacylglycerol; UDP-Gal, uridine diphosphate galactose; UDP-Glc, uridine diphosphate glucose; UDP-SQ, uridine di-phosphate-sulfoquinovose.

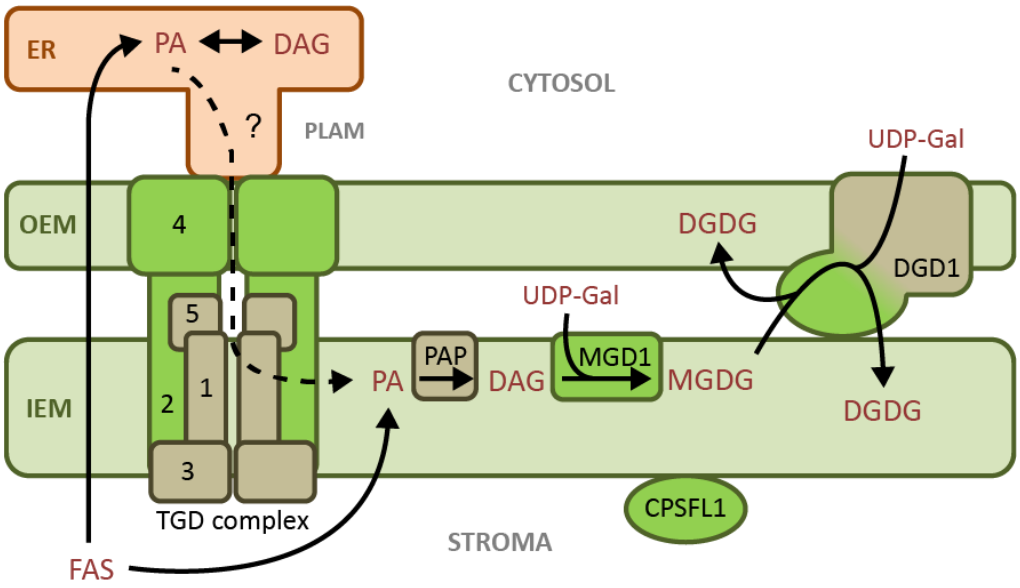

Figure 1.2. Roles of phosphatidic acid (PA) in chloroplast lipid metabolism. Proteins colored in green have specific interactions with PA, which may serve as a regulator, substrate, or both. The potential role of PA as the substrate for lipid import into the chloroplast is represented by a dotted arrow and a question mark, as this remains uncertain. List of abbreviations in alphabetical order: CPSFL1, CHLOROPLAST SEC14-LIKE1 protein; DAG, diacylglycerol; DGD1, UDP-galactose:MGDG galactosyltransferase; DGDG, digalactosyldiacylglycerol; ER, endoplasmic reticulum; MGD1, monogalactosyldiacylglycerol synthase; MGDG, monogalactosyldiacylglycerol; PA, phosphatidic acid; PAP, phosphatidic acid phosphatase; PLAM, plastid associated micro-somes; TGD complex, trigalactosyldiacylglycerol complex. The numbers refer to the TGD1-5 proteins forming the TGD complex.

REFERENCES

1. Cook, R., J. Lupette, and C. Benning, *The role of chloroplast membrane lipid metabolism in plant environmental responses.* Cells, 2021. **10**(3): p. 706.

2. Mackender, R. and R.M. Leech, *The Galactolipid, Phospholipid, and Fatty Acid Composition of the Chloroplast Envelope Membranes of Vicia faba. L.* Plant Physiol., 1974. **53**(3): p. 496-502.

3. Block, M.A., et al., *Preparation and characterization of membrane fractions enriched in outer and inner envelope membranes from spinach chloroplasts. II. Biochemical characterization.* J. Biol. Chem., 1983. **258**(21): p. 13281-13286.

4. Ohlrogge, J.B., D.N. Kuhn, and P. Stumpf, *Subcellular localization of acyl carrier protein in leaf protoplasts of Spinacia oleracea.* Proc. Natl. Acad. Sci. U.S.A., 1979. **76**(3): p. 1194-1198.

5. Bertrams, M. and E. Heinz, *Positional Specificity and Fatty Acid Selectivity of Purified sn-Glycerol 3-Phosphate Acyltransferases from Chloroplasts.* Plant Physiol., 1981. **68**(3): p. 653-657.

6. Kunst, L. and C. Somerville, *Altered regulation of lipid biosynthesis in a mutant of Arabidopsis deficient in chloroplast glycerol-3-phosphate acyltransferase activity.* Proc. Natl. Acad. Sci. U.S.A., 1988. **85**(12): p. 4143-4147.

7. Yu, B., et al., *Loss of plastidic lysophosphatidic acid acyltransferase causes embryo-lethality in Arabidopsis.* Plant Cell Physiol., 2004. **45**(5): p. 503-510.

8. Frentzen, M., et al., *Specificities and Selectivities of Glycerol-3-Phosphate Acyltransferase and Monoacylglycerol-3-Phosphate Acyltransferase from Pea and Spinach Chloroplasts.* Eur. J. Biochem., 1983. **129**(3): p. 629-636.

9. Sato, N. and K. Awai, *"Prokaryotic Pathway" Is Not Prokaryotic: Noncyanobacterial Origin of the Chloroplast Lipid Biosynthetic Pathway Revealed by Comprehensive Phylogenomic Analysis.* Genome Biol. Evol., 2017. **9**(11): p. 3162-3178.

10. Andrews, J. and K. Keegstra, *Acyl-CoA synthetase is located in the outer membrane and acyl-CoA thioesterase in the inner membrane of pea chloroplast envelopes.* Plant Physiol., 1983. **72**(3): p. 735-740.

11. Löhden, I. and M. Frentzen, *Role of plastidial acyl-acyl carrier protein: glycerol 3-phosphate acyltransferase and acyl-acyl carrier protein hydrolase in channelling the acyl flux through the prokaryotic and eukaryotic pathway.* Planta, 1988. **176**(4): p. 506-512.

12. Hares, W. and M. Frentzen, *Properties of the microsomal acyl-CoA: sn-1-acyl-glycerol-3-phosphate acyltransferase from spinach (Spinacia oleracea L.) leaves.* J. Plant Physiol., 1987. **131**(1-2): p. 49-59.

13. Koo, A.J., J.B. Ohlrogge, and M. Pollard, *On the export of fatty acids from the chloroplast.* J. Biol. Chem., 2004. **279**(16): p. 16101-10.

14. Li, N., et al., *FAX1, a novel membrane protein mediating plastid fatty acid export.* PLoS Biol., 2015. **13**(2): p. e1002053.

15. Tian, Y., et al., *FAX2 mediates fatty acid export from plastids in developing Arabidopsis seeds.* Plant Cell Physiol., 2019. **60**(10): p. 2231-2242.

16. Li, N., et al., *Two plastid fatty acid exporters contribute to seed oil accumulation in Arabidopsis.* Plant Physiol., 2020. **182**(4): p. 1910-1919.

17. Bugaeva, W., et al., *Plastid fatty acid export (FAX) proteins in Arabidopsis thaliana-the role of FAX1 and FAX3 in growth and development.* bioRxiv, 2023. DOI: https://doi.org/10.1101/2023.02.09.527856

18. Mongrand, S., et al., *The C16: 3\C18: 3 fatty acid balance in photosynthetic tissues from 468 plant species.* Phytochemistry, 1998. **49**(4): p. 1049-1064.

19. Block, M.A., et al., *The phosphatidic acid phosphatase of the chloroplast envelope is located on the inner envelope membrane.* FEBS Lett., 1983. **164**(1): p. 111-115.

20. Jarvis, P., et al., *Galactolipid deficiency and abnormal chloroplast development in the Arabidopsis MGD synthase 1 mutant.* Proc. Natl. Acad. Sci. U.S.A., 2000. **97**(14): p. 8175-8179.

21. Miège, C., et al., *Biochemical and topological properties of type A MGDG synthase, a spinach chloroplast envelope enzyme catalyzing the synthesis of both prokaryotic and eukaryotic MGDG.* Eur. J. Biochem., 1999. **265**(3): p. 990-1001.

22. Xu, C., et al., *Mutation of the TGD1 chloroplast envelope protein affects phosphatidate metabolism in Arabidopsis.* Plant Cell, 2005. **17**(11): p. 3094-110.

23. Roston, R.L., et al., *TGD1,-2, and-3 proteins involved in lipid trafficking form ATP-binding cassette (ABC) transporter with multiple substrate-binding proteins.* J. Biol. Chem., 2012. **287**(25): p. 21406-21415.

24. Cline, K. and K. Keegstra, *Galactosyltransferases Involved in Galactolipid Biosynthesis Are Located in the Outer Membrane of Pea Chloroplast Envelopes.* Plant Physiol., 1983. **71**(2): p. 366-372.

25. Heinz, E. and P.G. Roughan, *Similarities and differences in lipid metabolism of chloroplasts isolated from 18: 3 and 16: 3 plants.* Plant Physiol., 1983. **72**(2): p. 273-279.

26. Andrews, J., J.B. Ohlrogge, and K. Keegstra, *Final Step of Phosphatidic Acid Synthesis in Pea Chloroplasts Occurs in the Inner Envelope Membrane.* Plant Physiol., 1985. **78**(3): p. 459-465.

27. Siebertz, M. and E. Heinz, *Galactosylation of different monogalactosyldiacylglycerols by cell-free preparations from pea leaves.* Hoppe Seylers Z. Physiol. Chem., 1977. **358**(1): p. 27-34.

28. Dörmann, P., et al., *Isolation and characterization of an Arabidopsis mutant deficient in the thylakoid lipid digalactosyl diacylglycerol.* Plant Cell, 1995. **7**(11): p. 1801-1810.

29. Dörmann, P., I. Balbo, and C. Benning, *Arabidopsis galactolipid biosynthesis and lipid trafficking mediated by DGD1.* Science, 1999. **284**(5423): p. 2181-2184.

30. Froehlich, J.E., C. Benning, and P. Dörmann, *The digalactosyldiacylglycerol (DGDG) synthase DGD1 is inserted into the outer envelope membrane of chloroplasts in a manner independent of the general import pathway and does not depend on direct interaction with monogalactosyldiacylglycerol synthase for DGDG biosynthesis.* J. Biol. Chem., 2001. **276**(34): p. 31806-31812.

31. Kelly, A.A., J.E. Froehlich, and P. Dörmann, *Disruption of the two digalactosyldiacylglycerol synthase genes DGD1 and DGD2 in Arabidopsis reveals the existence of an additional enzyme of galactolipid synthesis.* Plant Cell, 2003. **15**(11): p. 2694-2706.

32. Kelly, A.A., et al., *Synthesis and transfer of galactolipids in the chloroplast envelope membranes of Arabidopsis thaliana.* Proc. Natl. Acad. Sci. U.S.A., 2016. **113**(38): p. 10714-10719.

33. Andrews, J. and J.B. Mudd, *Phosphatidylglycerol Synthesis in Pea Chloroplasts.* Plant Physiol., 1985. **79**(1): p. 259-265.

34. Xu, C., et al., *The pgp1 mutant locus of Arabidopsis encodes a phosphatidylglycerolphosphate synthase with impaired activity.* Plant Physiol., 2002. **129**(2): p. 594-604.

35. Hagio, M., et al., *Phosphatidylglycerol is essential for the development of thylakoid membranes in Arabidopsis thaliana.* Plant Cell Physiol., 2002. **43**(12): p. 1456-1464.

36. Babiychuk, E., et al., *Arabidopsis phosphatidylglycerophosphate synthase 1 is essential for chloroplast differentiation, but is dispensable for mitochondrial function.* Plant J., 2003. **33**(5): p. 899-909.

37. Lin, Y.C., et al., *Arabidopsis phosphatidylglycerophosphate phosphatase 1 involved in phosphatidylglycerol biosynthesis and photosynthetic function.* Plant J., 2016. **88**(6): p. 1022-1037.

38. Essigmann, B., et al., *Phosphate availability affects the thylakoid lipid composition and the expression of SQD1, a gene required for sulfolipid biosynthesis in Arabidopsis thaliana.* Proc. Natl. Acad. Sci. U.S.A., 1998. **95**(4): p. 1950-1955.

39. Shimojima, M. and C. Benning, *Native uridine 5'-diphosphate–sulfoquinovose synthase, SQD1, from spinach purifies as a 250-kDa complex.* Arch. Biochem. Biophys., 2003. **413**(1): p. 123-130.

40. Yu, B., C. Xu, and C. Benning, *Arabidopsis disrupted in SQD2 encoding sulfolipid synthase is impaired in phosphate-limited growth.* Proc. Natl. Acad. Sci. U.S.A., 2002. **99**(8): p. 5732-5737.

41. Tietje, C. and E. Heinz, *Uridine-diphospho-sulfoquinovose: diacylglycerol sulfoquinovosyltransferase activity is concentrated in the inner membrane of chloroplast envelopes.* Planta, 1998. **206**(1): p. 72-78.

42. Dubots, E., et al., *Role of phosphatidic acid in plant galactolipid synthesis.* Biochimie, 2012. **94**(1): p. 86-93.

43. Dubots, E., et al., *Activation of the chloroplast monogalactosyldiacylglycerol synthase MGD1 by phosphatidic acid and phosphatidylglycerol.* J. Biol. Chem., 2010. **285**(9): p. 6003-11.

44. Malherbe, A., et al., *Feedback inhibition of phosphatidate phosphatase from spinach chloroplast envelope membranes by diacylglycerol.* J. Biol. Chem., 1992. **267**(33): p. 23546-23553.

45. Awai, K., et al., *A phosphatidic acid-binding protein of the chloroplast inner envelope membrane involved in lipid trafficking.* Proc. Natl. Acad. Sci. U.S.A., 2006. **103**(28): p. 10817-10822.

46. Lu, B. and C. Benning, *A 25-amino acid sequence of the Arabidopsis TGD2 protein is sufficient for specific binding of phosphatidic acid.* J. Biol. Chem., 2009. **284**(26): p. 17420-17427.

47. Wang, Z., C. Xu, and C. Benning, *TGD4 involved in endoplasmic reticulum-to-chloroplast lipid trafficking is a phosphatidic acid binding protein.* Plant J., 2012. **70**(4): p. 614-623.

48. Xu, C., et al., *Lipid trafficking between the endoplasmic reticulum and the plastid in Arabidopsis requires the extraplastidic TGD4 protein.* Plant Cell, 2008. **20**(8): p. 2190-2204.

49. Wang, Z., N.S. Anderson, and C. Benning, *The phosphatidic acid binding site of the Arabidopsis trigalactosyldiacylglycerol 4 (TGD4) protein required for lipid import into chloroplasts.* J. Biol. Chem., 2013. **288**(7): p. 4763-71.

50. Hertle, A.P., et al., *A Sec14 domain protein is required for photoautotrophic growth and chloroplast vesicle formation in Arabidopsis thaliana.* Proc. Natl. Acad. Sci. U.S.A., 2020. **117**(16): p. 9101-9111.

51. Kim, E.H., et al., *Chloroplast-localized PITP7 is essential for plant growth and photosynthetic function in Arabidopsis.* Physiol. Plant., 2022. **174**(4): p. e13760.

52. Schroda, M., *Phosphoinositides regulate chloroplast processes.* Proc. Natl. Acad. Sci. U.S.A., 2020. **117**(17): p. 9154-9156.

53. Fritz, M., et al., *Channeling of eukaryotic diacylglycerol into the biosynthesis of plastidial phosphatidylglycerol.* J. Biol. Chem., 2007. **282**(7): p. 4613-25.

54. Muthan, B., et al., *Probing Arabidopsis chloroplast diacylglycerol pools by selectively targeting bacterial diacylglycerol kinase to suborganellar membranes.* Plant Physiol., 2013. **163**(1): p. 61-74.

55. Nakamura, Y., M. Tsuchiya, and H. Ohta, *Plastidic phosphatidic acid phosphatases identified in a distinct subfamily of lipid phosphate phosphatases with prokaryotic origin.* J. Biol. Chem., 2007. **282**(39): p. 29013-21.

56. Nguyen, V.C. and Y. Nakamura, *Distinctly localized lipid phosphate phosphatases mediate endoplasmic reticulum glycerolipid metabolism in Arabidopsis.* Plant Cell, 2023. **35**(5): p. 1548-1571.

57. Kolesnikov, Y., et al., *Phosphatidic acid in plant hormonal signaling: from target proteins to membrane conformations.* Int. J. Mol. Sci., 2022. **23**(6): p. 3227.

58. Lin, Y.T., et al., *Reduced Biosynthesis of Digalactosyldiacylglycerol, a Major Chloroplast Membrane Lipid, Leads to Oxylipin Overproduction and Phloem Cap Lignification in Arabidopsis.* Plant Cell, 2016. **28**(1): p. 219-32.

59. Yu, C.W., Y.T. Lin, and H.m. Li, *Increased ratio of galactolipid MGDG: DGDG induces jasmonic acid overproduction and changes chloroplast shape.* New Phytol., 2020. **228**(4): p. 1327-1335.

60. Ruan, J., et al., *Jasmonic acid signaling pathway in plants.* Int. J. Mol. Sci., 2019. **20**(10): p. 2479.

61. Wang, K., et al., *A Plastid Phosphatidylglycerol Lipase Contributes to the Export of Acyl Groups from Plastids for Seed Oil Biosynthesis.* Plant Cell, 2017. **29**(7): p. 1678-1696.

62. Wang, K., et al., *Two Abscisic Acid-Responsive Plastid Lipase Genes Involved in Jasmonic Acid Biosynthesis in Arabidopsis thaliana.* Plant Cell, 2018. **30**(5): p. 1006-1022.

CHAPTER 2:

Metabolic and developmental roles of chloroplast phosphatidate phosphatases

---

Chloroplast import experiments were conducted by John Froehlich. Photosynthetic experiments were conducted by Jeffrey Cruz in the David Kramer lab. EMS mutagenesis of seeds was performed by Linda Danhof.

Abstract

Galactolipids comprise the majority of chloroplast membranes in plants, and their biosynthesis requires dephosphorylation of phosphatidic acid (PA) at the chloroplast envelope membranes. In Arabidopsis, the lipid phosphate phosphatases LPPγ, LPPε1, and LPPε2 have been previously implicated in chloroplast lipid assembly, with LPPγ being essential, as null mutants were reported to exhibit embryo lethality. Here, we show that *lppγ* mutants are in fact viable, and that LPPγ, LPPε1, and LPPε2 do not appear to have central roles in the plastid pathway of membrane lipid biosynthesis. Redundant LPPγ and LPPε1 activity at the outer envelope membrane is important for plant development, and the respective *lppγ lppε1* double mutant exhibits reduced flux through the ER pathway of galactolipid synthesis. While LPPε2 is imported and associated with interior chloroplast membranes, its role remains elusive, and does not include basal nor phosphate limitation-induced biosynthesis of glycolipids. The specific physiological roles of LPPγ, LPPε1, and LPPε2 have yet to be uncovered, as does the identity of the PA phosphatase required for plastid MGDG biosynthesis.

Introduction

In plants, photosynthesis begins with the capture and photochemical conversion of light energy by densely-packed thylakoid membranes, and green tissues devote the majority of glycerolipid metabolism to generating and maintaining these chloroplast membranes. The potential for nutrient limitation imposed by a large phospholipid-based system is mitigated in plants, which have instead evolved photosynthetic membranes mostly composed of glycolipids.

The most abundant lipid constituent of chloroplast membranes is monogalactosyldiacylglycerol (MGDG), followed by digalactosyldiacylglycerol (DGDG). Together, these galactolipids account for more than two-thirds of chloroplast lipids [1-3]. The remainder is mainly phosphatidylglycerol (PG) and sulfoquinovosyldiacylglycerol (SQDG), the two major anionic lipids in chloroplasts. Phosphatidylcholine (PC) is also found in chloroplasts, where it is confined to the outer envelope membrane (OEM) [1, 3].

In 16:3 plants, which include Arabidopsis, tobacco, and spinach [4], two separate pathways of lipid biosynthesis converge to make MGDG: an endoplasmic reticulum (ER) pathway and a plastid

pathway (also referred to as the “eukaryotic” and “prokaryotic” pathways, respectively). 18:3 plants, including monocots and legumes, rely entirely on the ER pathway for galactolipid biosynthesis. In the ER pathway, fatty acid (FA) export from the chloroplast is followed by activation to acyl-CoAs and subsequent acyl transfer to glycerol 3-phosphate by ER acyltransferases [5, 6]. Acylation of the *sn-2* position is carried out in the ER by an acyltransferase with specific preference for 18-carbon substrates [7]. The phosphatidic acid (PA) product, or a PA derivative, is imported by the chloroplast to the inner envelope membrane (IEM) [8, 9], where the enzyme MGD1 galactosylates PA-derived diacylglycerol (DAG) to make MGDG [10-12].

In the plastid pathway of MGDG biosynthesis, acyl transfer from acyl-acyl carrier protein (acyl-ACP) to glycerol 3-phosphate takes place at the stroma-facing leaflet of the IEM [13, 14]. This is followed by dephosphorylation by a PA phosphatase (PAP), and galactosylation of DAG by MGD1 [10-12]. In contrast to the ER pathway, the chloroplast *sn-2* acyltransferase is specific to 16-carbon rather than 18-carbon substrates, allowing for MGDG synthesized through this pathway to be distinguished from the ER-derived lipid [15, 16].

Previously identified candidates for PAPs involved in MGDG biosynthesis in Arabidopsis include the cytosolic lipins PAH1 and PAH2 [17], and the lipid phosphate phosphatases LPPγ, LPPε1, and LPPε2 [18]. PAH1 and PAH2 may play a role in the ER pathway, while LPPγ, LPPε1, and LPPε2 are chloroplast-located and have enzymatic properties matching the PAP activity in chloroplast membranes. LPPε1 is associated with the OEM, where its activity has redundancy with that of the ER-located LPPα2 [19]. However, mutant studies in Arabidopsis report no phenotypic abnormalities in the *lppε1* and *lppε2* null mutants, the *lppε1 lppε2* double mutant, or reduced-function lines of *LPPγ*. Because a null mutant of *LPPγ* was deemed unattainable at the time, LPPγ was proposed to be essential for plant viability [18].

In this study, chloroplast *lpp* mutants were revisited for further characterization. It was hypothesized that LPPε1 and LPPε2 may function redundantly with other lipid metabolic enzymes, or may be involved in a response pathway to environmental challenges, thereby not showing aberrant mutant phenotypes at standard growth conditions. In addition, independent *lppγ* mutants were pursued for a more complete characterization of LPPγ function in chloroplasts.

Results

LPPγ null mutants are viable, and their lipid profile is unaltered

Three independent *lppγ* mutant alleles of Arabidopsis were confirmed as homozygous using PCR: *lppγ-1* (SAIL_1255_H02), *lppγ-2* (SALK_055510), and *lppγ-3* (SALK_048788), all of which have insertions within the coding sequence (Fig. 2.1A-B). In our hands, and in contrast to a previous report [18], the three *lppγ* insertional mutant alleles were viable and did not have abnormalities in growth or morphology under standard conditions (Fig. 2.1C). Subsequent experiments were conducted using *lppγ-1* (hereafter *lppγ*). The lipid profile of *lppγ* is comparable to the wild type, with the relative membrane lipid composition and their acyl compositions unaffected (Fig. 2.2).

LPPγ *and* LPPε1 *have redundant roles affecting plant growth*

The LPP family in Arabidopsis is subcategorized into LPPα, LPPβ, LPPγ, LPPδ, and LPPε, with a prior phylogenetic analysis showing that LPPγ and LPPε share a subclade, and microscopy and fractionation assays localizing LPPγ and LPPε to the chloroplast [18-20]. To account for potential functional redundancies among the different chloroplast LPP isoforms, single mutants were crossed to generate the double mutants *lppγ lppε1*, *lppγ lppε2*, and *lppε1 lppε2*, as well as the triple mutant *lppγ lppε1 lppε2*. As previously reported, *lppε1 lppε2* did not exhibit differences in growth or morphology [18], and this was also observed here for *lppγ lppε2*. Meanwhile, *lppγ lppε1* showed a reduction in both growth rate and size at maturity (Fig. 2.3A). This phenotype of *lppγ lppε1* was replicated in the triple mutant *lppγ lppε1 lppε2*, with no additive effect of introducing *lppε2*. These phenotypes show that the activities of LPPγ and LPPε1 are at least partially redundant and required for proper development under standard growth conditions, while LPPε2 activity is separate from that of LPPγ and LPPε1.

Complementation studies verified the redundancy of *LPPγ* and *LPPε1*, as either gene is sufficient to reverse the phenotype of *lppγ lppε1* when expressed using either native (Fig. 2.3B) or CaMV 35S (Fig. 2.3C) promoters. *LPPε2* overexpression in the *lppγ lppε1* background does not complement the mutant phenotype, further implicating the role of LPPε2 as discrete from LPPγ and LPPε1 (Fig. 2.3C).

LPP *localization within the chloroplast*

To characterize sub-chloroplast location of the three plastid LPP isoforms, we employed chloroplast import experiments with radioactive precursor proteins. For this purpose, LPPs labeled with ^{3}H-Leu were synthesized *in vitro* using wheat germ lysate and a coding sequence template, and the translation products were incubated with intact pea chloroplasts. All three LPPs appeared in pellets after chloroplast fractionation, confirming these are membrane-associated proteins (Fig. 2.4). LPPε2 was efficiently cleaved and imported to a trypsin-protected membrane, which could be either thylakoid or IEM. Meanwhile, LPPε1 import was inefficient, and LPPγ was not processed, but membrane-associated and protease-sensitive. The redundancy of LPPγ and LPPε1 is therefore likely at the chloroplast OEM, with LPPε2 unable to compensate due to its confinement to the IEM or thylakoids. Unexpectedly, the translation product of LPPε1 ran at approximately 25 kDa on polyacrylamide electrophoresis gels, despite an expected molecular weight of ~30 kDa and a high sequence similarity and equivalent length to LPPε2, which did run at the expected size.

To test whether chloroplast import separates LPPε2 from the redundant activity of LPPγ and LPPε1, a truncated LPPε2 lacking 59 N-terminal residues was introduced into *lppγ lppε1*. The wild-type growth phenotype was restored in these transgenic lines (Fig. 2.5), confirming that the redundant LPPγ and LPPε1 activity does not occur at the IEM nor thylakoids, and that the three LPPs have equivalent enzymatic activity. A rescue was also observed with a corresponding 51-residue N-terminal truncation of LPPε1, demonstrating that this region is not necessary for proper localization of LPPε1, and is possibly the missing component of the *in vitro* translation product.

Mutants lacking LPPγ*,* LPPε1*, and* LPPε2 *have largely unaltered membrane lipid profiles in leaves and unaffected lipid fluxes in isolated chloroplasts*

As previously reported, *lppε1 lppε2* did not show aberrations in relative quantities of membrane lipids, nor in lipid acyl composition [18]. The same was observed for *lppγ lppε2*. Differences in lipid composition, including PA content, were also not observed in *lppγ lppε1* (Fig. 2.6A). In addition, major lipids did not have altered acyl compositions, and the lipid profile of the *lppγ lppε1 lppε2* triple mutant was comparable to that of *lppγ lppε1* (Fig. 2.6B).

To test whether any of these LPPs have a significant role in the plastid pathway of galactolipid assembly, isolated chloroplasts from the *lppγ lppε1 lppε2* triple mutant were incubated with ^{14}C-acetate, and acyl flux through chloroplast lipid pools was determined based on pulse experiments. A deficiency in the PAP activity required for plastid MGDG biosynthesis would be observed as lower rates of PA conversion to MGDG [21]. Meanwhile, a decrease in flux caused by lower plastid PA production would be observed as higher relative PC accumulation, as plastid-synthesized FA transfer to PC continues to occur while PA and its derivatives accumulate more slowly [22]. Here, this is seen in isolated chloroplasts from the *ats1-1* mutant, which is deficient in plastid PA biosynthesis (Fig. 2.6C) [14]. Surprisingly, chloroplasts from *lppγ lppε1 lppε2* did not show slower conversion of PA to MGDG than wild-type chloroplasts, nor was there a relative decrease in labeling of PA, MGDG, or PG compared to PC (Fig. 2.6C). Therefore, the basal lipid biosynthetic pathways within the chloroplast do not appear to be dependent on the chloroplast LPPs.

LPPγ *and* LPPε1 *contribute to the ER pathway of galactolipid biosynthesis*

The role of chloroplast LPPs on the ER pathway contribution to galactolipid biosynthesis was tested by ^{14}C-acetate pulse-chase analysis of polar lipids in whole leaves. During the chase, both *lppγ lppε1* and *lppγ lppε1 lppε2* exhibited slower conversion of PC to MGDG than wild type, with no additive effect by the *LPPε2* deletion (Fig. 2.7). LPPγ and LPPε1 activity therefore facilitate MGDG biosynthesis from ER-derived phospholipids, while LPPε2 does not participate in either of the two galactolipid biosynthetic pathways.

Crosses of lppγ lppε1 to tgd and rbl10 mutants have additive phenotypes, while crossing to ats1 results in severely reduced fitness

In order to better contextualize the roles of LPPγ and LPPε1 in overall lipid metabolism, the double mutant was crossed to various characterized lipid mutants. Among these, *tgd1-1* and *tgd4-1* are deficient in lipid import from the ER pathway, *rbl10-1* has decreased PAP activity in the plastid pathway, and *ats1-1* is severely reduced in stromal PA biosynthesis [9, 14, 21, 23-25]. The triple mutants *lppγ lppε1 tgd1-1*, *lppγ lppε1 tgd4-1*, and *lppγ lppε1 rbl10-1* did not exhibit recovery nor

exacerbation of the *lppγ lppε1* growth defect, with *lppγ lppε1 tgd1-1* leaves additionally showing the pale color of *tgd1-1*.

The lipid profile of *tgd1-1* is changed by genetic stacking of *lppγ lppε1*, with the triple mutant showing a small relative decrease in DGDG and a restoration of fully desaturated 16-carbon chains on MGDG, while the acyl profile of DGDG in *lppγ lppε1 tgd1-1* remains identical to that of *tgd1-1* (Fig. 2.8A). The lipid profile *lppγ lppε1 rbl10-1* does not differ from that of *rbl10-1*, retaining the specific decrease in 16:3 acyl groups on MGDG (Fig. 2.8B).

While *lppγ ats1-1* plants were obtained and appear normal, the triple mutant was not successfully generated after crossing of *lppγ ats1-1* to *lppγ lppε1*. 192 seeds were sown from the *lppγ ats1-1* x *lppγ lppε1* F2 generation, of which approximately 12 (6.25%) would be expected to be triple mutants. Instead, only 171 seeds germinated, and none were determined to be *lppγ lppε1 ats1-1* triple mutants. Genetic linkage would not account for this result, as *ATS1* is on chromosome 1, *LPPγ* on chromosome 5, and *LPPε1* on chromosome 3. The ungerminated seeds represent ~11% of the F2 segregating population, and may include triple mutants that have a severe or complete decline in viability. Such effects on fitness have been previously witnessed in crosses of *ats1-1* to mutants disrupted in the ER pathway [9, 24, 26].

Light sensitivity is not the primary cause of growth inhibition in lppγ lppε1

In addition to its slow growth and stunted appearance, *lppγ lppε1* also visibly accumulates anthocyanins in leaves under standard growth conditions. This is particularly noticeable at the phase separation step of lipid extraction (Fig. 2.9A). Anthocyanin accumulation is associated with a wide range of stresses, including a photoprotective role in excess light. Chlorophyll fluorescence measurements showed lower photosystem II efficiency (ϕII) in the double mutant, which was mostly accounted for by higher energy-dependent quenching (qE) (Fig. 2.9B). To test whether excess light leads to a stress-induced growth inhibition in *lppγ lppε1*, plants were grown at a reduced light intensity of 35 µmol photons m^{-2} s^{-1}. These plants remained stunted, and their lipid profile was also unchanged, indicating that light sensitivity is not a major contributor to the growth phenotype of *lppγ lppε1* (Fig. 2.9C). Likewise, increasing the ambient CO_2 concentration to 1800 ppm did not alleviate the growth phenotype of the double mutant (Fig. 2.9D).

Salicylic acid signaling is not induced in lppγ lppε1

As discussed in chapters 1 and 3, chloroplast lipid mutants exist that are known to have hormone-driven changes to morphology. Among these, the *dgd1* mutant and *PLIP* overexpression lines have severe growth defects resulting from the constitutive production of jasmonic acid (JA) [27-30]. The phenotype *lppγ lppε1* does not resemble that of these constitutive JA mutants, as leaf and petiole elongation in *lppγ lppε1* is not disproportionately stunted, anthocyanins are not distributed in vascular tissues in the absence of light stress, and mutants have shown susceptibility to fungus gnats in the growth chambers. While these phenotypes differ from those of constitutive JA lines, we considered they may resemble previous descriptions of the constitutive salicylic acid (SA) mutant *cpr1-1*, among others [31, 32]. Stunted growth in these mutants is known to be suppressed at elevated temperature [32], so the morphology of *lppγ lppε1* was compared to that of *cpr1-1* at 22°C and 28°C. In our comparison, *lppγ lppε1* did not have a strong resemblance to *cpr1-1* at standard temperature (Fig. 2.10A), and growth was not rescued at elevated temperature (Fig. 2.10B). Furthermore, constitutive SA was tested in *lppγ lppε1* by probing for the response factor pathogenesis response 1 (PR1) using Western blotting, and PR1 accumulation was not observed in *lppγ lppε1* in the absence of applied stresses (Fig. 2.10C). The SA biosynthesis mutant *sid2-2* was also included as a negative control [33].

A screen in the lppγ lppε1 background has yielded preliminary suppressor mutants

In order to identify genes potentially responsible for the stunted growth of *lppγ lppε1*, the double mutant was mutagenized with EMS, and M2 plants subjected to a visual suppressor screen. Two mutants out of ~800 screened on soil, designated *sup3* and *sup25*, had strong suppression phenotypes and were chosen for backcrossing. Additional suppressors *sup30* and *sup32* were selected among ~4500 that were initially screened on agar plates, of which 24 had been transferred to soil for a secondary visual screen. These suppressor mutants are shown in Fig. 2.11. After mutant backcrossing to *lppγ lppε1*, the F2 segregating populations will be sequenced and causative mutations identified using the strategies applied in chapter 3.

Chloroplast-imported LPPs *are not required for lipid changes under phosphate deprivation, excess light, or low temperature*

While the phospholipid content in chloroplasts is already relatively low in nutrient-replete conditions, it is further decreased when SQDG is substituted for PG under phosphate deprivation [34]. Because *lppε2* has a wild-type phenotype under standard conditions, it is possible that LPPε2 instead plays a role in responding to environmental changes. Its import into the chloroplast and its PA phosphatase activity would suggest it may be important for the increase in SQDG under phosphate deprivation. Because the import assay also showed limited LPPε1 import, the single mutants *lppε1* and *lppε2* were examined under phosphate deprivation, along with the *lppε1 lppε2* double mutant. While root growth was slightly slower in the double mutant, this difference was not exacerbated on media with a 95% reduction in phosphate content (Fig. 2.12A). In addition, *lppε1 lppε2* did not appear to be impaired in its ability to accumulate SQDG in place of PG (Fig. 2.12B).

Other conditions in which a chloroplast PAP may be applied include transitions to excess light or decreased temperature, as these changes may require phosphatase-dependent lipid turnover or remodeling. To test this, three-week old plants grown at standard conditions (22°C, 120 µmol m^{-2} s^{-1} photons) were transferred to either low-temperature (10°C) or high-light (270 µmol m^{-2} s^{-1} photons) chambers. After one week at these conditions, no visible difference was seen between *lppε* mutants and wild-type plants (Fig. 2.13A). Likewise, no differential effects on lipid profiles were observed between Col-0 and *lppε1 lppε2* at reduced temperature or increased light (Fig. 2.13B).

Discussion

LPPγ*,* LPPε1*, and* LPPε2 *do not have major roles in the plastid pathway of galactolipid biosynthesis*

PA biosynthesis and conversion to MGDG in isolated *lppγ lppε1 lppε2* chloroplasts is equivalent to that of wild-type chloroplasts. In contrast, a mutant lacking the chloroplast rhomboid-like protein RBL10 has been shown to be deficient in the conversion of chloroplast PA to MGDG, indicating that PA dephosphorylation specific to the plastid pathway partially depends on functional RBL10 [21]. Because the conversion of plastid PA to MGDG is decreased in *rbl10*, but

not in *lppγ lppε1 lppε2*, these LPPs are not the RBL10-dependent PAPs involved in plastid galactolipid biosynthesis. Therefore, LPPγ, LPPε1, or LPPε2 serve other metabolic or physiological roles, while the identity of the plastid pathway PAP is still unknown (Fig. 2.14). Because the *rbl10-1* mutant phenotype does resemble that of an expected deficiency in plastid pathway PAP activity, additional investigation into the role of RBL10 in the plastid may reveal its identity.

LPPγ*,* LPPε1*, and* LPPε2 *have the same catalytic activity, with* LPPγ *and* LPPε1 *located at the chloroplast OEM, and* LPPε2 *within the IEM or thylakoids.*

With chloroplast import assays showing an efficient import of LPPε2 into the trypsin-protected internal compartments of chloroplasts, and little to no equivalent import of LPPγ nor LPPε1, it is likely that LPPε2 is the only characterized PA phosphatase exclusively located at internal chloroplast membranes (Fig. 2.14). LPPε1 may be dual-localized to both envelope membranes, as import assays have shown inefficient chloroplast import to trypsin-protected compartments. Published protease assays on chloroplasts from epitope-tagged LPPε1 lines in Arabidopsis have shown OEM association [19]. LPPγ is likely exclusively at the OEM, as it has redundant activity with LPPε1, no apparent processing or import, and has been shown to be chloroplast-associated [18]. The complementation of the *lppγ lppε1* phenotype by an N-terminal truncation of LPPε2 confirms the equivalent enzymatic activity, previously shown to be PAP activity [18], among the three enzymes.

LPPε2 may associate with either thylakoids or the IEM. Because the bulk of chloroplast membrane lipid biosynthesis takes place in the envelope membranes, the location of LPPε2 in thylakoids would explain why *lppε2* mutants are unaffected in lipid phenotypes. In such case, LPPε2 may be involved in turnover of thylakoid lipids, although it is likely not involved in mild transitions to low temperature or high light. On the other hand, if LPPε2 is IEM-associated, it would not be the primary PAP in the plastid pathway of galactolipid or sulfolipid biosynthesis, as mutants can accumulate these glycolipids without hinderance under standard and phosphate-limited growth conditions.

LPPγ *and* LPPε1 *contribute to the ER pathway of galactolipid biosynthesis*

With LPPγ and LPPε1 located in the OEM, we would expect that if they are involved in one of the galactolipid biosynthetic pathways, it would be the ER pathway (Fig. 2.14). Indeed, based on the radiolabeling results in whole leaves and chloroplasts of *lppγ lppε1*, the double mutant appears to be specifically impaired in the ER pathway of MGDG biosynthesis. In addition, the failure to obtain homozygous *lppγ lppε1 ats1-1* triple mutants, with *ats1-1* being deficient in the plastid pathway, is also reported for known ER pathway mutants *tgd1-1*, *tgd4-1*, and *tgd5-1* [9, 24, 26]. This is in contrast to the viability of *lppγ lppε1 tgd1-1* and *lppγ lppε1 tgd4-1* triple mutants, which remain deficient in just the ER pathway, and in line with a disruption of both galactolipid biosynthetic pathways in *lppγ lppε1 ats1-1*.

Activity of the desaturase FAD5 *may be altered in the tgd1-1 mutant*

The differences between *tgd1-1* and *lppγ lppε1 tgd1-1* in DGDG content and MGDG acyl composition may both derive from a decrease in FAD5 activity. In the *tgd1-1* mutant, the majority of acyl chains on the *sn*-2 position of DGDG are 16:0, as opposed to 18:3 in the wild type [23]. Likewise, the *sn*-2 position of MGDG in *tgd1-1* is not only depleted of 18-carbon chains, but also enriched in saturated 16-carbon moieties, which is seen affecting the total acyl composition of *tgd1-1* in Fig. 2.8A. This would suggest that DGD1 cannot utilize plastid-derived MGDG as a substrate if the *sn*-2 position is desaturated, and in *tgd1-1* this desaturation is downregulated to provide compensatory substrate for DGD1. In *lppγ lppε1 tgd1-1*, desaturation of MGDG *sn*-2 chains is restored and 16:3 levels are recovered, which deprives DGD1 of substrate and results in decreased DGDG content. The desaturase FAD5 is responsible for the initial desaturation of *sn*-2 chains on chloroplast MGDG [35, 36]. *FAD5* expression or activity may therefore be downregulated in *tgd1-1*, and repression of *FAD5* is reversed in *lppγ lppε1 tgd1-1*.

PA at the intermembrane-facing leaflet of the OEM may negatively regulate plant growth in lppγ lppε1

Despite evidence for the involvement of LPPγ and LPPε1 in the ER pathway of galactolipid biosynthesis, the acyl profile of MGDG in *lppγ lppε1* strongly resembles that of the wild type. This would suggest that Arabidopsis is somehow able to compensate for the decreased lipid flux from

the ER in the double mutant. Meanwhile, the *tgd1-1* mutant shows a similar pattern of lipid fluxes in whole leaves labeled using ^{14}C-acetate, but is also affected in the acyl profile of MGDG and DGDG, and accumulates high levels of PA [9, 23]. In addition, unlike *lppγ lppε1*, it has pale leaves, likely due to an overall decrease in thylakoid membrane content. Based on these data, it appears that the ER pathway is more severely affected in *tgd1-1* than in *lppγ lppε1*. However, in *tgd1-1*, as well as similar mutants affecting import complex components TGD2-5, plant growth is not inhibited as it is in *lppγ lppε1* [24, 26, 37, 38]. The growth deficiency in *lppγ lppε1* is therefore likely distinct from the broad effects on lipid flux from the ER to the chloroplast, and may rather result specifically from PA accumulation in a particular membrane compartment.

In a previous Arabidopsis study, a bacterial DAG kinase was targeted to stromal-facing, intermembrane-facing, or cytosolic-facing leaflets of the chloroplast membranes. Among these, only the lines in which DAG kinase was introduced to the intermembrane space appeared stunted in growth [39]. As in *lppγ lppε1*, the membrane lipid composition appeared unaffected despite the growth inhibition. Given these results, and because LPPγ is exclusive to the OEM, it can be reasoned that the phenotype of *lppγ lppε1* is a specific result of PA accumulation at the intermembrane-facing leaflet of the OEM (Fig. 2.14). This PA pool would be negligible relative to total PA content, resulting in the apparent lack of difference in PA during quantification.

There is currently no insight into the means by which PA at the inner leaflet of the OEM affects plant development in *lppγ lppε1*. It appears as though the hormone pathways of JA and SA are not involved, based on morphological, physiological, and biochemical observations. The retention of growth inhibition at low light and high CO_2 suggests that it is not a direct result of constraints or inhibition of photosynthesis. The severity of growth inhibition in *lppγ lppε1* may itself be the reason for the double mutant's light sensitivity, with quenching mechanisms activated to prevent photosynthetic sink limitations from leading to oxidative stress. In this absence of obvious leads, the mutant screen for suppressors of *lppγ lppε1* will provide opportunities for elucidating the roles of PA and chloroplast LPPs in the regulation of plant development.

LPPε2 *has an unknown role in the interior chloroplast membranes*

The role of LPPε2 is yet more elusive, with no discernable phenotypic differences in *lppε1* or *lppε2* mutants at standard, phosphate-limited, high-light, or low-temperature conditions. The enzyme may therefore be involved in responses to environmental conditions that have not yet been tested, with possible roles in lipid signaling, remodeling, or degradation. LPPε2 may have redundancies with LPPε1, depending on their specific locations at the interior membranes of the chloroplast. Therefore, future studies introducing various environmental challenges would be appropriate using the *lppε1 lppε2* double mutant.

LPPs *and PA in the chloroplast*

Our continued investigation of chloroplast LPPs has confirmed that LPPγ and LPPε1 are involved in basal lipid metabolism, but as part of the ER-derived galactolipid biosynthesis pathway and not the plastid pathway. The stunted growth of *lppγ lppε1* implicates PA as a potential regulatory molecule at the site of LPPγ and LPPε1 activity, and consequently these enzymes' function may not be limited to just metabolism. LPPε2 is imported into the inner envelope or thylakoids, but like the other LPPs, does not significantly contribute to plastid-derived galactolipid biosynthesis. Its role has yet to be discovered, as does the identity of the plastid pathway PA phosphatase.

Methods

Plants

Insertional mutant lines of *Arabidopsis thaliana* were ordered from the Arabidopsis Biological Resource Center (ABRC). The T-DNA lines with insertions in *LPPγ* were SAIL_1255_H02, SALK_055510, and SALK_048788, corresponding to *lppγ-1*, *lppγ-2*, and *lppγ-3* [40-42]. The *lppε1* and *lppε2* mutants refer to T-DNA lines SALK_000157 and SALK_055964, respectively. *cpr1-1* seeds were obtained from the Sarah Lebeis lab, and *sid2-2* seeds from the Federica Brandizzi lab. *ats1-1*, *tgd1-1*, *tgd4-1*, and *rbl10-1* mutant seeds were available in the Benning lab stock. Double and triple mutants were generated by crossing, which entailed removal of petals and stamens from unopened flowers, cross-pollination of the emasculated flowers by the male, and protection of pollinated pistils using plastic cling film for ~1 week, until silique formation [43].

EMS mutagenesis

Approximately 13,000 PLIP3-OX seeds were incubated in 0.1% Tween®20 (Sigma-Aldrich) for 15 minutes in a tube rotator, after which seeds were allowed to settle, and the solution was removed. 0.2% Ethyl methanesulfonate (EMS) in water was added, and seeds were incubated overnight (~16 hrs) in tube rotator. Seeds were washed 7 times with water, incubated in water for 2 hours, and washed with water one more time.

Growth conditions

Unless otherwise stated, plants were grown in SUREMIX™ Professional All-Purpose Perlite Mix (Michigan Grower Products, Inc.) at a temperature of 22°C, a long-day 16/8-hr light/dark cycle, and a light intensity of approximately 120 µmol m^{-2} s^{-1}. Plants for phosphate response assays were grown on vertical plates on medium containing half-strength Murashige and Skoog (MS), 1% sucrose, 1% Phytoblend™ agar (Caisson labs), and buffered with 2.5 mM MES at pH 5.7 [44]. For low-phosphate plates, MS was replaced with a mixture of 5% MS and 95% phosphate-free MS. Plants used for chloroplast isolation were grown on horizontal plates containing full-strength MS, 1% sucrose, and 0.8% Phytoblend™ agar, buffered with 2.5 mM MES at pH 5.7. Plate-grown plants were all incubated at 22°C, a long-day 16/8-hr light/dark cycle, and a light intensity of approximately 120 µmol m^{-2} s^{-1}.

Constructs and transformation

For overexpression lines, coding sequences were amplified using cDNA templates synthesized from Arabidopsis leaf mRNAs. These were cloned into pENTR using the pENTR™ /D-TOPO® kit (ThermoFisher), and recombined to pH35GY expression vectors [45] using Gateway™ LR Clonase™ II (ThermoFisher). Stop codons were excluded to generate C-terminal YFP fusions. Constructs for N-terminal truncations were made using the Q5® Site-Directed Mutagenesis Kit (New England Biolabs). For constructs using native promoters, target genes were amplified together with ~2 kb upstream regions from Arabidopsis gDNA using primers that include AscI and SalI restriction sites. These were then integrated into pCAMBIA1390 vectors using restriction digests and ligation. Primer sequences are listed and defined in Table 2.1. Vectors were used to transform *Agrobacterium tumefaciens* strain GV3101, and plants were transformed via vacuum-

mediated floral dip [46]. For the *in vitro* translation step of the chloroplast import experiment, *LPP* sequences from pENTR were recombined with pDEST14 expression vectors.

Lipid profiling

Tissue was harvested from 4-week-old soil-grown plants, and lipids were extracted, separated, and analyzed as described [47]. In brief, lipids were extracted from leaves in 20:10:1 methanol:chloroform:formic acid solution, after which a half-volume of 0.2 M phosphoric acid, 1 M KCl solution was added and vortexed. After phase separation, the bottom organic phase was transferred to a new tube, dried with pure nitrogen, resuspended in chloroform, and loaded onto an ammonium sulfate-impregnated thin layer chromatography (TLC) plate. TLC was run using a mobile phase of 91:30:7.5 acetone:toluene:water. PA was separated using 2-dimensional TLC on unimpregnated plates, with a mobile phase of 65:25:4 chloroform:methanol:water for the first dimension, and 50:20:10:10:5 chloroform:acetone:methanol:acetic acid:water for the second [9]. Lipids were briefly stained with iodine for identification, then scraped into glass tubes and derivatized to fatty acid methyl esters (FAMEs) by adding 1 M methanolic HCl for a 25-minute incubation at 80°C. Equal volumes of 0.9% aqueous sodium chloride and hexane were then added, and phases were separated after vortexing. The FAME-containing hexane phase was transferred to a new tube, dried under N_2 gas, and resuspended with hexane. FAMEs were identified and quantified using gas chromatography-flame ionization detection.

Chloroplast isolation from Arabidopsis

Intact chloroplasts were isolated as described in [48]. In brief, two-week old plants grown on horizontal plates were harvested in the morning using a razor blade, and suspended in ice-cold chloroplast buffer (330 mM sorbitol, 50 mM HEPES, 1 mM $MgCl_2$, 1M $MnCl_2$, 2 mM EDTA, 0.1% BSA, KOH to pH 7.3). In the buffer, leaves were promptly cut with scissors and then homogenized for 10-30 s using a T25 digital ULTRA-TURRAX® homogenizer (IKA) with a 15-mm probe at 8,000 rpm. Homogenate was filtered through two layers of Miracloth (Millipore), pelleted at 700 x *g* for 5 min, and resuspended in buffer, which was loaded onto tubes containing a step gradient. The step gradient consisted of 85% Percoll® (Sigma) at the bottom, upon which 40% Percoll® was gently loaded (Percoll® solutions were prepared with the same solute composition as the

chloroplast buffer). After centrifugation at 2000 x *g* for 10 min with no brake, intact chloroplasts were transferred from the interphase to a new tube, washed once with buffer, pelleted, and resuspended in a small volume of buffer. To determine µg/mL chlorophyll, absorbance at 652 nm was measured in 80% acetone, and multiplied by an extinction coefficient of 28 [49].

^{14}C-acetate labeling

^{14}C-acetate labeling was carried out for intact chloroplasts at 100 µg/mL chlorophyll in chloroplast buffer (330 mM sorbitol, 50 mM HEPES, 1 mM $MgCl_2$, 1M $MnCl_1$, 2 mM EDTA, 0.1% BSA, KOH to pH 7.3) with 0.6 mM UDP-galactose. 10 µCi/mL ^{14}C-acetate (American Radiolabeled Chemicals, Inc., Catalog No. ARC 0173) was added in the dark and on ice. Samples were transferred to a 24-well plate on a shaker, at room temperature and with an LED light source of ~100 µmol m^{-2} s^{-1}. ^{14}C-acetate labeling of leaves was carried out in 10 cm petri plates, with leaves floating on 25 mM MES pH 5.7 buffer. The 1-hr pulse and first wash included 0.001% Tween®20, and the pulse included 1 µCi/mL ^{14}C-acetate. After the pulse, leaves were washed once with the same buffer, containing no radioactivity. Equivalent MES buffer excluding the Tween was used for the second and third washes, and as the chase incubation buffer. Leaf samples also used an LED light source of ~100 µmol m^{-2} s^{-1}. For both leaves and isolated chloroplasts, samples were harvested at the designated timepoints, and polar lipids were extracted and separated using TLC as previously described. Plates were imaged using phosphor screens, and radioactivity was measured for scraped lipids by addition of 4a20™ counting cocktail (Research Products International) and quantification using a liquid scintillation counter.

Photosynthesis measurements

Photosynthetic measurements were obtained from 4-week-old plants grown in soil at a temperature of 22°C, a long-day 16/8-hr light/dark cycle, and a light intensity of approximately 120 µmol m^{-2} s^{-1}. Chlorophyll fluorescence images were recorded using dynamic environmental phenotype imager (DEPI) chambers as previously described [50], but with a series of constant actinic intensities. Briefly, plants were dark-adapted for 30 min, and relative yields of chlorophyll fluorescence were estimated for the fully dark-adapted state (F0) and during an intense flash (~0.3 s, 10,000 µmol m^{-2} s^{-1}) to saturate photosystem II (PSII) photochemistry. A series of actinic

light intensities (50, 100, 200, 300, 400, 500, 600 µmol photons m^{-2} s^{-1}) were then applied in sequence. After five minutes of illumination at each intensity, relative chlorophyll fluorescence yields were in the steady state (Fs) and during saturation flashes (Fm'). Photosynthetic parameters were calculated for photosystem II efficiency (ϕII) and energy-dependent quenching (qE) as previously described [50, 51].

Protein extraction, SDS-PAGE, and immunoblotting

~50-100 mg of leaf tissue was harvested into 2 mL tubes containing 5-10 zirconia/silica beads (2.3 mm, BioSpec Products, Cat. No. 11079125z) and frozen in liquid nitrogen. Cells were broken using bead-beater at 30 Hz for 3 min. 150 µL loading buffer (4% sodium dodecyl sulfate (SDS), 20% glycerol, 10% β-mercaptoethanol, 0.125 M Tris-HCl, pH 6.8) containing plant protease inhibitor cocktail (Sigma-Aldrich Cat. No. P9599) was added to the sample. The sample was incubated at room temperature for 15 minutes with occasional vortexing, then centrifuged at 15,000 x *g* for 2 minutes. Supernatant was transferred to new tube, allowed to incubate at room temperature for 15 minutes, then loaded onto Bio-Rad 4-20% Mini-PROTEAN® TGX™ precast polyacrylamide gels (Cat. No. 4561094). Gels were run at 150 V for 45-60 minutes, using Tris-glycine-SDS running buffer (25 mM Tris, 192 mM glycine, 0.1% SDS), and transferred to a PVDF membrane at 100 V for 80 minutes using Tris-glycine transfer buffer (25 mM Tris, 192 mM glycine, 20% methanol), with chilling and stirring. Membranes were washed in PBS-T (137 mM NaCl, 2.7 mM KCl, 10 mM Na_2HPO_4, 1.8 mM KH_2PO_4, 0.04% Tween®20), and blocked using PBS-T with 5% nonfat dry milk. Membranes were incubated with antibodies for 1 hr, then washed 4 times for 5 minutes with PBS-T. The primary antibody used was the rabbit PR-1 antibody from Agrisera (Cat. No. AS10 687), and the secondary antibody was the HRP-conjugated donkey anti-rabbit IgG, from Agrisera (Cat No. AS10 845). An undergraduate student expressed concern for the fate of the donkey. Chemiluminescence was detected using Bio-Rad Clarity Western ECL Substrate (Cat. No. 1705061).

Chloroplast import assays

Chloroplast import assays were carried out as previously described in [52]. In summary, chloroplasts were extracted from 8- to 12-day-old pea seedlings, isolated by centrifugation using

a 40% Percoll cushion, and resuspended in import buffer (IB; 330 mM sorbitol, 50 mM HEPES-KOH, pH 8.0) at 1 mg/mL chlorophyll. Separately, pDEST14 vectors with *LPP* or control sequences were translated using the Promega TNT® Coupled Wheat-germ Lysate System, with the addition of 0.05 mCi ^{3}H-leucine in each 50 µL reaction. After translation, the radiolabeled reaction product was diluted with an equal volume of 2x IB containing 50 mM unlabeled L-leucine. Equal volumes of 1 mg/mL chloroplasts in IB and 12 mM Mg-ATP in IB were added to the translation product (final Mg-ATP concentration of 4 mM), and the mixture was incubated at room temperature and ambient room light (~10 µmol m^{-2} s^{-1}) for 30 min. The sample was then divided in half, one of which was incubated with trypsin (final conc. 0.1 mg/mL) for 20 minutes on ice, and then quenched with trypsin inhibitor (final conc. 0.2 mg/mL). The other half was the negative control. After protease treatment, chloroplasts were recovered by centrifugation using a 40% percoll cushion, resuspended in lysis buffer (25 mM HEPES-KOH, 4.0 mM $MgCl_2$, pH 8.0), and centrifuged to fractionate into total soluble (S) and total membranes (P). Fractions were analyzed using SDS-PAGE, followed by fluorography and exposure to X-ray film.

FIGURES AND TABLES

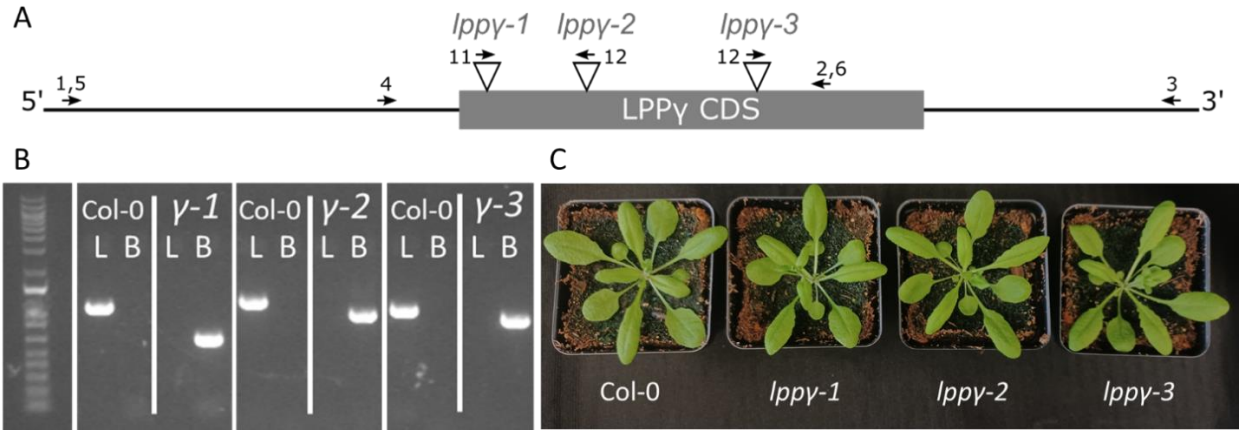

Figure 2.1. Insertional sites and genotyping primers (**A**), PCR genotyping confirmations (**B**), and growth phenotypes (**C**) of the three independent *lppγ* mutants. Pictured plants are 4 weeks old. L, left primer paired with right primer; B, insertion border primer paired with right primer; for *lppγ-1*: L, 1+2; B, 11+2; for *lppγ-2*: L, 3+4; B, 12+4; for *lppγ-3*: L, 5+6; B, 12+6; see Table 2.1 for primer descriptions and sequences.

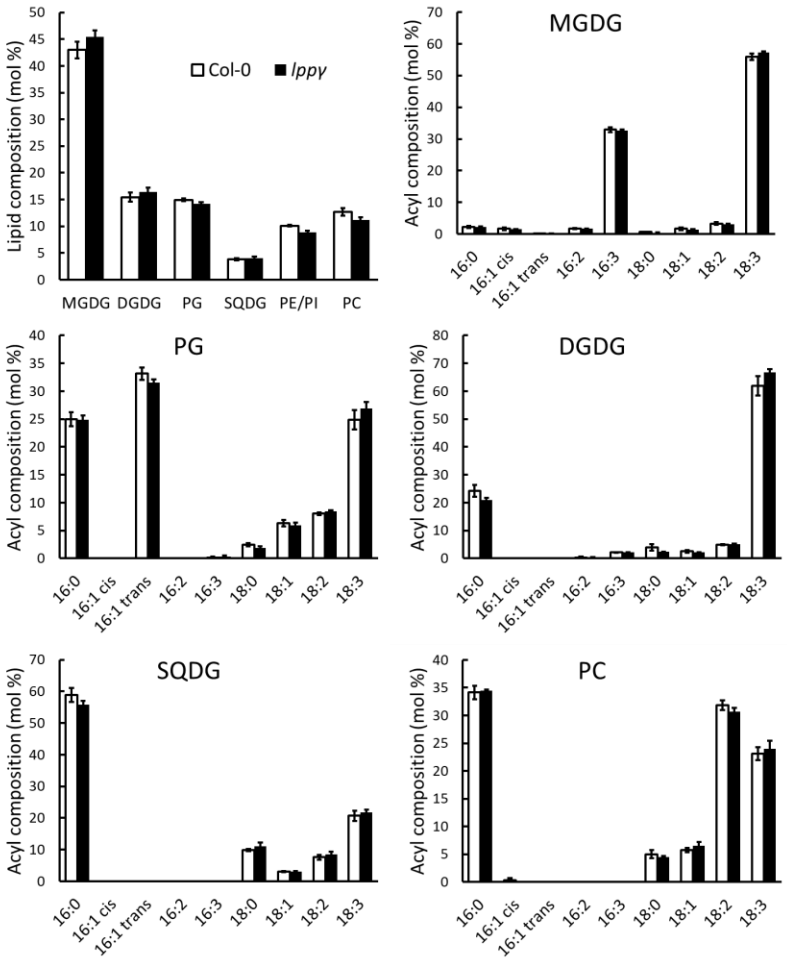

Figure 2.2. Relative lipid content and acyl composition of major membrane lipids in *lppγ*. MGDG, monogalactosyldiacylglycerol; DGDG, digalactosyldiacylglycerol; PG, phosphatidylglycerol; SQDG, sulfoquinovosyldiacylglycerol; PE, phosphatidylethanolamine; PI, phosphatidylinositol; PC, phosphatidylcholine. Three biological replicates; bars indicate standard deviation.

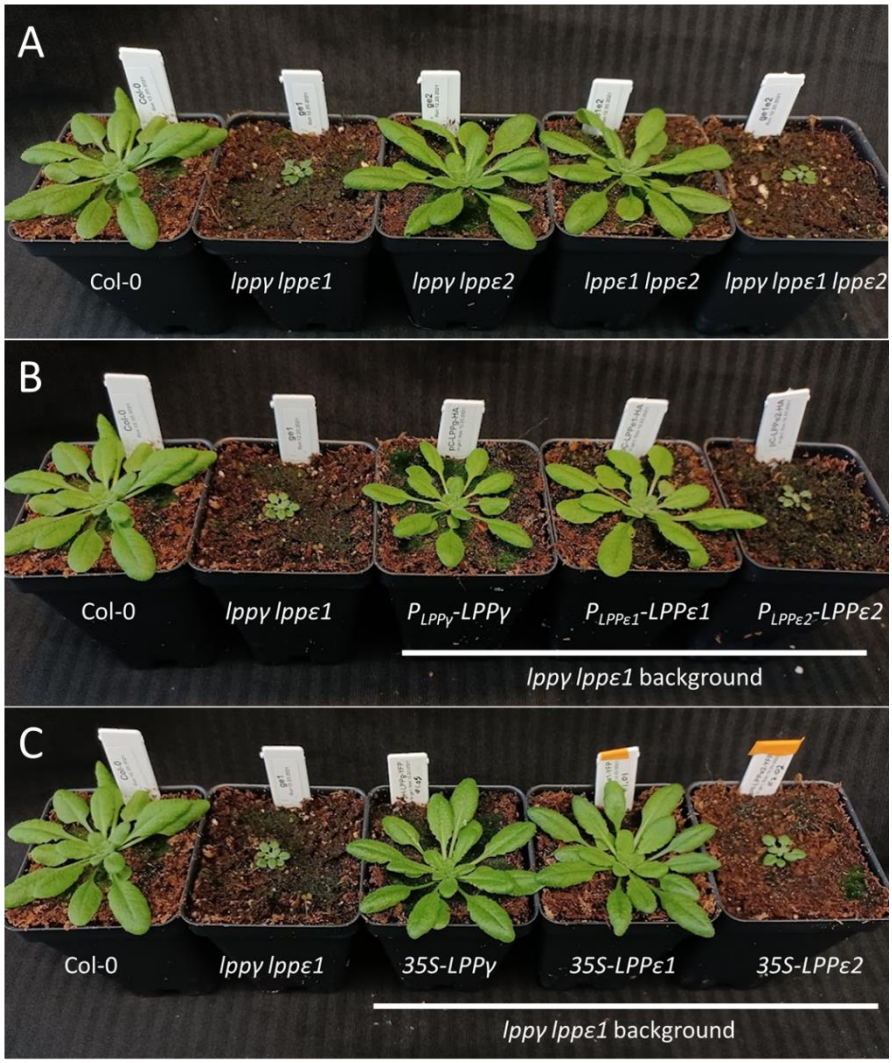

Figure 2.3. (**A**) Morphology of *lpp* double mutants and triple mutant. Complementation of *lppγ lppε1* by *LPP* genes driven by native (**B**) or overexpression (**C**) promoters. 5-week-old plants, grown in a 12/12 hr light/dark cycle.

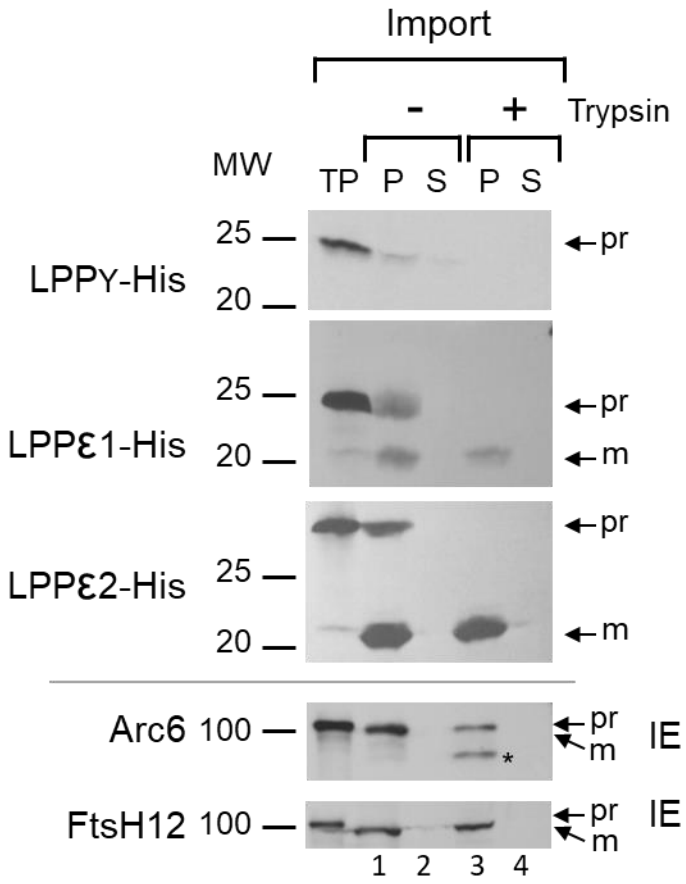

Figure 2.4. Import of ^{3}H-labeled *in vitro* translation products in isolated pea chloroplasts. Arc6 and FtsH12 are IEM-localized controls, with Arc6 containing a domain that extends into the intermembrane space, which upon digestion results in a smaller protein indicated by the asterisk. TP, translation product; P, pellet from fractionated chloroplasts; S, supernatant from fractionated chloroplasts; pr, protein prior to cleavage of transit peptide; m, mature protein; IE, inner envelope-localized. This experiment was performed by John Froehlich.

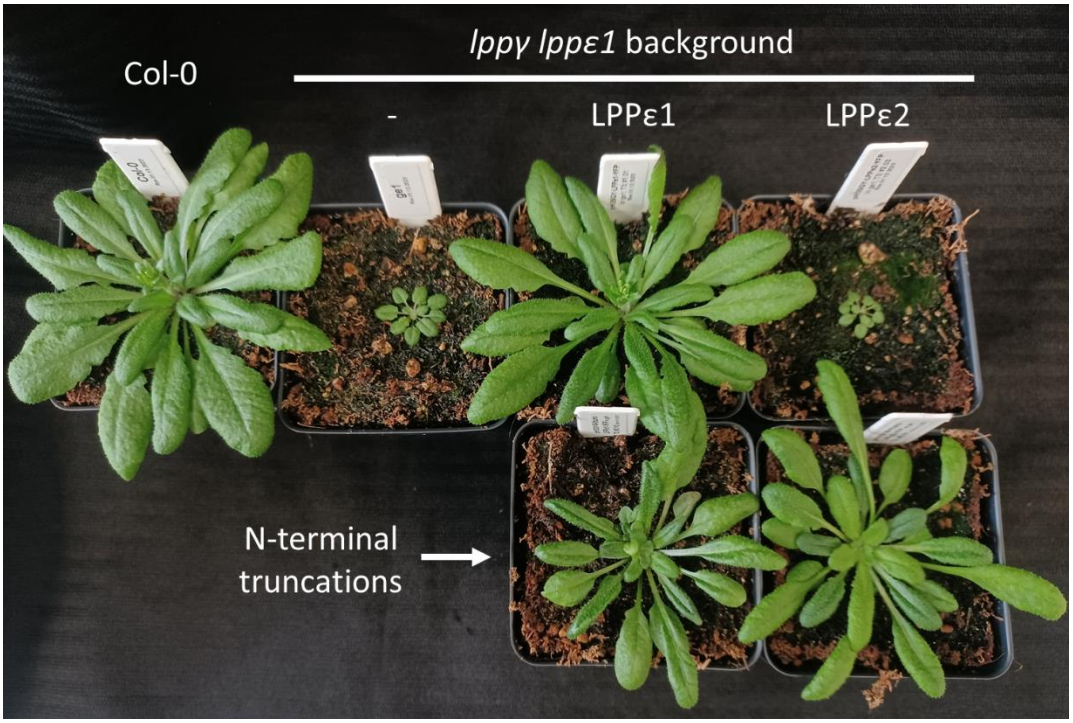

Figure 2.5. Rescue of *lppγ lppε1* phenotype with N-terminal truncations of LPPε1 and LPPε2. Genes are expressed under 35S CaMV promoter. 6-week-old plants, grown in a 12/12 hr light/dark cycle.

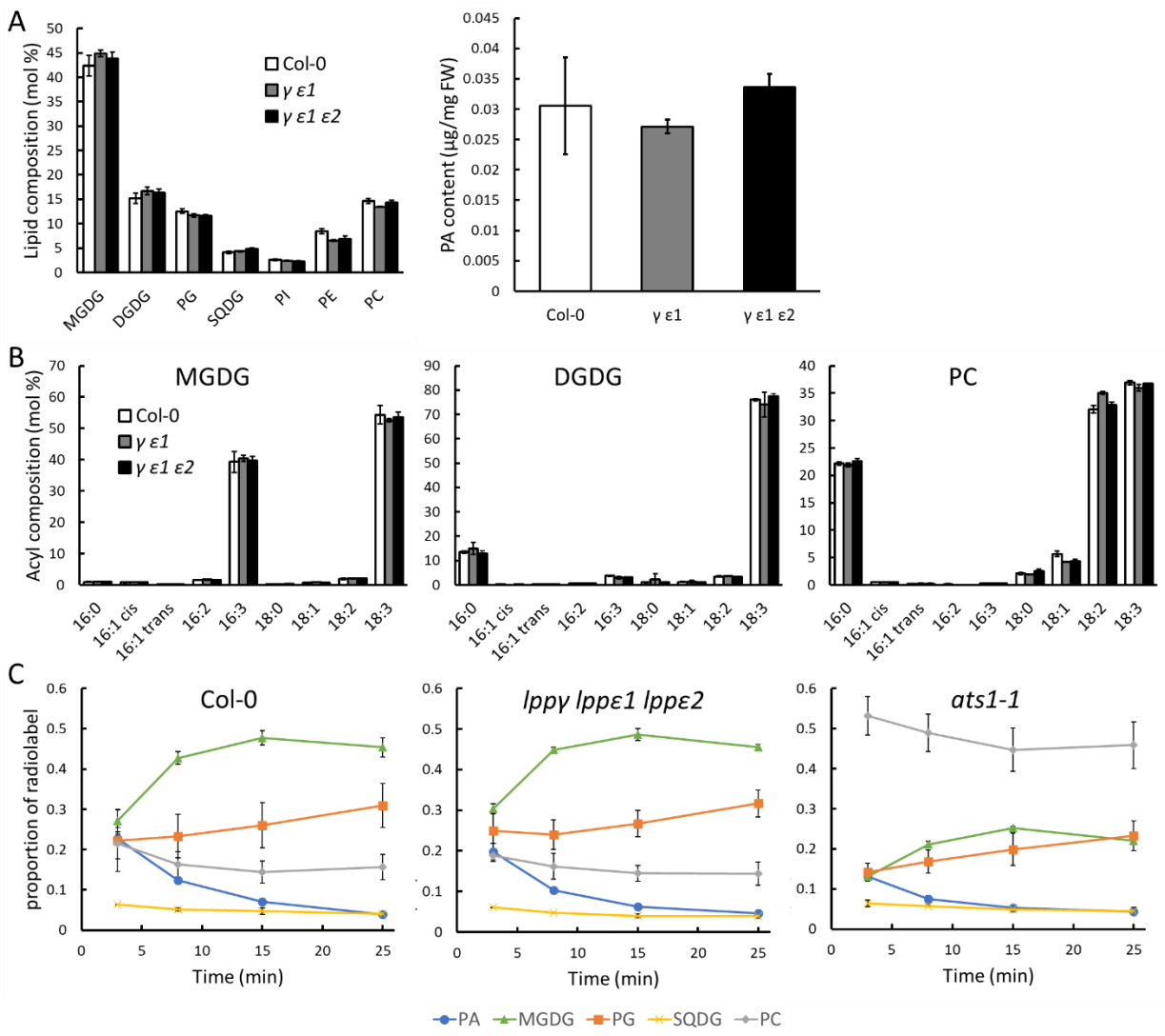

Figure 2.6. (**A**) Lipid compositions and (**B**) lipid acyl compositions of *lppγ lppε1* and *lppγ lppε1 lppε2*. (**C**) Relative incorporation of radioactivity into membrane lipids in isolated chloroplasts fed with ^{14}C-acetate. MGDG, monogalactosyldiacylglycerol; DGDG, digalactosyldiacylglycerol; PG, phosphatidylglycerol; SQDG, sulfoquinovosyldiacylglycerol; PE, phosphatidylethanolamine; PI, phosphatidylinositol; PC, phosphatidylcholine. Three biological replicates; bars indicate standard deviation.

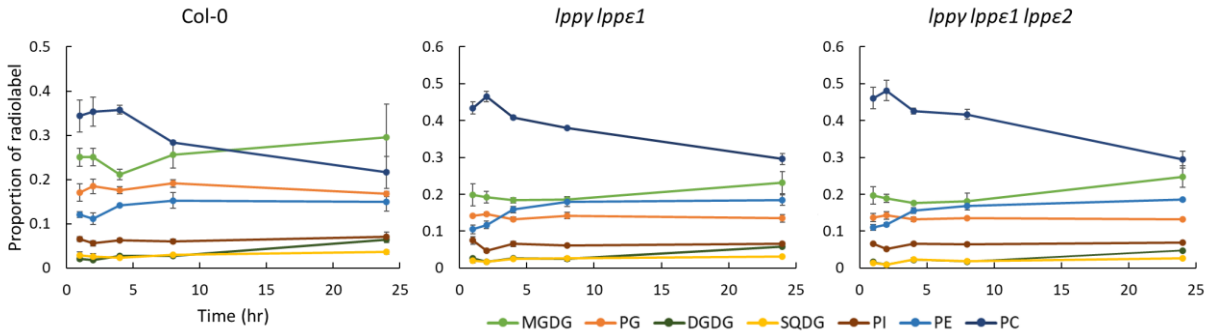

Figure 2.7. Relative incorporation of radioactivity to membrane lipids in leaves after feeding with ^{14}C-acetate. x-axis represents time after removal of radioactive acetate. MGDG, monogalactosyldiacylglycerol; PG, phosphatidylglycerol; DGDG, digalactosyldiacylglycerol; SQDG, sulfoquinovosyldiacylglycerol; PI, phosphatidylinositol; PE, phosphatidylethanolamine; PC, phosphatidylcholine. Three biological replicates; bars indicate standard deviation.

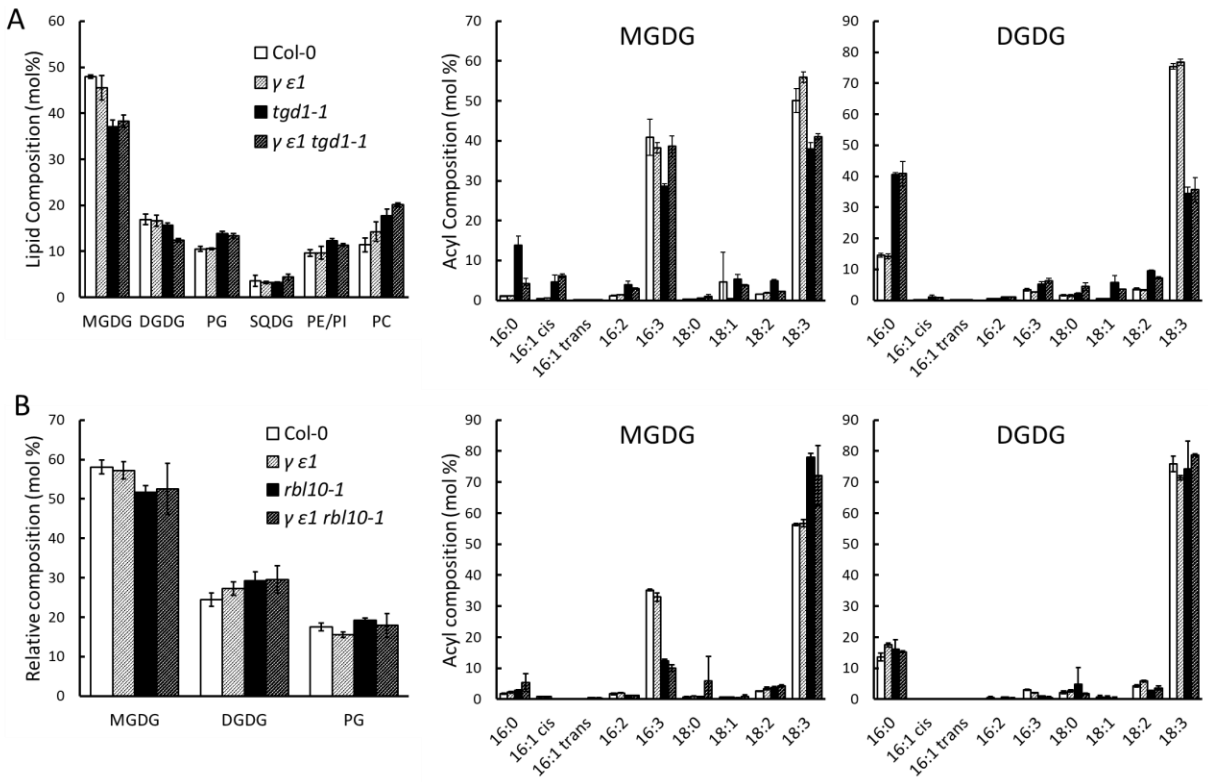

Figure 2.8. Relative lipid content and galactolipid acyl compositions of (A) *lppγ lppε1 tgd1-1* and (B) *lppγ lppε1 rbl10-1*. MGDG, monogalactosyldiacylglycerol; PG, phosphatidylglycerol; DGDG, digalactosyldiacylglycerol; SQDG, sulfoquinovosyldiacylglycerol; PI, phosphatidylinositol; PE, phosphatidylethanolamine; PC, phosphatidylcholine. Three biological replicates; bars indicate standard deviation.

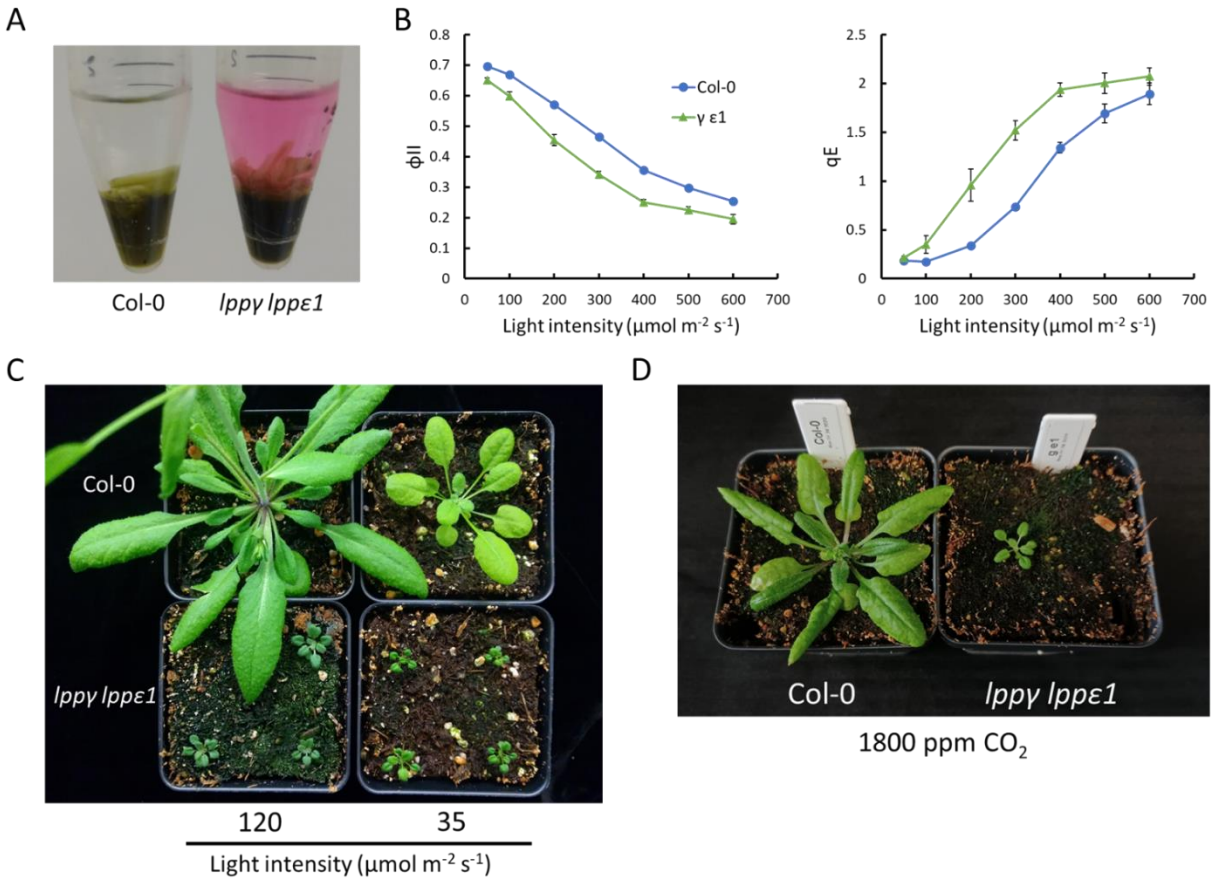

Figure 2.9. (**A**) Anthocyanin in aqueous phase in extract from Col-0 vs *lppγ lppε1*. (**B**) Photosystem II efficiency (ϕII) and energy-dependent quenching (qE) in Col-0 vs *lppγ lppε1*. (**C**) Growth of Col-0 vs *lppγ lppε1* under low light. (D) Growth of Col-0 vs l*ppγ lppε1* at elevated CO_2. Three biological replicates; bars indicate standard deviation.

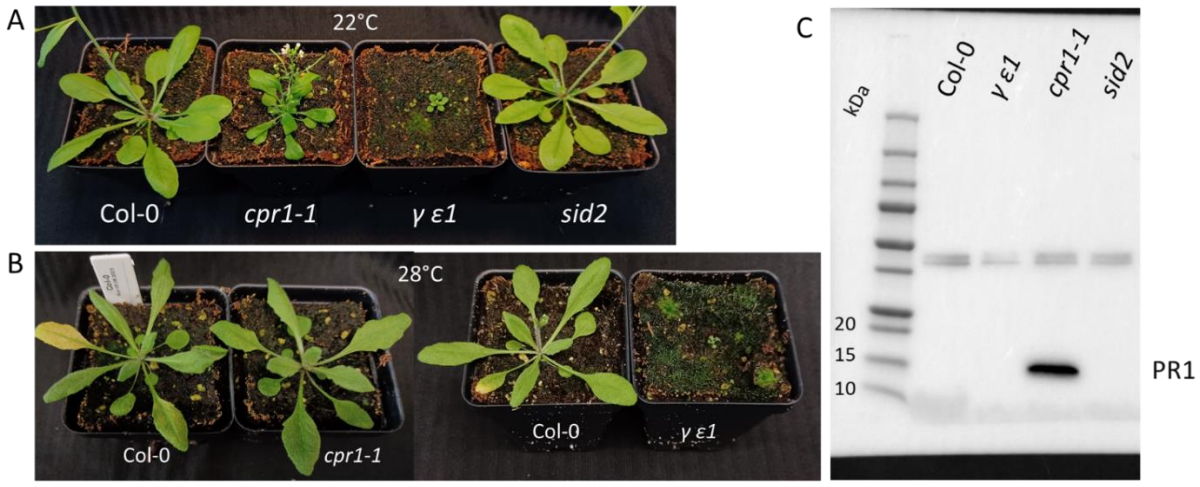

Figure 2.10. Growth of *lppγ lppε1* compared with constitutive SA mutant *cpr1-1* or SA-deficient mutant *sid2-2* at (**A**) 22°C and (**B**) 28°C. Plants are approximately 4 weeks old. (**C**) Probing of the SA response factor PR1 in *lppγ lppε1* compared with wild-type and SA mutant controls.

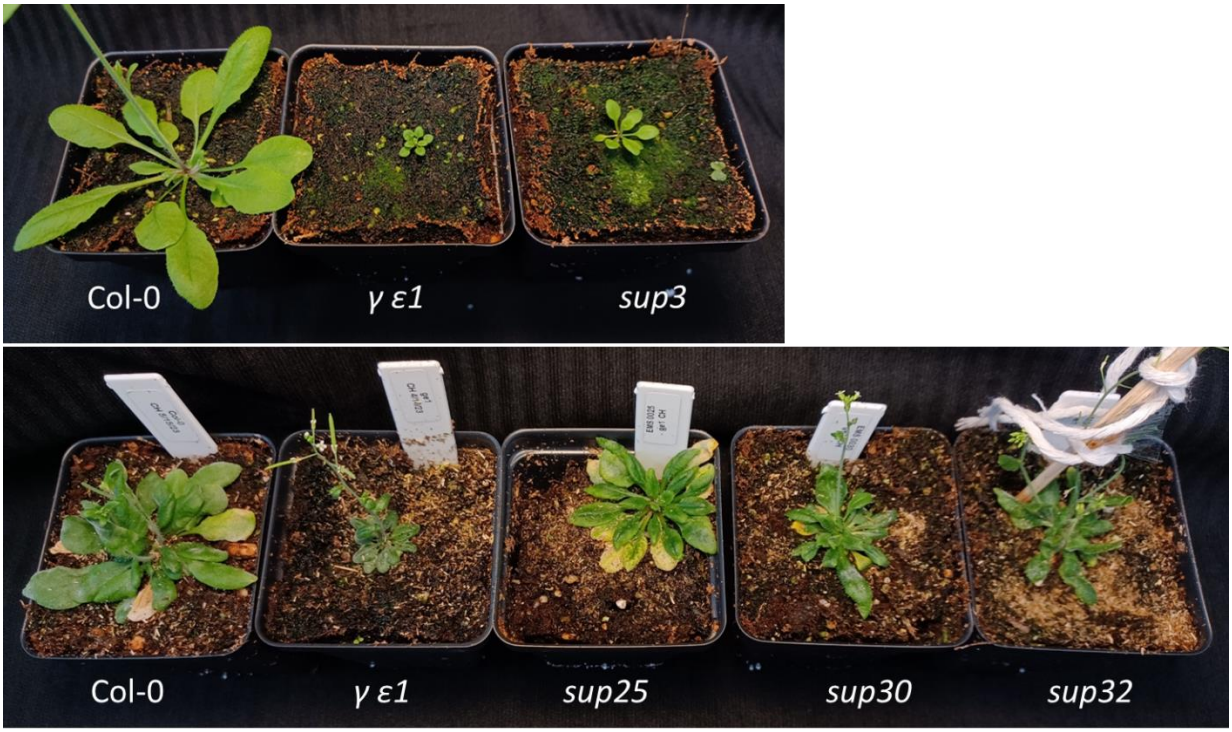

Figure 2.11. Suppressor mutants of *lppγ lppε1*. Plants in the upper panel are approximately 4 weeks old, plants in lower panel are 5-8 weeks old.

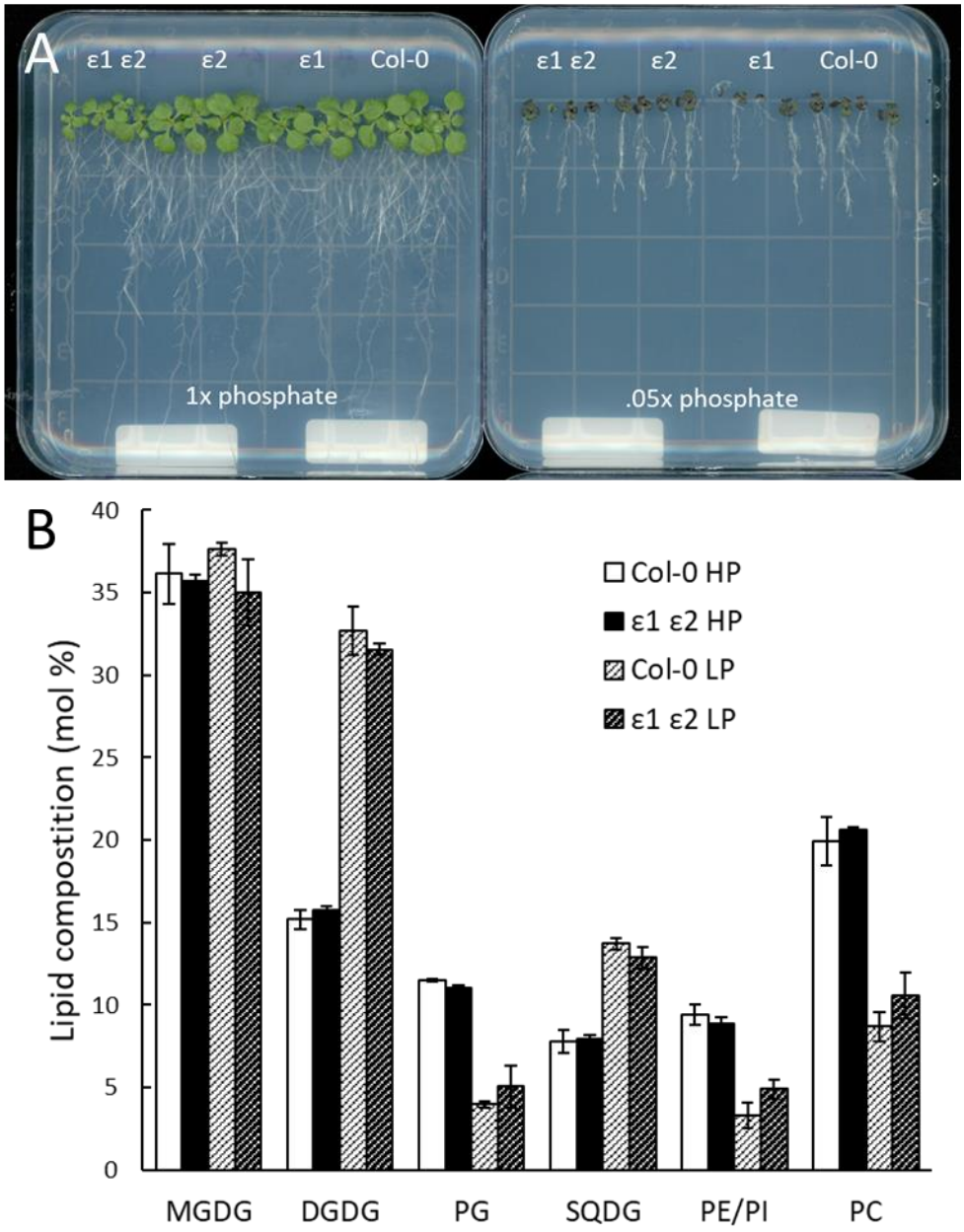

Figure 2.12. Effect of low phosphate on growth (**A**) and lipid profile (**B**) of *lppε* mutants. HP, 1x phosphate; LP, 0.05x phosphate; MGDG, monogalactosyldiacylglycerol; DGDG, digalactosyldiacylglycerol; PG, phosphatidylglycerol; SQDG, sulfoquinovosyldiacylglycerol; PE, phosphatidylethanolamine; PI, phosphatidylinositol; PC, phosphatidylcholine. Three biological replicates; bars indicate standard deviation.

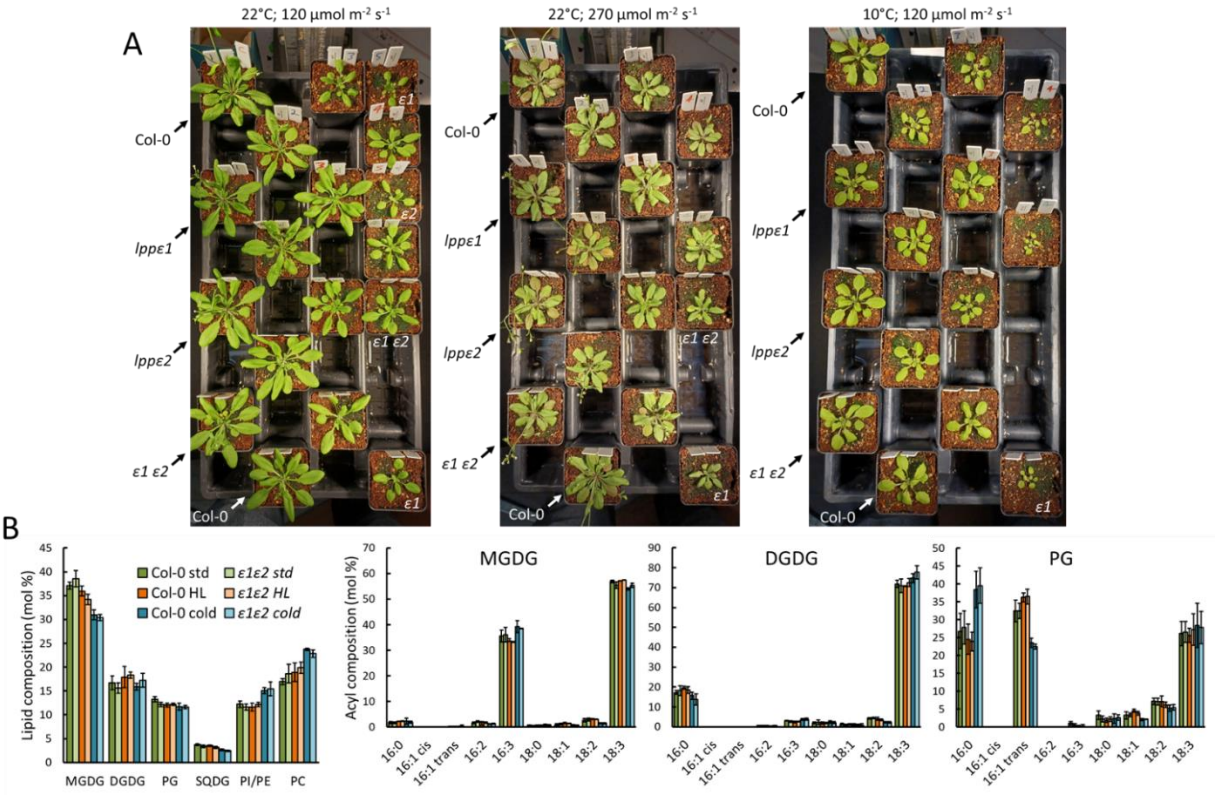

Figure 2.13. (A) Size and morphology of *lppε* mutants after one week at high light or low temperature. (B) Lipid composition and acyl compositions of major chloroplast lipids in *lppε* mutants at high light or low temperature. Std, standard light and temperature (22°C, 120 µmol m^{-2} s^{-1} photons); HL, high light (270 µmol m^{-2} s^{-1} photons); cold, 10°C. Three biological replicates; bars indicate standard deviation.

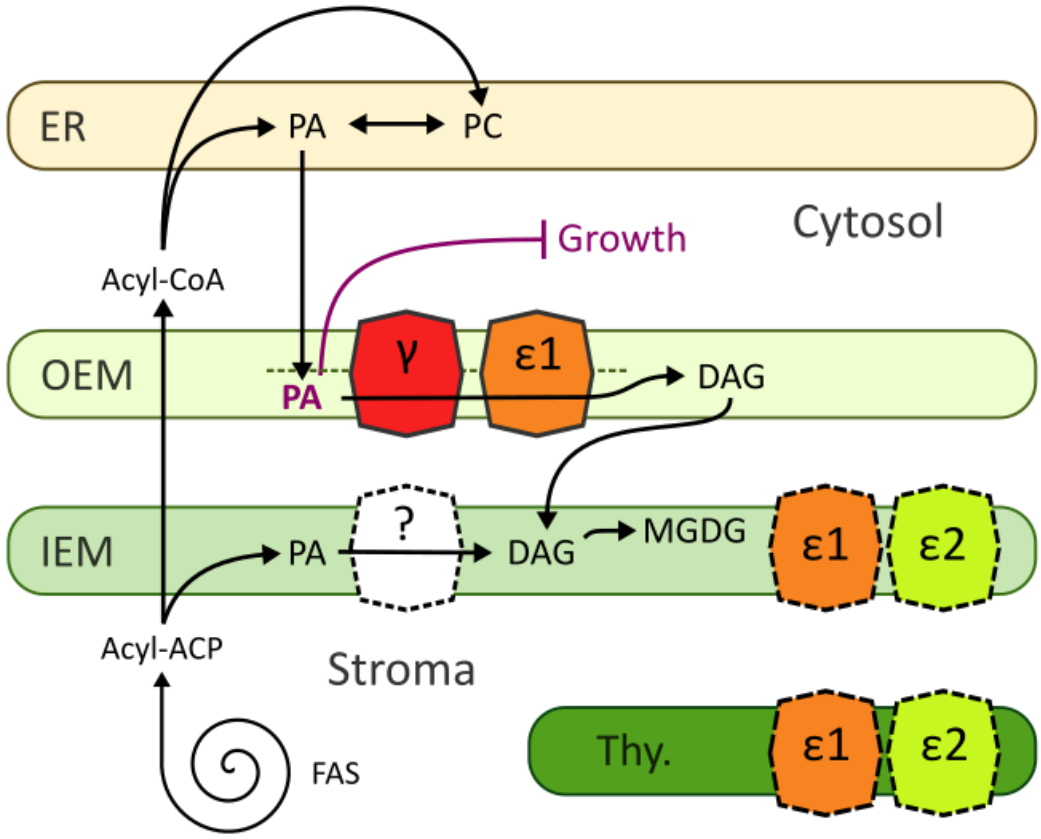

Figure 2.14. Model illustrating the localizations and activities of chloroplast LPPs, denoted by their Greek letters. Dotted lines represent uncertain localization. The unknown RBL10-dependent PA phosphatase is represented by a white box and question mark. Bolded "PA" in purple represents PA at the inner leaflet of the outer envelope, which may have an inhibitory effect on plant growth. ACP, acyl carrier protein; CoA, coenzyme A; DAG, diacylglycerol; ER, endoplasmic reticulum; FAS, fatty acid synthesis; IEM, chloroplast inner envelope membrane; MGDG, monogalactosyldiacylglycerol; OEM, chloroplast outer envelope membrane; PA, phosphatidic acid; PC, phosphatidylcholine; Thy, thylakoid membranes.

No.	Primer Sequence	Description
1	CCATTGAAGAAGCTTGAGCAC	*lppγ-1* genotyping left primer
2	ACCAACTCGCACCAACAATAC	*lppγ-1* genotyping right primer
3	ATGGAATCTCCCATCTCCTTG	*lppγ-2* genotyping left primer
4	CACTTTTCCGTCACTTTCTCG	*lppγ-2* genotyping right primer
5	CCATTGAAGAAGCTTGAGCAC	*lppγ-3* genotyping left primer
6	ACCAACTCGCACCAACAATAC	*lppγ-3* genotyping right primer
7	TCTGTTGATACCAGAGGTGGC	*lppε1* genotyping left primer
8	GGATCGATTTCGAATTCTGCT	*lppε1* genotyping right primer
9	CAAGAGAGTTCCAAGTTACA	*lppε2* genotyping left primer
10	GAATCGTTTGATTTGACTTATAG	*lppε2* genotyping right primer
11	GCCTTTTCAGAAATGGATAAATAGCCTTGCTTCC	LB1 genotyping border primer, paired with right primer for *lppγ-1*
12	ATTTTGCCGATTTCGGAAC	LBb1.3 genotyping border primer, paired with right primers of *lppγ-2*, *lppγ-3*, *lppε1*, and *lppε2*
13	CACCATGGACCTAATACCTCAGC	*LPPγ* for cloning to pENTR, forward
14	ATCAGATTTAGCAGAATCCATATC	*LPPγ*, no stop, reverse
15	TTAATCAGATTTAGCAGAATCC	*LPPγ*, stop, reverse
16	CACCATGGCAGCGTCGTCTTC	*LPPε1* for cloning to pENTR, forward
17	TCTCTCGTCTTTGAACCAGTT	*LPPε1*, no stop, reverse
18	TTATCTCTCGTCTTTGAACCAG	*LPPε1*, stop, reverse
19	CACCATGGCAGCGTCATCATCTTC	*LPPε2* for cloning to pENTR, forward
20	TCTGTCATCTTTAAACCAGTTAAG	*LPPε2*, no stop, reverse
21	TCATCTGTCATCTTTAAACCAG	*LPPε2*, stop, reverse
22	CTGAAGGCGCGCcaaaattgaacaatagaatatc	*LPPγ* 2 kb upstream forward, with AscI,
23	GTCAAGTCGACttgcattgaagcttgttcctag	*LPPγ* genomic reverse, with SalI
24	CTGAAGGCGCGCCaaaatcaaccaaaaaacctaaacc	*LPPε1* 2 kb upstream forward, with AscI,
25	GTCAAGTCGACttgattttaacaaacgggctctg	*LPPε1* genomic reverse, with SalI
26	CTGAAGGCGCGCCataacgatatctcggccggac	*LPPε2* 2 kb upstream forward, with AscI,
27	GTCAAGTCGActatggatgtatggttgatctgc	*LPPε2* genomic reverse, with SalI
28	ATGACCGTTAAAAGATTCTCTAG	LPPε1 alternative start for 51-residue N-terminal truncation, for use with NEB Q5 SDM kit, forward
29	ATGGCCGATTTGGTTAAAACCAATG	LPPε2 alternative start for 59-residue N-terminal truncation, for use with NEB Q5 SDM kit, forward
30	GGTGAAGGGGGCGGCCGC	pENTR/D-TOPO immediate upstream, for use with NEB Q5 SDM kit, reverse

Table 2.1. Primers used for cloning of *LPP* genes, and genotyping of *lpp* mutants.

REFERENCES

1. Block, M.A., et al., *Preparation and characterization of membrane fractions enriched in outer and inner envelope membranes from spinach chloroplasts. II. Biochemical characterization.* J. Biol. Chem., 1983. **258**(21): p. 13281-13286.

2. Mackender, R. and R.M. Leech, *The Galactolipid, Phospholipid, and Fatty Acid Composition of the Chloroplast Envelope Membranes of Vicia faba. L.* Plant Physiol., 1974. **53**(3): p. 496-502.

3. Dörmann, P. and C. Benning, *Galactolipids rule in seed plants.* Trends Plant Sci., 2002. **7**(3): p. 112-118.

4. Mongrand, S., et al., *The C16: 3\C18: 3 fatty acid balance in photosynthetic tissues from 468 plant species.* Phytochemistry, 1998. **49**(4): p. 1049-1064.

5. Andrews, J. and K. Keegstra, *Acyl-CoA synthetase is located in the outer membrane and acyl-CoA thioesterase in the inner membrane of pea chloroplast envelopes.* Plant Physiol., 1983. **72**(3): p. 735-740.

6. Löhden, I. and M. Frentzen, *Role of plastidial acyl-acyl carrier protein: glycerol 3-phosphate acyltransferase and acyl-acyl carrier protein hydrolase in channelling the acyl flux through the prokaryotic and eukaryotic pathway.* Planta, 1988. **176**(4): p. 506-512.

7. Hares, W. and M. Frentzen, *Properties of the microsomal acyl-CoA: sn-1-acyl-glycerol-3-phosphate acyltransferase from spinach (Spinacia oleracea L.) leaves.* J. Plant Physiol., 1987. **131**(1-2): p. 49-59.

8. Roston, R.L., et al., *TGD1,-2, and-3 proteins involved in lipid trafficking form ATP-binding cassette (ABC) transporter with multiple substrate-binding proteins.* J. Biol. Chem., 2012. **287**(25): p. 21406-21415.

9. Xu, C., et al., *Mutation of the TGD1 chloroplast envelope protein affects phosphatidate metabolism in Arabidopsis.* Plant Cell, 2005. **17**(11): p. 3094-110.

10. Jarvis, P., et al., *Galactolipid deficiency and abnormal chloroplast development in the Arabidopsis MGD synthase 1 mutant.* Proc. Natl. Acad. Sci. U.S.A., 2000. **97**(14): p. 8175-8179.

11. Miège, C., et al., *Biochemical and topological properties of type A MGDG synthase, a spinach chloroplast envelope enzyme catalyzing the synthesis of both prokaryotic and eukaryotic MGDG.* Eur. J. Biochem., 1999. **265**(3): p. 990-1001.

12. Shimojima, M., et al., *Cloning of the gene for monogalactosyldiacylglycerol synthase and its evolutionary origin.* Proc. Natl. Acad. Sci. U.S.A., 1997. **94**(1): p. 333-337.

13. Bertrams, M. and E. Heinz, *Positional Specificity and Fatty Acid Selectivity of Purified sn-Glycerol 3-Phosphate Acyltransferases from Chloroplasts.* Plant Physiol., 1981. **68**(3): p. 653-657.

14. Kunst, L. and C. Somerville, *Altered regulation of lipid biosynthesis in a mutant of Arabidopsis deficient in chloroplast glycerol-3-phosphate acyltransferase activity.* Proc. Natl. Acad. Sci. U.S.A., 1988. **85**(12): p. 4143-4147.

15. Yu, B., et al., *Loss of plastidic lysophosphatidic acid acyltransferase causes embryo-lethality in Arabidopsis.* Plant Cell Physiol., 2004. **45**(5): p. 503-510.

16. Frentzen, M., et al., *Specificities and Selectivities of Glycerol-3-Phosphate Acyltransferase and Monoacylglycerol-3-Phosphate Acyltransferase from Pea and Spinach Chloroplasts.* Eur. J. Biochem., 1983. **129**(3): p. 629-636.

17. Nakamura, Y., et al., *Arabidopsis lipins mediate eukaryotic pathway of lipid metabolism and cope critically with phosphate starvation.* Proc. Natl. Acad. Sci. U.S.A., 2009. **106**(49): p. 20978-20983.

18. Nakamura, Y., M. Tsuchiya, and H. Ohta, *Plastidic phosphatidic acid phosphatases identified in a distinct subfamily of lipid phosphate phosphatases with prokaryotic origin.* J. Biol. Chem., 2007. **282**(39): p. 29013-21.

19. Nguyen, V.C. and Y. Nakamura, *Distinctly localized lipid phosphate phosphatases mediate endoplasmic reticulum glycerolipid metabolism in Arabidopsis.* Plant Cell, 2023. **35**(5): p. 1548-1571.

20. Sato, N. and K. Awai, *"Prokaryotic Pathway" Is Not Prokaryotic: Noncyanobacterial Origin of the Chloroplast Lipid Biosynthetic Pathway Revealed by Comprehensive Phylogenomic Analysis.* Genome Biol. Evol., 2017. **9**(11): p. 3162-3178.

21. Lavell, A., et al., *A predicted plastid rhomboid protease affects phosphatidic acid metabolism in Arabidopsis thaliana.* Plant J., 2019. **99**(5): p. 978-987.

22. Karki, N., B.S. Johnson, and P.D. Bates, *Metabolically distinct pools of phosphatidylcholine are involved in trafficking of fatty acids out of and into the chloroplast for membrane production.* Plant Cell, 2019. **31**(11): p. 2768-2788.

23. Xu, C., et al., *A permease-like protein involved in ER to thylakoid lipid transfer in Arabidopsis.* EMBO J., 2003. **22**(10): p. 2370-2379.

24. Xu, C., et al., *Lipid trafficking between the endoplasmic reticulum and the plastid in Arabidopsis requires the extraplastidic TGD4 protein.* Plant Cell, 2008. **20**(8): p. 2190-2204.

25. Wang, Z., C. Xu, and C. Benning, *TGD4 involved in endoplasmic reticulum-to-chloroplast lipid trafficking is a phosphatidic acid binding protein.* Plant J., 2012. **70**(4): p. 614-623.

26. Fan, J., et al., *Arabidopsis TRIGALACTOSYLDIACYLGLYCEROL5 interacts with TGD1, TGD2, and TGD4 to facilitate lipid transfer from the endoplasmic reticulum to plastids.* Plant Cell, 2015. **27**(10): p. 2941-2955.

27. Dörmann, P., et al., *Isolation and characterization of an Arabidopsis mutant deficient in the thylakoid lipid digalactosyl diacylglycerol.* Plant Cell, 1995. **7**(11): p. 1801-1810.

28. Lin, Y.T., et al., *Reduced Biosynthesis of Digalactosyldiacylglycerol, a Major Chloroplast Membrane Lipid, Leads to Oxylipin Overproduction and Phloem Cap Lignification in Arabidopsis.* Plant Cell, 2016. **28**(1): p. 219-32.

29. Wang, K., et al., *A Plastid Phosphatidylglycerol Lipase Contributes to the Export of Acyl Groups from Plastids for Seed Oil Biosynthesis.* Plant Cell, 2017. **29**(7): p. 1678-1696.

30. Wang, K., et al., *Two Abscisic Acid-Responsive Plastid Lipase Genes Involved in Jasmonic Acid Biosynthesis in Arabidopsis thaliana.* Plant Cell, 2018. **30**(5): p. 1006-1022.

31. Bowling, S.A., et al., *A mutation in Arabidopsis that leads to constitutive expression of systemic acquired resistance.* Plant Cell, 1994. **6**(12): p. 1845-1857.

32. Van Wersch, R., X. Li, and Y. Zhang, *Mighty dwarfs: Arabidopsis autoimmune mutants and their usages in genetic dissection of plant immunity.* Front. Plant Sci., 2016. **7**: p. 1717.

33. Wildermuth, M.C., et al., *Isochorismate synthase is required to synthesize salicylic acid for plant defence.* Nature, 2001. **414**(6863): p. 562-565.

34. Cook, R., J. Lupette, and C. Benning, *The role of chloroplast membrane lipid metabolism in plant environmental responses.* Cells, 2021. **10**(3): p. 706.

35. Kunst, L., J. Browse, and C. Somerville, *A mutant of Arabidopsis deficient in desaturation of palmitic acid in leaf lipids.* Plant Physiol., 1989. **90**(3): p. 943-947.

36. Heilmann, I., et al., *Identification of the Arabidopsis palmitoyl-monogalactosyldiacylglycerol Δ7-desaturase gene FAD5, and effects of plastidial retargeting of Arabidopsis desaturases on the fad5 mutant phenotype.* Plant Physiol., 2004. **136**(4): p. 4237-4245.

37. Awai, K., et al., *A phosphatidic acid-binding protein of the chloroplast inner envelope membrane involved in lipid trafficking.* Proc. Natl. Acad. Sci. U.S.A., 2006. **103**(28): p. 10817-10822.

38. Lu, B., et al., *A Small ATPase Protein ofArabidopsis, TGD3, Involved in Chloroplast Lipid Import.* J. Biol. Chem., 2007. **282**(49): p. 35945-35953.

39. Muthan, B., et al., *Probing Arabidopsis chloroplast diacylglycerol pools by selectively targeting bacterial diacylglycerol kinase to suborganellar membranes.* Plant Physiol., 2013. **163**(1): p. 61-74.

40. Sessions, A., et al., *A High-Throughput Arabidopsis Reverse Genetics System.* Plant Cell, 2002. **14**(12): p. 2985-2994.

41. Alonso, J.M., et al., *Genome-Wide Insertional Mutagenesis of Arabidopsis thaliana.* Science, 2003. **301**(5633): p. 653-657.

42. Alonso, J.M., et al., *Genome-wide insertional mutagenesis of Arabidopsis thaliana.* Science, 2003. **301**(5633): p. 653-657.

43. Cook, R., *How to cross Arabidopsis thaliana*. 2021: YouTube. https://www.youtube.com/watch?v=0Tvkco9fa-E&ab_channel=roncook9.

44. Murashige, T. and F. Skoog, *A revised medium for rapid growth and bio assays with tobacco tissue cultures.* Physiol. Plant., 1962. **15**(3): p. 473-497.

45. Kubo, M., et al., *Transcription switches for protoxylem and metaxylem vessel formation.* Genes Dev., 2005. **19**(16): p. 1855-1860.

46. Logemann, E., et al., *An improved method for preparing Agrobacterium cells that simplifies the Arabidopsis transformation protocol.* Plant Methods, 2006. **2**(1): p. 1-5.

47. Wang, Z. and C. Benning, *Arabidopsis thaliana polar glycerolipid profiling by thin layer chromatography (TLC) coupled with gas-liquid chromatography (GLC).* J. Vis. Exp., 2011(49): p. e2518.

48. Aronsson, H. and P. Jarvis, *A simple method for isolating import-competent Arabidopsis chloroplasts.* FEBS Lett., 2002. **529**(2-3): p. 215-220.

49. Arnon, D.I., *Copper enzymes in isolated chloroplasts. Polyphenoloxidase in Beta vulgaris.* Plant Physiol., 1949. **24**(1): p. 1-15.

50. Cruz, J.A., et al., *Dynamic environmental photosynthetic imaging reveals emergent phenotypes.* Cell Syst., 2016. **2**(6): p. 365-377.

51. Baker, N.R. and K. Oxborough, *Chlorophyll fluorescence as a probe of photosynthetic productivity*, in *Chlorophyll a Fluorescence: A Signature of Photosynthesis*. 2004. p. 66-79.

52. Froehlich, J., *Studying Arabidopsis Envelope Protein Localization and Topology Using Thermolysin and Trypsin Proteases*, in *Chloroplast Research in Arabidopsis: Methods and Protocols*, R.P. Jarvis, Editor. 2011, Humana Press: Totowa, NJ. p. 351-367.

CHAPTER 3:

A suppressor screen targeting novel components of OPDA conversion to jasmonic acid

---

EMS mutagenesis of seeds was performed by Linda Danhof. Portions of this chapter have been published in Liu et al. 2021 [1]. My contribution to the published work was to optimize the growth and screening protocol, and provide instructional videos for students on seed sowing and plant crossing.

Abstract

Fatty acid export from chloroplasts is basal to plant lipid metabolism, and it is a complex process due to the amphipathic nature of the mobile molecule, and the multiple organic and aqueous barriers it must cross. Here, a forward genetic screen was implemented in the background of a transgenic Arabidopsis line, *PLIP3*-OX, that excessively produces and exports the fatty acid derivative 12-oxo-phytodienoic acid (OPDA). Because cytosolic OPDA is efficiently converted into the defense hormone jasmonic acid (JA), *PLIP3*-OX plants have a distinctive JA-induced morphological phenotype that is dependent on OPDA production, export, and conversion. To identify plants with impaired OPDA export capacity, mutagenized *PLIP3*-OX plants were screened for suppression of the JA-induced phenotype. Two lines isolated from the screen were determined to exhibit *PLIP3*-OX suppression due to mutations in *KEG4* and *CDK8*. KEG4 may be involved in abscisic acid (ABA)-JA signal coordination by stabilizing a transcriptional repressor of the JA response, while targeting activators of the ABA response for degradation; CDK8 is likely itself a transcriptional activator of JA response genes.

Introduction

Nearly all fatty acid (FA) biosynthesis in plants occurs in the chloroplast stroma, and FA export from the chloroplast feeds the various lipid pathways in the plant cell. Free FAs generated in the stroma must cross two envelope membranes and an aqueous intermembrane space, a process complicated by their amphipathic nature (Fig. 3.1). FA export therefore cannot depend on diffusion alone, and protein factors must be involved in transport [2]. However, because FA export is essential for plant viability, null mutants of FA export factors would be lethal and therefore difficult to identify.

The chloroplast inner envelope membrane (IEM) transporter FAX1 has been characterized as a component of the FA export machinery, with *fax1* null mutants retaining much of their transport capacity, and exhibiting various mild phenotypes such as reduced cuticle deposition and a higher 16:3 acyl content of MGDG [3]. It is therefore not surprising that FAX1 was identified using a reverse genetic approach, rather than through a phenotype-driven genetic screen. Subsequent research on FAX1 homologs identified IEM FA transporters FAX2-4, with FAX3 operating in

vegetative tissues alongside FAX1 [4-6]. While these may account for much or all of the FA transport across the IEM, factors facilitating transfer across the intermembrane space and outer envelope membrane (OEM) are still unknown. Because FA export is the basis for a metabolic network that is both extensive and essential, forward genetic approaches could miss null mutants due to lethality, while potentially overlooking reduced-function mutants with indistinct phenotypes.

Chloroplast FA export is not limited to the precursors of glycerolipids and cuticular constituents, but also includes various FA-derived oxylipins which are involved in environmental responses [7]. Among these, chloroplast-derived 12-oxo-phytodienoic acid (OPDA) is exported as part of the jasmonic acid (JA) biosynthetic pathway [8]. As an FA derivative, OPDA faces the same physical constraints that require export mediation, namely a charged carboxyl end which must cross two hydrophobic membranes, and a hydrocarbon tail which must dissociate from membranes and cross the intermembrane space. While an OEM OPDA transporter, JASSY, has been identified, proteins required for OPDA transport across the IEM and intermembrane space remain undetermined [9].

18:3 FA precursors can be directed towards OPDA production by lipase activity, which releases the linolenoyl substrates from glycerolipids [10]. Such lipases include the plastid lipases PLIP1, PLIP2, and PLIP3, which contribute to excess OPDA production and conversion to JA in *PLIP*-OX transgenic Arabidopsis plants (Fig. 3.2) [11, 12]. The distinctive JA-induced phenotype of these plants includes stunted growth, altered relative dimensions of leaves and petioles, and anthocyanin accumulation in vascular tissues (Fig. 3.3). The clarity of this phenotype makes it a strong background for suppressor screening, and because the phenotype depends on OPDA export, a suppressor screen may uncover mutants in OPDA or general FA transport. Therefore, a suppressor screen in the *PLIP3*-OX transgenic background was designed and implemented to discover new factors in OPDA or FA export, in a forward genetic approach that had previously been unfeasible.

Results

Screen design and preparation

Of the three described *PLIP* overexpression lines, *PLIP1*-OX has the mildest JA phenotype, *PLIP2*-OX has the most severe phenotype, which severely limits seed production, and *PLIP3*-OX has an intermediate phenotype, which is clearly distinguishable from the wild type while maintaining reproductive capacity [11, 12]. *PLIP3*-OX was therefore chosen as the background for mutant suppressor screening.

PLIP3-OX seeds were previously mutagenized with ethyl methanesulfonate (EMS), grown, allowed to self-fertilize, and M2 seeds were harvested in 96 separate batches. M2 plants were screened visually for suppression. Initially, vertical plates were considered as an option for visual screening. However, *PLIP3*-OX plants do not exhibit a strong JA-induced phenotype in early stages of growth, rendering plate screening unfeasible (Fig. 3.4). EMS mutants were therefore grown in soil, with visual screening taking place at approximately four weeks after sowing.

Primary screen

The primary screen for *PLIP3*-OX suppressor mutants was performed according to the following visual criteria: rosette diameter relative to Col-0, anthocyanin content and distribution, ratio of leaf length to petiole length, and ratio of leaf length to leaf width. Approximate values for these parameters in Col-0, PLIP3-OX, and suppressor mutants are provided in Table 3.1. Inflorescence apical dominance, plant fertility, and leaf color were also noted, though not used as selection criteria. Plants were selected for secondary screening if a stronger resemblance to wild type than *PLIP3*-OX was observed in two or more of these characteristics. Selected plants that were ultimately sequenced are shown in Fig. 3.3. In total, approximately 5000 plants were screened visually, with 90 mutants selected for secondary screening.

Integration of primary screen into a lab course

Primary screening was also integrated into a Course-based Undergraduate Research Experience (CURE) [1]. Undergraduate students enrolled in an entry-level biology laboratory course engaged in sowing Arabidopsis seeds, maintaining plants, characterizing the phenotypes of Col-0 and

PLIP3-OX controls, and screening for suppressor mutants. After selecting the mutants, students used PCR analysis to confirm the presence of the *PLIP3*-OX transgene in the suppressor lines. Mutants were then independently analyzed according to the previously described criteria, and suppressor lines meeting these criteria were chosen for secondary screening. In total, approximately 1200 of the ~5000 visually screened plants were screened by undergraduates through CURE, yielding 17 of the 90 mutants carried into secondary screening.

Secondary screen

Mutants isolated from the primary screen may show suppression due to various causes, beyond the targeted defects in OPDA export. These are expected to include mutants in OPDA biosynthesis, JA perception, and downstream JA signaling. In order to mitigate these possibilities, a secondary screen was implemented in which OPDA, JA, and the JA catabolite 12-OH JA were directly quantified. Mutants lacking OPDA were discounted as OPDA biosynthetic mutants, and mutants retaining high JA were discounted as defective in JA perception or downstream signaling. Out of the 90 mutants screened, 23 were determined to have non-zero levels of OPDA, and lower levels of JA than *PLIP3*-OX. Results of the JA metabolite concentrations are shown in Table 3.2. The 23 suppressor mutants passing the secondary screen were designated candidates for OPDA export, appropriate for subsequent mutation mapping.

Candidates were back-crossed to *PLIP3*-OX, and the F1 phenotype was monitored to determine whether mutations were dominant, semi-dominant, or recessive. F2 seeds were harvested separately for each F1 plant and used in subsequent F2 segregation analyses and mutation mapping.

Whole genome sequencing and mutation mapping

Mutants with recessive suppression alleles were prioritized for mapping. These were determined based on an unsuppressed *PLIP3*-OX phenotype in the F1 backcross to *PLIP3*-OX, and one-quarter or fewer F2 plants showing *PLIP3*-OX suppression. Four such mutants were selected: *sup11*, *sup12*, *sup53*, and *sup72*, as these had clear phenotypes, sufficient seeds, and recessive suppression alleles (Fig. 3.3). For each, the segregating F2 population from the *PLIP3*-OX backcross was grown, and gDNA extracted from individual plants showing suppression and background

phenotypes. The extracted gDNA was pooled based on phenotype, with each suppressor or background pool consisting of DNA from 30-200 plants. Pooled gDNA was submitted for whole genome sequencing, and results were analyzed using the SIMPLE pipeline developed for causal mutation mapping [13]. Plots generated by SIMPLE remove uncorrelated mutations, and then use LOESS smoothing when plotting the remaining mutations [13]. This provides an accessible visualization of the region containing the causal mutation, shown for each mutant in Fig. 3.5. Lists of potential causal mutations in Tables 3.3-3.6. Causal gene candidates were pursued further for the suppressor mutants *sup72* and *sup11*.

A mutation in KEG may lead to PLIP3-OX suppression in sup72

Sequencing data analysis for *sup72* indicated co-segregation of *PLIP3*-OX suppression with a cytosine to thymine base substitution, at nucleotide position 4369 in the coding sequence of *KEEP ON GOING* (*KEG*). The substitution corresponds to a change of the histidine residue at position 1457 to tyrosine. KEG is a RING-type E3 ligase, with a negative regulatory role in the abscisic acid (ABA) and JA signaling pathways [14, 15]. It is composed of RING and ankyrin domains, a kinase domain, and a C-terminal domain of 12 HERC2-like repeats [14]. The H1457Y mutation is in the 10th HERC2-like repeat and may alter the protein-protein interactions associated with the HERC2-like domain. A previous study on the mutant *keg-4* had determined that alterations to the HERC2-like domain increases the repressive role of KEG in the ABA pathway, and it is therefore likely that a similar effect is witnessed in *sup72* with respect to JA signaling [16].

A mutation in CDK8 leads to PLIP3-OX suppression in sup11

Sequencing data analysis for *sup11* showed co-segregation of *PLIP3*-OX suppression with the introduction of an early stop codon to the gene *CDK8*, corresponding to residue position 149. Unpublished data from the Howe lab demonstrates a similar suppression of the *jazD* phenotype by mutation of *CDK8*. The *jazD* phenotype resembles that of *PLIP3*-OX, as it lacks ten transcriptional repressors of JA response genes [17]. *cdk8* suppression of *jazD* indicates that CDK8 has an important role in driving expression of JA response genes, and the elimination of CDK8 in *sup11* likely results in the same suppression.

In order to test whether the mutation of *CDK8* was indeed causal for *PLIP3*-OX phenotypic suppression, *sup11* was crossed to a null *cdk8* insertional mutant (SALK_138675). The F1 generation, which is heterozygous for the *PLIP3*-OX transgene, showed suppression for *cdk8* x *sup11*, while the control cross of *cdk8* x *PLIP3*-OX background retained the JA response phenotype (Fig. 3.6). These F1 results confirm that two non-functional alleles of *CDK8* suppress the JA response in *PLIP3*-OX, while one functional *CDK8* allele is sufficient to maintain the response.

Crosses of insertional mutants of candidate genes to sup12 and sup53 will determine causal mutations

While suppressor mutants *sup12* and *sup53* have been sequenced, the co-segregating mutations do not include obvious candidates for suppression. Causal mutations for suppression will be determined by crossing the suppressor mutant to insertional mutants for each of the co-segregating altered genes. The cross in which the insertional mutant is in the same gene as the causal suppressor mutation will appear suppressed in the F1 generation, while the others should retain the *PLIP3*-OX phenotype.

Discussion

Primary screen and course integration

Based on the mutants identified, the visual primary screen was effective in targeting JA-related genes. The distinct phenotypes allow for rapid identification of suppressor mutants, in a manner accessible to contributors who are otherwise unexperienced with Arabidopsis. Thus, integration of the primary screen with a lab course was successful, and undergraduate students were able to identify promising suppression phenotypes. In fact, primary screening continued solely through CURE would be sufficient for providing future mutants, as the downstream backcrossing, growing, sequencing, and analysis of selected candidates represent a more significant bottleneck than the initial screen. The CURE also provided the Benning lab with opportunities to recognize and recruit capable undergraduates. From the undergraduate perspective, direct exposure to an academic research project was useful in gauging their interest in a future academic career.

Secondary screen

The purpose of the secondary screen was to eliminate mutants deficient in OPDA biosynthesis or JA perception and downstream signaling, thereby narrowing the candidate pool to mutants deficient in the conversion of OPDA to JA. This was accomplished by measuring OPDA and JA levels in the plants and eliminating mutants that appeared to accumulate high JA or no OPDA. While the secondary screen was successful in reducing the number of candidates from 90 to 23, the results from *sup11* and *sup72* indicate that false positives do pass through secondary screening. Both of the presumed causative mutations in these suppressors affect expression of JA response genes, rather than JA biosynthesis. False positives are likely a result of the variability in the JA response values, which was witnessed in both wild-type and *PLIP3*-OX controls included in each batch of hormone quantification. While it is not ideal for such off-target mutants to pass through secondary screening, false positives may be preferable to elimination of true JA biosynthetic mutants.

KEG mutation in sup72 likely results in greater JAZ12 *stability and repression of the JA response*

The substitution in *sup72* results in a single residue change from histidine to tyrosine at the 10th HERC2-like repeat in the C-terminal domain of KEG. The full protein is composed of an N-terminal RING-HCa domain, a kinase domain, and ankyrin repeats, followed by the HERC2-like repeats, and its repressive role in the ABA pathway is essential for plant viability [14]. In the absence of ABA, KEG maintains low levels of the transcriptional activator ABSCISIC ACID INSENSITIVE 5 (ABI5) by continually ubiquitinating ABI5. In response to ABA, KEG self-ubiquitinates, allowing ABI5 to accumulate and activate the ABA response [18, 19]. Early development is therefore arrested in null *keg* mutants, due to excess ABA signaling, while *KEG* overexpression results in reduced ABA sensitivity [14, 18]. However, the *keg-4* mutant, which contains a substitution in the 5th HERC2-like repeat, exhibits low ABA sensitivity rather than hypersensitivity [16]. Comparative localization of native and mutant KEG revealed that in *keg-4*, the protein is less strongly associated with the trans-Golgi network (TGN) and more abundant in the cytosol, indicating that the HERC2-like domain helps to sequester the protein at the TGN, where KEG is less effective in repression of the ABA response [20]. More recently, KEG has been implicated in JA signaling, as the JA response

repressor JAZ12 is stabilized through interaction with the HERC2-like domain of KEG, and *KEG* overexpression protected JAZ12 from degradation [15].

In this context, there are two likely models for KEG-mediated suppression of the JA response in *sup72*. In the first, the mutation in the HERC2-like domain of KEG in *sup72* directly affects the interaction of KEG and JAZ12, in such a way as to increase the stability and repressive role of the JAZ repressor. While this is the most straightforward explanation, the *keg-4* phenotype would suggest that a more general role of the HERC2-like domain in subcellular targeting could be affected in *sup72*. If the effect of an altered HERC2-like domain in *sup72* is comparable to that of *keg-4*, the increase in cytosolic KEG would amplify its repressive role in the ABA pathway through increased degradation of ABI5, and similarly repress the JA response due to increased interactions with JAZ12 (Fig. 3.7). These models can be tested by directly studying the stability of the JAZ12-KEG4 interactions, as well as determining the sensitivity of *sup72* to ABA.

CDK8 *may be involved in transcriptional activation of JA response genes*

Using a genetic approach, phenotypic suppression of *PLIP3*-OX was shown here to be caused by a nonsense mutation of *CDK8* in *sup11*. The suppression is likely the result of a muted transcriptional response to JA, as opposed to decreased JA biosynthesis. CDK8 is known to be a nuclear-localized protein, involved in activation of various stress-responsive regulatory pathways [21]. In addition, unpublished data from the Howe lab shows *cdk8* mutant suppression of the *jazD* phenotype. Because the *jazD* phenotype results from de-repression of JA response genes, and does not directly depend on JA biosynthesis, CDK8 likely acts as a positive regulator of these response genes.

Methods

Plant strains

PLIP3-OX lines had been previously developed in the Benning lab and were obtained from the lab seed stocks [12]. The *cdk8* insertional mutant, SALK_138675, was ordered from the Arabidopsis Biological Resource Center (ABRC).

EMS mutagenesis

Approximately 13,000 *PLIP3*-OX seeds were incubated in 0.1% Tween©20 (Sigma-Aldrich) for 15 minutes in a tube rotator, after which seeds were allowed to settle, and the solution was removed. 0.2% Ethyl methanesulfonate (EMS) in water was added, and seeds were incubated overnight (~16hrs) in tube rotator. Seeds were washed 7 times with water, incubated in water for 2 hours, and washed one more time.

Plant growth conditions

Plants were grown in SUREMIX™ Professional All-Purpose Perlite Mix (Michigan Grower Products, Inc.) at 22°C and a light intensity of approximately 120 µmol m^{-2} s^{-1}, under a 16/8-hr light/dark cycle in a growth chamber. Plants grown in the classroom for the CURE-based primary screen had a less stable environment as they were grown on open, lighted racks, and may have experienced some deviations from this regime.

Hormone quantification

Fresh plant tissue was harvested, flash-frozen, ground, and incubated in extraction buffer (80:20 methanol:water, 0.1% formic acid, 100 mg/L butylated hydroxytoluene) containing internal standard (100 nM abscisic acid-d6) for 24 hr at 4°C. Samples were analyzed using liquid chromatography/mass spectrometry as described [11].

Genome sequencing and analysis

Genomic DNA was isolated from segregating F2 plants using the Promega Wizard® Genomic DNA Purification Kit, and quantified using a Qubit fluorometer. Equal amounts of DNA from 30-200 plants were pooled based on phenotype, and then sent to BGI genomics for paired-end 150 Illumina sequencing, or the BGI DNBseq™ platform. At least 10 Gb was sequenced for each sample. Sequencing data was processed using the SIMPLE pipeline [13]. Modifications to the SIMPLE pipeline were made by undergraduate student Yash Manne, for compatibility with data arriving from the DNBseq™ platform.

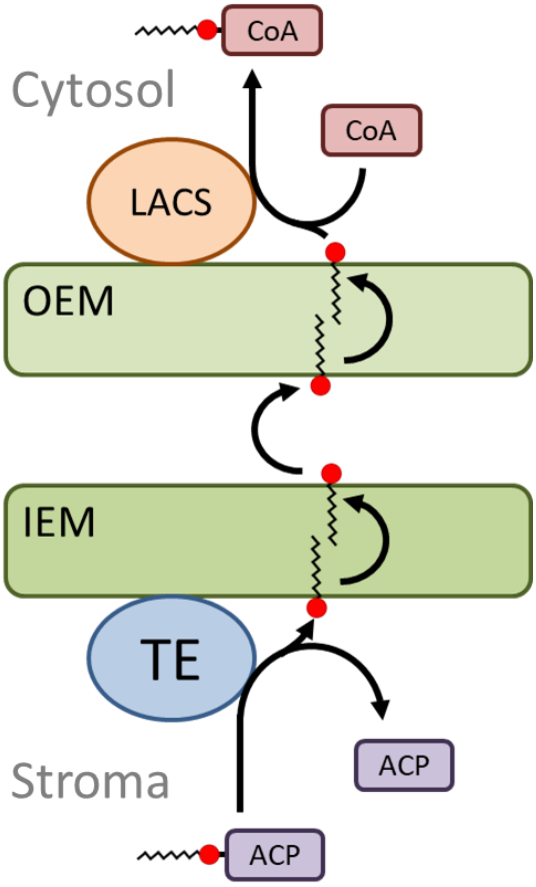

Figure 3.1. Fatty acid (FA) export from the chloroplast requires an amphipathic molecule to cross both hydrophobic membranes and an aqueous intermembrane space. This process requires facultative protein factors in order to be thermodynamically favorable. ACP, acyl carrier protein; CoA, coenzyme A; IEM, chloroplast inner envelope membrane; LACS, long-chain acyl-CoA synthetase; OEM, chloroplast outer envelope membrane; TE, thioesterase.

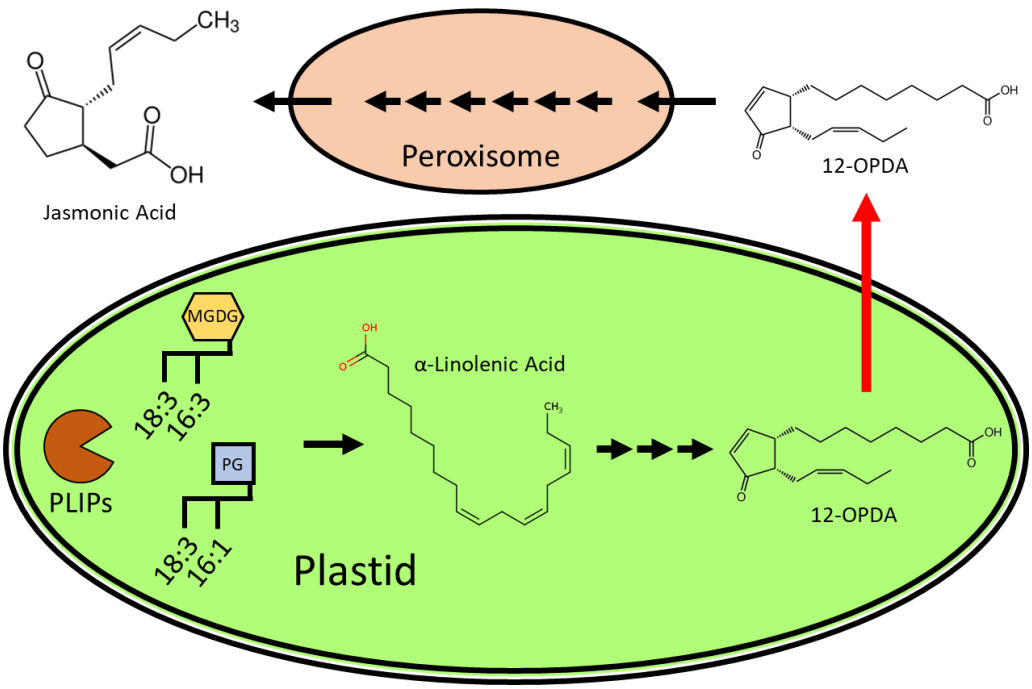

Figure 3.2. Schematic of jasmonic acid (JA) biosynthesis in plants. The red arrow represents OPDA export from the chloroplast, the primary target of the *PLIP3*-OX suppressor screen. MGDG, monogalactosyldiacylglycerol; 12-OPDA, 12-oxo-phytodienoic acid; PG, phosphatidylglycerol; PLIPs, plastid lipases.

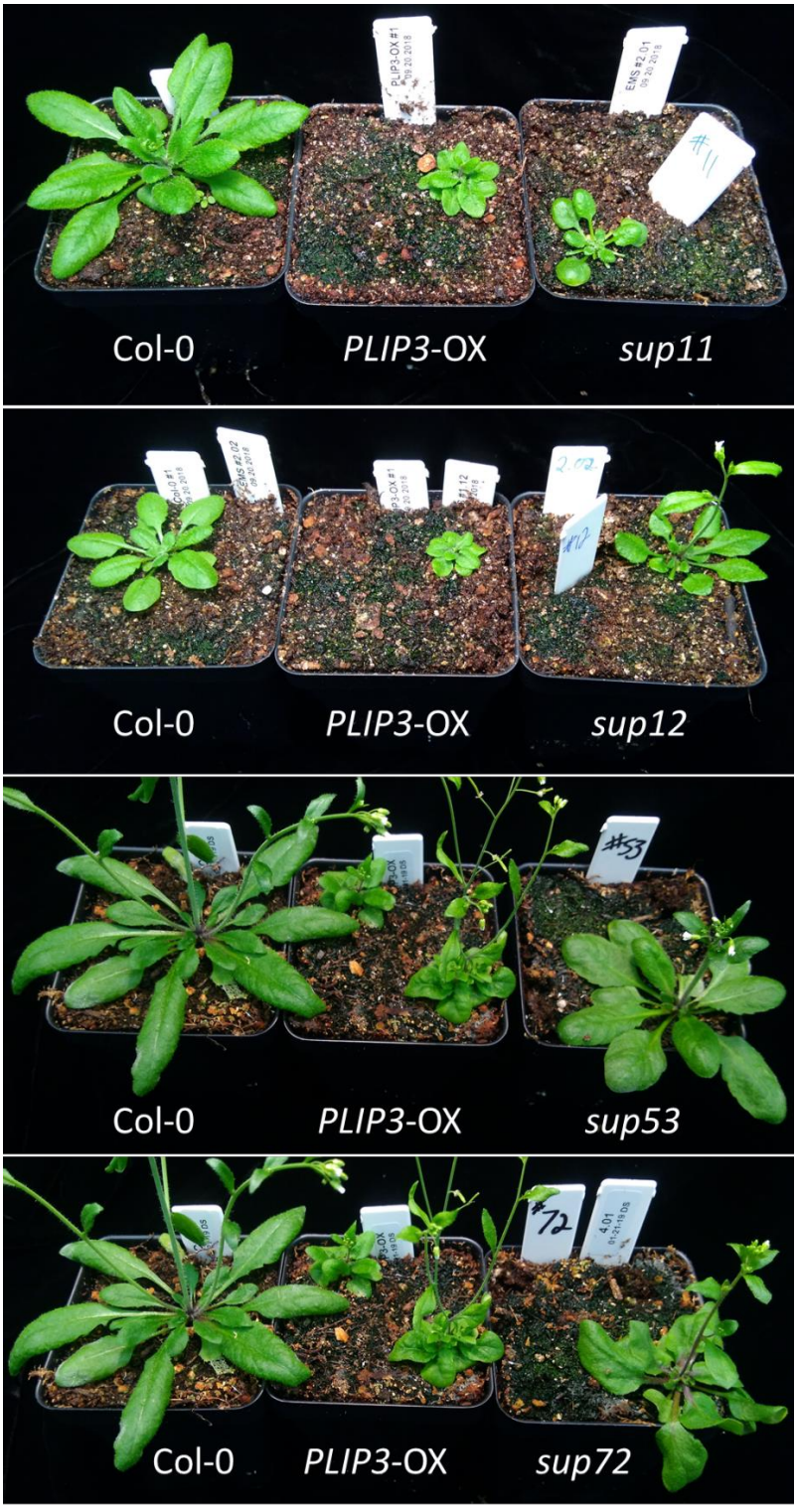

Figure 3.3. *PLIP3*-OX suppressor mutants selected for genomic sequencing. These M2 plants were backcrossed to *PLIP3*-OX, and the F2 generation was sequenced.

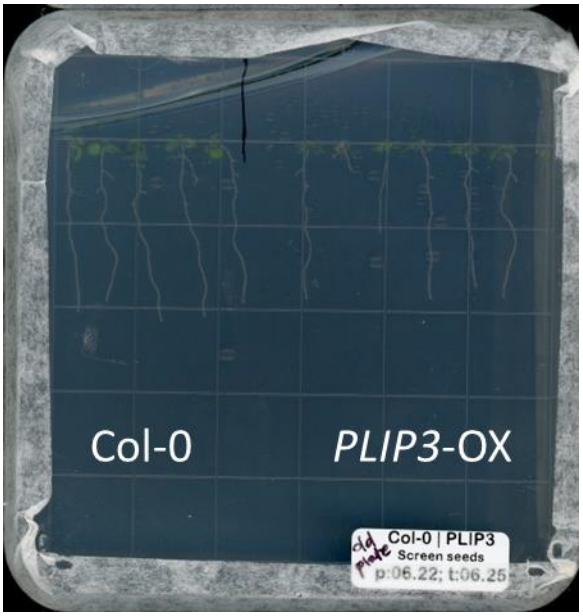

Figure 3.4. 8-day-old plants grown on vertical plates, as a test for a plate-based primary screen. The JA-induced *PLIP3*-OX phenotype does not appear in young seedlings.

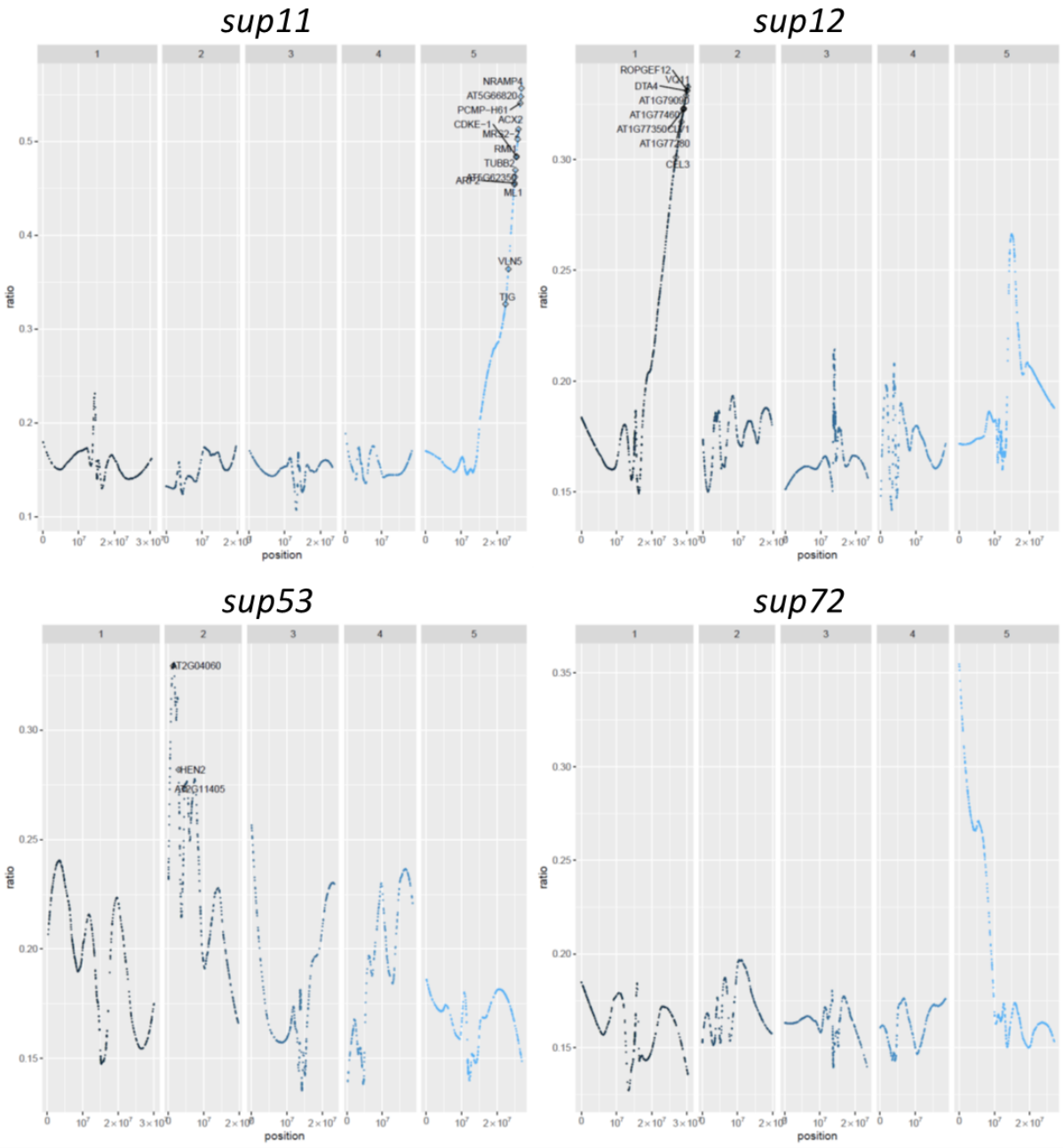

Figure 3.5. LOESS plots generated from the SIMPLE pipeline, showing chromosomal regions in which mutations co-segregate with suppression phenotypes in *sup11*, *sup12*, *sup53*, and *sup72*.

Figure 3.6. F1 generation of *sup11* crossed to *cdk8*, in which the JA-induced *PLIP3*-OX phenotype remains suppressed. In contrast, *cdk8* crossed to *PLIP3*-OX retains its JA-induced phenotype. Two independent F1 plants are shown for each cross.

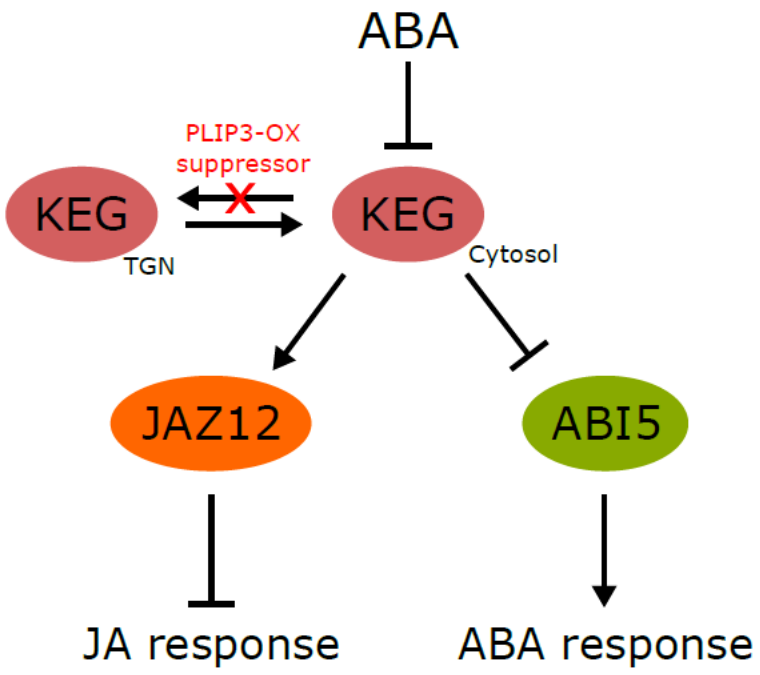

Figure 3.7. A model for *PLIP3*-OX suppression in *sup72*. A substitution in the HERC2-like domain weakens KEG association with the TGN, and the resulting higher KEG concentration at the cytosol increases stabilization of JAZ12 and subsequent repression of JA response genes.

batch date	batch #	mutant #	relative rosette diameter	anthocyanin	inflorescence apical dominance	fertility	color	leaf length: petiole length	leaf length: leaf width	notes
N/A	N/A	col-0	1.00		strong AD			2	3.00	
N/A	N/A	PLIP3-OX	0.20		weak AD			10	1.25	
08.17.2018	#1.02	1	0.75	wt distribution	near-wt AD		wt	3	1.50	
08.17.2018	#1.05	2	0.30	wt distribution	weak AD	weak	wt	?	2.00	attacked by herbivores, indistinguishible from mutant #3
08.17.2018	#1.05	3	0.30	wt distribution	weak AD	weak	wt	?	2.00	attacked by herbivores, indistinguishible from mutant #2
08.17.2018	#1.08	4	0.50	less than wt	weak-intermediate AD		slight pale	2	1.50	
08.17.2018	#1.09	5	0.40	less than wt	weak AD	yes	pale	?	2.00	bolted very early (~week2-3), and senesced early (rosette already completeley senesced at week 6). Had to harvest cauline leaves for hormone analysis
	#8.01	6				no				Seems infertile, filament doesn't elongate. Could be a JA-deficient phenotype
	#8.03	7				yes				
	#8.04	8				yes				
	#8.07	9				yes				
09.20.2018	#1.11	10	0.67	low	strong AD	yes	normal	3	1.75	
09.20.2018	#2.01	11	0.40	low -> high at later stage	strong AD	no	normal -> dark	1.5	1.50	slow to grow, slow to bolt. Only started bolting after week 7, and rosette had many more leaves. Only started bolting in week 7
09.20.2018	#2.02	12	0.80	low	strong AD	yes	normal	3	1.75	
09.20.2018	#2.02	13	0.50	low	moderate AD	yes	pale	3	1.40	
09.20.2018	#2.04	14	0.60	low	moderate AD	yes	pale	3	1.25	
09.20.2018	#2.05	15	1.00	high	strong AD	yes	dark	2	2.00	appears to retain JA phenotype with the exception of growth inhibition. Update: growth more stunted in later weeks (~5-8)
09.20.2018	#2.06	16	0.50	low		yes	slight pale	3	3.00	
09.20.2018	#2.06	17	0.40	low		yes	slight pale	2	2.00	
10.24.2018	#2.08	18	0.33	low	strong AD	yes	normal	2	1.50	
10.24.2018	#2.09	19	0.50	moderate			normal	3	3.00	slightly late to bolt
10.24.2018	#2.09	20	0.30	moderate	strong AD		normal	1.5	1.70	flat leaves, low trichome density
10.24.2018	#2.09	21	0.40	high			slight dark	3	2.00	slow to bolt
10.24.2018	#2.10	22	0.30				normal			immature?
10.24.2018	#2.10	23	0.15	high?			normal	5	1.25	JA not measured; Plant had strong JA phenotype 12/12/2018
10.24.2018	#2.11	24	0.40	low	moderate AD		normal	2	3.00	
10.24.2018	#2.11	25	0.40	low	moderate AD	yes	nomal	3	2.00	
10.24.2018	#2.11	26	0.70	low	strong AD		normal	2.5	2.50	
10.24.2018	#3.01	27	0.15	moderate			slight pale	4	1.25	JA not measured; Plant had strong JA phenotype 12/12/2018
10.24.2018	#3.01	28	0.30	low			normal	2	2.00	
10.24.2018	#3.01	29	0.25	low	moderate AD		normal	1	2.00	spindly
10.24.2018	#3.01	30	0.40	high	moderate AD	yes	slight pale?	3	2.00	
10.24.2018	#3.01	31	0.45	low	moderate AD	yes	slight dark	1.5	2.00	folded leaves
10.24.2018	#3.01	32	0.20	low			pale	2	1.50	JA not measured; Apparent recovery from JA phenotype: back-cross necessary.
11.12.2018	unknown	33	0.60	low			very pale	4	2.00	very pale plant, seed was in PLIP3-OX control vial, JA not measured
12.11.2018	#3.03	34	0.20	moderate			normal	2	1.33	
12.11.2018	#3.03	35	0.20	moderate			normal	2	1.33	
12.11.2018	#3.04	36	0.20	low	moderate AD		normal	2	1.33	
12.11.2018	#3.06	37	0.25	low	moderate AD		normal	2	1.50	crumpled, bushy leaves, looks like butter lettuce
12.11.2018	#3.07	38	0.20	low			normal	1.5	1.00	strange, smooth, few leaves, some circular others very skinny. Early senescence
12.11.2018	#3.07	39	0.25	moderate	strong AD		normal	2	2.00	spiky leaves
01.08.2019	#7.09	40								not backcrossed - too old
01.08.2019	#7.11	41				no				sterile
01.08.2019	#8.08	42								
01.08.2019	#7.04	43								
01.08.2019	#8.08	44								
01.08.2019	#8.08	45								not backcrossed
01.08.2019	#7.02	46				no				sterile
01.08.2019	#7.02	47								not backcrossed
01.08.2019	#7.05	48								no hormone measurments - sample lost
01.08.2019	#7.05	49								promising
01.08.2019	#7.05	50								too small for JA meas., too old to backcross
01.08.2019	#7.01	51								too young to backcross
01.08.2019	#7.01	52								too young to backcross
01.21.2019	#3.08	53								
01.21.2019	#3.08	54								
01.21.2019	#3.08	55								
01.21.2019	#3.09	56								
01.21.2019	#3.09	57								
01.21.2019	#3.09	58								
01.21.2019	#3.09	59								
01.21.2019	#3.09	60								
01.21.2019	#3.10	61								
01.21.2019	#3.10	62								
01.21.2019	#3.10	63								
01.21.2019	#3.10	64								
01.21.2019	#3.10	65								
01.21.2019	#3.10	66								
01.21.2019	#3.11	67								
01.21.2019	#3.11	68								
01.21.2019	#3.12	69								
01.21.2019	#3.12	70								
01.21.2019	#3.12	71								
01.21.2019	#4.01	72								
01.21.2019	#4.01	73								
02.24.2019	#4.02	74	0.40	low			normal	1.5	4.00	leaves are completely vertical, no apparent bolt for flowers as of 03.27.2019. crumpled leaf appearance
02.24.2019	#4.02	75	0.70	moderate		04.08.19: unclear	normal	3	2.00	
02.24.2019	#4.02	76	0.20	moderate			dark	1	1.00	
02.24.2019	#4.03	77	0.35	low			slight pale	2	2.00	
02.24.2019	#4.03	78	0.35	moderate			slight pale	2	1.50	
02.24.2019	#4.03	79	0.35	low			slight pale	2	1.25	
02.24.2019	#4.03	80	0.35	moderate			slight pale	1	1.30	
02.24.2019	#4.04	81	0.80	low	strong AD	04.08.19: appears sterile	pale	2	2.00	pale. 04.08.2019: similar phenotype to #83 (coi1?)
02.24.2019	#4.04	82	0.40	low			slight pale	2	1.80	
02.24.2019	#4.04	83	0.50	low		04.08.19: appears sterile	normal	2	3.00	04.08.2019: similar phenotype to #81 (coi1?)
02.24.2019	#4.04	84	0.40	moderate			slight pale	2	2.00	
02.24.2019	#4.06	85	0.25	moderate			normal	2	1.60	
02.24.2019	#4.06	86	0.25	low			slight pale	2	2.00	
02.24.2019	#4.06	87	0.30	moderate			slight pale	6	3.00	
02.24.2019	#4.07	88	0.35	low			slight pale	3	1.50	
02.24.2019	#4.07	89	0.35	low			normal	3	2.00	
02.24.2019	#4.07	90	0.60	low	strong AD	fertile	slight pale	2	2.00	

Table 3.1. Phenotypic data collected on mutants selected from visual primary screen.

			raw				total				nmol per g			
harvest date		harvest mass (g)	OPDA (nM)	JA (nM)	JA-Ile (nM)	12-OH JA (response)	OPDA (pmol)	JA (pmol)	JA-Ile (pmol)	12-OH JA (response)	OPDA	JA	JA-Ile	12-OH JA (response)
	wt	0.085	72.03874	0.2924		0.2827	57.630992	0.23392	0	0.22616	0.678	0.003	0.000	0.003
	PLIP3-OX	0.05	55.55396	1.89235		4.5056	44.443168	1.51388	0	3.60448	0.889	0.030	0.000	0.072
	#1	0.08	86.99594	3.2662	0.12569	5.4923	69.597	2.613	0.101	4.394	0.870	0.033	0.001	0.055
	#2	0.03	71.21643	11.95392		15.1647	56.973	9.563	0.000	12.132	1.899	0.319	0.000	0.404
	#3	0.044	45.98224	4.54166		26.445	36.786	3.633	0.000	21.156	0.836	0.083	0.000	0.481
	#4	0.055	82.98276	5.5287	0.1147	1.4263	66.386	4.423	0.092	1.141	1.207	0.080	0.002	0.021
	#5	0.041	36.98417	3.20263		1.6751	29.587	2.562	0.000	1.340	0.722	0.062	0.000	0.033
10.22.2018	wt	0.0487	6.7083	0.22438		0.0381	4.02498	0.134628	0	0.02286	0.083	0.003	0.000	0.000
10.22.2018	PLIP3-OX	0.0464	8.7123	3.70176	0.1847	10.1446	5.22738	2.221056	0.11082	6.08676	0.113	0.048	0.002	0.131
10.22.2018	#6	0.0125	0.4378	0.10353	0.0001	0.1378	0.26268	0.062118	0.00006	0.08268	0.021	0.005	0.000	0.007
10.22.2018	#7	0.032	1.9508	0.1212	0.1103	0.2292	2.34096	0.14544	0.13236	0.27504	0.073	0.005	0.004	0.009
10.22.2018	#8	0.0435	3.8457	2.06935	0.3455	0.1715	2.30742	1.24161	0.2073	0.1029	0.053	0.029	0.005	0.002
10.22.2018	#9	0.011	2.3625	0.11746	0.0045	2.329	1.4175	0.070476	0.0027	1.3974	0.129	0.006	0.000	0.127
10.22.2018	wt	0.0548	6.4949	0.08971	0.0025	0.0392	3.89694	0.053826	0.0015	0.02352	0.071	0.001	0.000	0.000
10.22.2018	PLIP3-OX	0.039	29.1363	1.87841	0.3664	45.8129	17.48178	1.127046	0.21984	27.48774	0.448	0.029	0.006	0.705
10.22.2018	#10	0.0463	3.315	0.26712	0.0835	0.2209	1.989	0.160272	0.0501	0.13254	0.043	0.003	0.001	0.003
10.22.2018	#11	0.0464	2.7488	0.14357	0.0078	0.0569	1.64928	0.086142	0.00468	0.03414	0.036	0.002	0.000	0.001
10.22.2018	#12	0.0483	3.8768	0.09514	0.0004	0.0349	2.32608	0.039084	0.00024	0.02094	0.052	0.001	0.000	0.000
10.22.2018	#13	0.0335	0.0903	0.0131	0.0012	0.0475	0.05418	0.00786	0.00072	0.0285	0.002	0.000	0.000	0.001
10.22.2018	#14	0.0406	1.5502	0.37421	0.2387	0.1477	0.93012	0.224526	0.14322	0.08862	0.023	0.006	0.004	0.002
10.22.2018	#15	0.0592	11.7861	0.44529	0.1627	2.7687	7.07166	0.267174	0.09762	1.66122	0.119	0.005	0.002	0.028
10.22.2018	#16	0.0423	3.3474	2.36828	0.2818	5.5637	2.00844	1.420968	0.16908	3.33822	0.047	0.034	0.004	0.079
10.22.2018	#17	0.0251	0.8033	0.02793	0.022	0.2805	0.48198	0.016758	0.0132	0.1683	0.019	0.001	0.001	0.007
12.04.2018	wt #1	0.0654	17.9026	3.20226	0.0068	1.3193	10.74156	1.921356	0.00408	0.79158	0.164	0.029	0.000	0.012
12.04.2018	wt #2	0.0541	4.4491	0.19189		0.9067	2.66946	0.115134	0	0.54402	0.049	0.002	0.000	0.010
12.04.2018	PLIP3-OX #1	0.0434	2.6228	2.3626	0.0088	2.1371	1.57368	1.41756	0.00528	1.28226	0.036	0.033	0.000	0.030
12.04.2018	PLIP3-OX #2	0.0231	2.4752	2.19751	0.0067	0.4715	1.48512	1.318506	0.00402	0.2829	0.064	0.057	0.000	0.012
12.04.2018	#18	0.0542	1.2916	0.77275	0.0028	0.4847	0.77496	0.46365	0.00168	0.29082	0.014	0.009	0.000	0.005
12.04.2018	#19	0.0497	4.2542	1.93718	0.0202	0.8285	2.55252	1.162308	0.01212	0.4971	0.051	0.023	0.000	0.010
12.04.2018	#20	0.0274	6.7092	1.21785		0.5166	4.02552	0.73071	0	0.30996	0.147	0.027	0.000	0.011
12.04.2018	#21	0.0513	4.1468	5.70458	0.0031	4.2144	2.48808	3.422748	0.00186	2.52864	0.049	0.067	0.000	0.049
12.04.2018	#22	0.0081	0.1112	0.57461	0.0022	0.0624	0.06672	0.344766	0.00132	0.03744	0.008	0.043	0.000	0.005
	#23						0	0	0	0	#DIV/0!	#DIV/0!	#DIV/0!	#DIV/0!
12.04.2018	#24	0.0451			0.0002	0.1894	0	0	0.00012	0.11364	0.000	0.000	0.000	0.003
12.04.2018	#25	0.0526	5.945	1.93372	0.0018	1.2677	3.567	1.160232	0.00108	0.76062	0.068	0.022	0.000	0.014
12.04.2018	#26	0.0394	3.8877	0.6738	0.0151	0.3326	2.33262	0.40428	0.00906	0.19956	0.059	0.010	0.000	0.005
	#27						0	0	0	0	#DIV/0!	#DIV/0!	#DIV/0!	#DIV/0!
12.04.2018	#28	0.0221	0.9739	0.36067	0.0041	0.0687	0.58434	0.216402	0.00246	0.04122	0.026	0.010	0.000	0.002
12.04.2018	#29	0.0167	0.3745	0.79272	0.0064	0.4379	0.2247	0.475632	0.00384	0.26274	0.013	0.028	0.000	0.016
12.04.2018	#30	0.0354	1.9402	2.71679	0.0634	1.4812	1.16412	1.630074	0.03804	0.88872	0.033	0.046	0.001	0.025
12.04.2018	#31	0.0489	4.4346	1.0784	0.1155	0.6942	2.66076	0.64704	0.0693	0.41652	0.054	0.013	0.001	0.009
	#32													
01.16.2019	wt #1	0.0475	112.90915	5.36159		0.1624	67.74549	3.216954	0	0.09744	1.426	0.068	0.000	0.002
01.16.2019	wt #2	0.0437	85.57158	7.03778		0.1864	51.342948	4.222668	0	0.11184	1.175	0.097	0.000	0.003
01.16.2019	PLIP3-OX #1	0.0258	98.04684	22.71287	0.0709	9.4297	58.828104	13.62772	0.04254	5.65782	2.280	0.528	0.002	0.219
01.16.2019	PLIP3-OX #2	0.0263	121.65531	60.86976	0.1904	32.6805	72.993186	36.52186	0.11424	19.6083	2.775	1.389	0.004	0.745
01.16.2019	#34	0.0295	119.75275	53.54001	0.1288	11.493	71.85165	32.12401	0.07728	6.8958	2.436	1.089	0.003	0.234
01.16.2019	#35	0.0322	39.81831	86.36901	0.096	1.736	23.890986	51.82141	0.0576	1.0416	0.742	1.609	0.002	0.032
01.16.2019	#36	0.032	58.09106	24.98605	0.0224	0.6661	34.854636	14.99163	0.01344	0.39966	1.089	0.468	0.000	0.012
01.16.2019	#37	0.0349	25.24707	13.36276	0.2349	0.061	15.148242	8.017656	0.14094	0.0366	0.434	0.230	0.004	0.001
01.16.2019	#38	0.0133	74.26895	34.82444	0.0577	9.6309	44.56137	20.89466	0.03462	5.77854	3.350	1.571	0.003	0.434
01.16.2019	#39	0.0485	74.82114	44.68281	0.2691	0.8187	44.892684	26.80969	0.16146	0.49122	0.926	0.553	0.003	0.010
02.15.2019	7.02 col-0	0.0364	195.79588	11.41731	0.0017	0.2282	117.477528	6.850386	0.00102	0.13692	3.227	0.188	0.000	0.004
02.15.2019	7.05 col-0	0.052	170.56108	3.81673	0.0034	0.013	102.336648	2.290038	0.00204	0.0078	1.968	0.044	0.000	0.000
02.15.2019	7.11 col-0	0.0302	110.3321	72.44077	1.3701	0.0961	66.19926	43.46446	0.82206	0.05766	2.192	1.439	0.027	0.002
02.15.2019	8.08 col-0	0.097	197.22041	12.21968	0.1039	0.1817	118.332246	7.331808	0.06234	0.10902	1.220	0.076	0.001	0.001
02.15.2019	7.02 PLIP3	0.0259	1281.42606	103.7661	0.2331	1.8158	768.855636	62.25968	0.13986	1.08948	29.686	2.404	0.005	0.042
02.15.2019	7.05 PLIP3	0.0299	695.74883	31.59615	0.05	10.6858	417.449298	18.95769	0.03	6.41148	13.962	0.634	0.001	0.214
02.15.2019	7.11 PLIP3	0.037	721.29385	29.99369	0.0396	8.8643	432.77631	17.99621	0.02376	5.31858	11.697	0.486	0.001	0.144
02.15.2019	8.08 PLIP3	0.0539	579.26309	96.22145	0.2413	11.3042	347.557854	57.73287	0.14478	6.78252	6.448	1.071	0.003	0.126
02.15.2019	#40	0.0345	95.4666	3.6102	0.0047	0.2765	57.27996	2.16612	0.00282	0.1659	1.660	0.063	0.000	0.005
02.15.2019	#41	0.05	1.44622	10.56269	0.0062	0.0662	0.867732	6.337614	0.00372	0.03972	0.017	0.127	0.000	0.001
02.15.2019	#42	0.0533	171.27429	60.49172	0.0824	7.8148	102.764574	36.29503	0.04944	4.68888	1.928	0.681	0.001	0.088
02.15.2019	#43	0.0385	38.73274	25.56334	0.0567	0.0159	23.239644	15.338	0.03402	0.00954	0.604	0.398	0.001	0.000
02.15.2019	#44	0.0183	49.69856	22.49813	0.1367	0.4806	29.819136	13.49888	0.08202	0.28836	1.629	0.738	0.004	0.016
02.15.2019	#45	0.02	14.01517	7.85793	0.0497	0.2807	8.409102	4.714758	0.02982	0.16842	0.420	0.236	0.001	0.008
02.15.2019	#46	0.047	1.1468	1.64607	0.0025	0.2523	0.68808	0.987642	0.0015	0.15138	0.015	0.021	0.000	0.003
02.15.2019	#47	0.0266	228.87213	140.6353	0.2343	5.3846	137.323278	84.3812	0.14058	3.23076	5.163	3.172	0.005	0.121
02.15.2019	#49	0.0375	318.36933	22.16193	0.0374		191.021598	13.29716	0.02244	0	5.094	0.355	0.001	0.000
02.15.2019	#51	0.0217	216.08026	84.97542	1.0423	0.2518	129.648156	50.98525	0.62538	0.15108	5.975	2.350	0.029	0.007
02.15.2019	#52	0.0204	210.45005	9.02369	0.0468	0.0624	126.27003	5.414214	0.02808	0.03744	6.190	0.265	0.001	0.002
02.20.2019	col-0	0.0483	226.37421	86.05322	0.5806	0.158	135.824526	51.63193	0.34836	0.0948	2.812	1.069	0.007	0.002
02.20.2019	col-0	0.0417	185.84344	9.89529	0.0209	0.126	111.506064	5.937174	0.01254	0.0756	2.674	0.142	0.000	0.002
02.20.2019	PLIP3-OX	0.0244	141.77249	119.5056	0.6842	39.5023	85.063494	71.70335	0.41052	23.70138	3.486	2.939	0.017	0.971
02.20.2019	PLIP3-OX	0.0168	61.05935	11.9301	0.0402	19.836	36.63561	7.15806	0.02412	11.9016	2.181	0.426	0.001	0.708
02.19.2019	#48	0.0167	158.39526	5.11149	0.1555	0.7013	95.037156	3.066894	0.0933	0.42078	5.691	0.184	0.006	0.025
02.20.2019	#50	0.015	26.37566	3.76101	0.0168	0.3355	15.825396	2.256606	0.01008	0.2013	1.055	0.150	0.001	0.013
02.20.2019	#53	0.0174	50.23476	7.7665	0.0094	0.0446	30.140856	4.6599	0.00564	0.02676	1.732	0.268	0.000	0.002
02.20.2019	#54	0.0296	95.25968	44.95067	0.1433	3.9033	57.155808	26.9704	0.08598	2.34198	1.931	0.911	0.003	0.079
02.20.2019	#55	0.001	10.02346	86.03486	0.0202	2.0665	6.014076	51.62092	0.01212	1.2399	6.014	51.621	0.012	1.240
02.20.2019	#56	0.0201	10.91416	14.27315	0.0491	0.1131	6.548496	8.56389	0.02946	0.06786	0.326	0.426	0.001	0.003
02.20.2019	#57	0.0192	29.99098	16.38774	0.015	3.6354	17.994588	9.832644	0.009	2.18124	0.937	0.512	0.000	0.114
02.20.2019	#58	0.0144	24.53178	4.77357	0.0009	2.3749	14.719068	2.864142	0.00054	1.42494	1.022	0.199	0.000	0.099
02.20.2019	#59	0.0102	22.90658	15.85929	0.0427	1.6005	13.743948	9.515574	0.02562	0.9603	1.347	0.933	0.003	0.094
02.20.2019	#60	0.0086	15.58063	6.64687	0.0208	0.6123	9.348378	3.988122	0.01248	0.36738	1.087	0.464	0.001	0.043
02.20.2019	#61	0.0247	14.71152	6.33016	0.0038	0.8354	8.826912	3.798096	0.00228	0.50124	0.357	0.154	0.000	0.020
02.20.2019	#62	0.0419	47.70498	108.3485	1.4091	0.1304	28.622988	65.00911	0.84546	0.07824	0.683	1.552	0.020	0.002
02.20.2019	#63	0.0095	8.07935	4.47188	0.0264	1.7166	4.84761	2.683128	0.01584	1.02996	0.510	0.282	0.002	0.108
02.20.2019	#64	0.0066	3.97369	5.83019	0.0009	0.2511	2.384214	3.498114	0.00054	0.15066	0.361	0.530	0.000	0.023
02.20.2019	#65	0.0185	12.79721	16.17166	0.0387	0.0375	7.678326	9.702996	0.02322	0.0225	0.415	0.524	0.001	0.001
02.20.2019	#66	0.0378	98.37841	22.15578	0.3563	14.2387	59.027046	13.29347	0.21378	8.54322	1.562	3.517	0.006	0.226
02.20.2019	#67	0.026	43.83424	0.85212	0.0001	0.1616	26.300544	0.511272	0.00006	0.09696	1.012	0.020	0.000	0.004
02.20.2019	#68	0.022	30.82893	18.02843	0.023	0.6749	18.497358	10.81706	0.0138	0.40494	0.841	0.492	0.001	0.018
02.20.2019	#69	0.0383	55.90096	80.16986	0.5281	0.1369	33.540576	48.10192	0.31686	0.08214	0.876	1.256	0.008	0.002
02.20.2019	#70	0.0257	17.80209	22.44234	0.0679	0.6237	10.681254	13.4654	0.04074	0.37422	0.416	0.524	0.002	0.015
02.20.2019	#71	0.0326	121.20451	30.66939	0.0853	3.1245	72.722706	18.40163	0.05118	1.8747	2.231	0.564	0.002	0.058
02.20.2019	#72	0.0367	56.49604	13.26511	0.0034	0.123	33.897624	7.959066	0.00204	0.0738	0.924	0.217	0.000	0.002
02.20.2019	#73	0.0301	54.19367	9.39152	0.0384	0.0552	32.516202	5.634912	0.02304	0.03312	1.080	0.187	0.001	0.001
04.03.2019	col-0 #1	0.0676	393.96	36.87	0.041	3.0506	236.376	22.122	0.0246	1.83036	3.497	0.327	0.000	0.027
04.03.2019	col-0 #2	0.0604	742.87	40.35	0.002	0.0615	445.722	24.21	0.0012	0.0369	7.380	0.401	0.000	0.001
04.03.2019	PLIP3-OX #1	0.0406	165.77	118.71	0.4093	20.3691	99.462	71.226	0.24558	12.22146	2.450	1.754	0.006	0.301
04.03.2019	PLIP3-OX #2	0.0692	383.63	101.38	0.6558	12.0709	230.178	60.828	0.39348	7.24254	3.326	0.879	0.006	0.105
04.03.2019	#74	0.0333	46.56	12.86	0.0432	2.8522	27.936	7.716	0.02592	1.71132	0.839	0.232	0.001	0.051
04.03.2019	#75	0.0371	283.17	33.86	0.0564	7.9707	169.902	20.316	0.03384	4.78242	4.580	0.548	0.001	0.129
04.03.2019	#76	0.0172	22.75	62.24	0.3109	0.6754	13.65	37.344	0.18654	0.40524	0.794	2.171	0.011	0.024
04.03.2019	#77	0.0483	68.17	508.19	2.2286	0.3205	40.902	304.914	1.33716	0.1923	0.847	6.313	0.028	0.004
04.03.2019	#78	0.039	71.38	389.48	0.4468	44.3897	42.828	233.688	0.26808	26.63382	1.098	5.992	0.007	0.683
04.03.2019	#79	0.041	59.6	52.58	0.2281	0.6124	35.76	31.548	0.13686	0.36744	0.872	0.769	0.003	0.009
04.03.2019	#80	0.0318	103.9	389.91	0.7571	47.722	62.34	233.946	0.45426	28.6332	1.960	7.357	0.014	0.900
04.03.2019	#81	0.0724	10.1	10.21	0.0621	0.1091	6.06	6.126	0.03726	0.06546	0.084	0.085	0.001	0.001
04.03.2019	#82	0.0426	95.27	104.57	0.3654	1.7009	57.162	62.742	0.21924	1.02054	1.342	1.473	0.005	0.024
04.03.2019	#83	0.0422	7.08	23.5	0.4786	0.1953	4.248	14.1	0.28716	0.11718	0.101	0.334	0.007	0.003
04.03.2019	#84	0.0483	62.02	90.9	0.1665	6.8208	37.212	54.54	0.0999	4.09248	0.770	1.129	0.002	0.085
04.03.2019	#85	0.024	76.25	46.77	0.1564	20.2348	45.75	28.062	0.09384	12.14088	1.906	1.169	0.004	0.506
04.03.2019	#86	0.0432	80.79	64.77	0.2539	1.5846	48.474	38.862	0.15234	0.95076	1.122	0.900	0.004	0.022
04.03.2019	#87	0.0406	84.62	112.39	0.449	2.5267	50.772	67.434	0.2694	1.51602	1.251	1.661	0.007	0.037
04.03.2019	#88	0.0461	68.78	144.3	0.6818	0.3611	41.268	86.58	0.40908	0.21666	0.895	1.878	0.009	0.005
04.03.2019	#89	0.0527	310.63	81.48	0.1828	0.0977	186.378	48.888	0.10968	0.05862	3.537	0.928	0.002	0.001
04.03.2019	#90	0.0626	187.02	34.72	0.247	0.1475	112.212	20.832	0.1482	0.0885	1.793	0.333	0.002	0.001

Table 3.2. Hormone data collected from plants selected in primary screen. Light green highlights represent plants determined to meet the criteria for passing the hormone-based secondary screen.

chr	pos	ref	alt	mutation_effect	gene	At_num	CDS_change	protein_change	EMS_mut.ref	EMS_mut.alt	EMS_wt.ref	EMS_wt.alt	notes	insertional lines
5	22400218	C	T	stop_gained	TIG	AT5G55220	1366C>T	Gln456*	4	63	42	29	homozygous apparently fine (Rohr et al 2019, plant phys), and homozygous line SALK_089907C apparently available	SALK_089907C
5	23213868	C	T	missense_variant	VLN5	AT5G57320	721C>T	Pro241Ser	1	57	35	12	*vln5* SAIL_512_F03 and GABI_225F09 homozygous mutants were fertile (zhang 2010)	CS863116 (homoSAIL)
5	24883408	C	T	missense_variant&splice_region_variant	ML1	AT5G61960	76G>A	Glu26Lys	2	59	46	24	mutant viable and fertile according to Anderson 2005	SALK_015088C
5	24914071	C	T	stop_gained	ARF2	AT5G62000	2146C>T	Gln716*	3	58	40	18	early flowers infertile, later flowers fertile (Okushima 2005)	CS24602
5	25037961	C	T	missense_variant	AT5G62350	AT5G62350	458C>T	Ala153Val	0	56	38	21	mutation looks less likely to cause problems (Ala->Val). No publications on this gene specifically. Predictions: Plant invertase/pectin methylesterase inhibitor superfamily protein; plastid-localized; there is line SALK_134445C, which is homozygous	SALK_134445C
5	25182210	C	T	missense_variant	TUBB2	AT5G62690	563C>T	Ser188Phe	0	44	42	17	hard to find papers on this, because it is used in many studies as a housekeeping gene for looking at expression. "Phenotype curated by ABRC: Left-handed helical growth in the root and other rapidly elongating organs. Strong severity of defects in cell expansion, cytokinesis, and vascular development." This does not resemble my mutant	CS68678
5	25444029	C	T	stop_gained	RMI1	AT5G63540	345G>A	Trp115*	0	65	46	23	homozygous sterile, both male and female "We examined the reproductive development of these mutants and found that blap75 sterility is due to abortion of male and female gametophytes (data not shown)" (Chelysheva 2008). Sterility detailed more in Bonnet 2013. This would not explain rescue by MeJA application. However, stop codon is in the essential DUF domain (Bonnet 2013), so this mutant is expected to be sterile here, so I don't know what to think	SALK_093589 SALK_093519
5	25464611	C	T	stop_gained	CDKE-1	AT5G63610	447G>A	Trp149*	1	59	39	21	AKA HEN3. no mention of infertility in Wang 2004, although shorter siliques were described for mutant. Floral development gene. Homozygous line SALK_072781C exists	SALK_072781C
5	25807197	C	T	missense_variant	MRS2-2	AT5G64560	1103G>A	Arg368Lys	0	49	48	17	Mg transporter essential for pollen development (Chen 2009). Homozygous lethal. Very possible that R->K change in residue 368 out of 394 does not cause loss of function	SALK_030174 (het)
5	26011654	C	T	missense_variant	ACX2	AT5G65110	601G>A	Ala201Thr	2	50	42	17	Acyl-CoA oxidase 2; used in catabolism of long-chain FAs in peroxisome, no problems germinating or setting seed for *acx2-1 null* mutant, and wound-induced JA response is not compromised either (Pinfield-Wells 2005)	SALK_030578C SALK_006464-het
5	26552651	C	T	missense_variant	PCMP-H61	AT5G66520	773C>T	Ala258Val	2	64	40	27	aka Chloroplast RNA Editing Factor 7 (CREF7). Mutant strain SALK_078415 "displayed no aberrant visible phenotype" (Yagi 2013)	SALK_078415C
5	26689989	C	T	missense_variant	AT5G66820	AT5G66820	439C>T	Pro147Ser	1	54	40	23	519-residue "transmembrane protein". SALK_016436C (homozygous) exists, but this insertion is ~100bp upstream of start codon. High-throughput phenotyping shows reduced tolerance of cold and oxidative stress for SALK_016436C, and no change for heat, osmotic, NaCl, ABA, or hypoxia stress tolerance (Luhua 2013)	SALK_016436C WiscDsLoxHs015_03G (CS901367)
5	26863128	C	T	missense_variant	NRAMP4	AT5G67330	1087C>T	Leu363Phe	2	55	34	18	Mn transporter? Vacuole localized. *nramp4-1* null mutant "displays no obvious phenotype" (Lanquar 2005)	CS859760
5	23247163	C	T	missense_variant	VIN3	AT5G57380	1238G>A	Gly413Glu	5	56	33	32		CS875198 het
5	23905083	C	T	missense_variant	AT5G59250	AT5G59250	592C>T	Leu198Phe	6	67	51	21	HP59; PSUT; PLASTIDIC SUGAR TRANSPORTER	CS67300
5	23925623	C	T	synonymous_variant	LTP4	AT5G59310	150G>A	Pro50Pro	5	60	36	16		CS416473 (5'utr, not homo)
5	25166065	C	T	missense_variant	NPF2.11	AT5G62680	1216G>A	Gly406Arg	3	64	40	26	GLUCOSINOLATE TRANSPORTER-2	SALK_052811C
5	26474855	C	T	missense_variant	AT5G66270	AT5G66270	170G>A	Arg57Gln	10	48	51	24	Zinc finger C-x8-C-x5-C-x3-H type family protein	CS863998 (WISCDSLOX297300_11N)
5	26947794	C	T	missense_variant	AT5G67550	AT5G67550	826G>A	Glu276Lys	4	47	39	14	transmembrane protein	SALK_127997C, SALK_052167 (het)

Table 3.3. Outputs from SIMPLE following genomic sequencing of *sup11*, showing possible causative mutations that co-segregate with suppression phenotype. A list of insertional mutants was also included here, for crossing to *sup11* to identify the causal suppressor mutation.

chr	pos	ref	alt	mutation_effect	gene	At_num	CDS_change	protein_change	EMS_mut.ref	EMS_mut.alt	EMS_wt.ref	EMS_wt.alt
1	17046048	C	T	upstream_gene_variant	AT1G45100	AT1G45100	-4583C>T		0	1	8	5
1	26401359	G	A	missense_variant	GATL9	AT1G70090	433G>A	Val145Ile	2	55	41	25
1	26901261	G	A	missense_variant	CEL3	AT1G71380	415C>T	Pro139Ser	2	26	32	19
1	28464675	G	A	missense_variant	CLV1	AT1G75820	1978C>T	Arg660Cys	5	56	41	25
1	29034238	G	A	missense_variant	AT1G77280	AT1G77280	322C>T	Leu108Phe	3	32	47	21
1	29071522	G	A	missense_variant	AT1G77350	AT1G77350	346G>A	Glu116Lys	5	47	46	27
1	29108381	C	T	missense_variant	AT1G77460	AT1G77460	3541C>T	Leu1181Phe	2	50	42	17
1	29751567	C	T	stop_gained	AT1G79090	AT1G79090	366G>A	Trp122*	1	47	44	18
1	30012292	C	T	missense_variant	DTA4	AT1G79760	239C>T	Thr80Ile	1	27	38	19
1	30043481	C	T	missense_variant	ROPGEF12	AT1G79860	529G>A	Asp177Asn	0	47	31	26
1	30244604	C	T	missense_variant	VQ11	AT1G80450	85G>A	Val29Ile	2	38	30	16

Table 3.4. Outputs from SIMPLE following genomic sequencing of *sup12*, showing possible causative mutations that co-segregate with suppression phenotype.

chr	pos	ref	alt	mutation_effect	gene	At_num	CDS_change	protein_change	EMS_mut.ref	EMS_mut.alt	EMS_wt.ref	EMS_wt.alt	ratio
2	1343761	C	T	splice_region_variant&intron_variant	AT2G04060	AT2G04060	463+7G>A		2	34	40	22	0.589606
2	1600559	C	T	downstream_gene_variant	AT2G04570	AT2G04570	*4430C>T		1	37	28	15	0.624847
2	2895400	C	T	missense_variant	HEN2	AT2G06990	266C>T	Ser89Phe	0	37	29	25	0.537037
2	4539413	C	T	upstream_gene_variant	AT2G11405	AT2G11405	-3762C>T		0	43	28	19	0.595745
2	368009	C	T	missense_variant	AHK4	AT2G01830	8G>A	Arg3Lys	9	41	34	20	0.44963
2	466905	C	T	upstream_gene_variant	AT2G01990	AT2G01990	-408G>A		4	40	31	21	0.505245
2	935961	C	T	missense_variant	AT2G03110	AT2G03110	448C>T	Pro150Ser	2	25	31	13	0.630471
2	2342483	GA	G	upstream_gene_variant	AT2G06020	AT2G06020	-51delA		10	7	20	0	0.411765
2	2992124	C	T	upstream_gene_variant	AT2G07210	AT2G07210	n.-22G>A		0	36	22	21	0.511628
2	3161788	C	T	non_coding_exon_variant	AT2G07550	AT2G07550	n.3722G>A		0	32	29	11	0.725
2	3232139	C	T	upstream_gene_variant	AT2G07660	AT2G07660	n.-439G>A		0	40	26	20	0.565217
2	3434738	T	G	missense_variant	AT2G07721	AT2G07721	143A>C	Glu48Ala	2	3	7	0	0.6
2	4595941	G	A	upstream_gene_variant	AT2G11465	AT2G11465	n.-507G>A		21	26	39	0	0.553191
2	4989494	C	T	upstream_gene_variant	AT2G12380	AT2G12380	n.-136G>A		1	35	24	22	0.493961
2	6341031	G	A	upstream_gene_variant	AT2G14780	AT2G14780	n.-334C>T		13	17	51	0	0.566667
2	6589845	C	T	missense_variant	AT2G15180	AT2G15180	323G>A	Gly108Glu	13	24	41	0	0.648649
2	7394275	C	T	missense_variant	AT2G17010	AT2G17010	1309G>A	Asp437Asn	22	14	43	0	0.388889
2	7406858	C	T	upstream_gene_variant	anac036	AT2G17040	-265C>T		20	31	76	0	0.607843
2	7411519	C	T	missense_variant	AT2G17050	AT2G17050	3595G>A	Val1199Met	17	15	58	0	0.46875
2	14770384	C	T	missense_variant	AT2G35050	AT2G35050	677C>T	Pro226Leu	6	20	38	19	0.435897
1	11267234	G	A	missense_variant	SGR2	AT1G31480	634G>A	Ala212Thr	26	18	49	0	0.409091
2	368009	C	T	missense_variant	AHK4	AT2G01830	8G>A	Arg3Lys	9	41	34	20	0.44963
2	935961	C	T	missense_variant	AT2G03110	AT2G03110	448C>T	Pro150Ser	2	25	31	13	0.630471
2	2895400	C	T	missense_variant	HEN2	AT2G06990	266C>T	Ser89Phe	0	37	29	25	0.537037
2	6589845	C	T	missense_variant	AT2G15180	AT2G15180	323G>A	Gly108Glu	13	24	41	0	0.648649
2	7411519	C	T	missense_variant	AT2G17050	AT2G17050	3595G>A	Val1199Met	17	15	58	0	0.46875
2	13754645	C	T	missense_variant	GLR3.7	AT2G32400	1240G>A	Val414Ile	9	26	37	19	0.403571
2	14770384	C	T	missense_variant	AT2G35050	AT2G35050	677C>T	Pro226Leu	6	20	38	19	0.435897
4	10665994	C	T	missense_variant	AT4G19570	AT4G19570	479C>T	Ala160Val	28	22	47	0	0.44
4	14063045	C	T	missense_variant	AT4G28450	AT4G28450	732G>A	Met244Ile	22	18	49	0	0.45
4	15648149	C	T	missense_variant	CYP95	AT4G32420	2126G>A	Arg709Lys	20	20	44	0	0.5

Table 3.5. Outputs from SIMPLE following genomic sequencing of *sup53*, showing possible causative mutations that co-segregate with suppression phenotype.

		change		mut.ref	mut.alt	wt.ref	wt.alt	ratio	notes
AT5G01010	retinal-binding protein		Leu112Leu	20	37	64	11	0.502456	
AT5G02320	ARABIDOPSIS THALIANA MYB DOMAIN PROTEIN 3R5, ATMYB3R5, MYB DOMAIN PROTEIN 3R-5, MYB3	-4181G>A (upstream variant)		16	27	56	3	0.57706	mutant in 2017 Chen Nature paper is SALK_031972. MYB3R5 is transcriptional repressor. Myb3r5 mutant continues to grow during zeocin treatment (inducer of double-stranded breaks)
AT5G02502	Oligosaccaryltransferase; OST4B	-1G>A (splice region variant)		17	28	34	6	0.472222	part of protein glycosylation complex?
AT5G13530	Encodes KEEP ON GOING (KEG), a RING E3 ligase involved in abscisic acid signaling. KEG is essential for Arabidopsis growth and development. ABA promotes KEG degradation via the ubiquitin dependent 26S proteasome pathway	4369C>T	His1457Tyr	11	38	43	4	0.690404	KEG is essential for development past the seedling stage. Full protein is 1625 residues. Mutation H1457Y is in Herc2-like repeat.
AT5G12850	TANDEM ZINC FINGER 8, TZF8	185C>T	Ser62Phe	15	46	54	8	0.625066	excluded from nucleus (Koroleva 2004 plant journal); otherwise not much info
AT5G10220	ANN6, ANNAT6, ANNEXIN 6, ANNEXIN ARABIDOPSIS THALIANA 6	823G>A	Glu275Lys	15	39	47	15	0.480287	annexins are Ca-dependent membrane binding proteins involved in signaling
AT5G06830	hypothetical protein	-416G>A		20	46	50	10	0.530303	no info in literature
AT5G03370	acylphosphatase family	-4271G>A		15	31	52	9	0.526372	don't know
AT5G03340	ATCDC48C, CELL DIVISION CYCLE 48C	-1646G>A		27	41	51	7	0.482252	"Critical Roles in Cell Division, Expansion, and Differentiation" 2008 Park Plant Physiology
AT5G02290	NAK, PBL11, PBS1-LIKE 11	1006G>A	Asp336Asn	27	40	54	10	0.440765	kinase, involved in signaling
AT5G01950	Leucine-rich repeat protein kinase family protein	1642+3G>A		20	39	60	18	0.430248	no info in literature
AT5G01100	FRB1, FRIABLE 1	430G>A	Gly144Arg	26	30	59	10	0.390787	important for cell adhesion (fucosyltranferase?). Mutants have very crumpled appearance.
AT5G17090	Cystatin/monellin superfamily protein	322G>A	Glu108Lys	15	28	50	11	0.470835	no info in literature
AT5G26010		-873C>T		15	45	41	10	0.553922	
AT2G33470	GLTP1	-2993_-2992insT		10	5	22	0	0.333333	glycosphingolipid transfer protein
AT5G05480		1136G>A	Gly379Glu	20	29	41	9	0.411837	
AT5G05560		3133-21C>T		13	39	47	16	0.496032	
AT5G06150		532G>A	Ala178Thr	17	35	38	14	0.403846	
AT5G07740		*278G>A		13	27	32	7	0.495513	
AT5G12980	NOT9B	550G>A	Glu184Lys	19	25	53	10	0.409452	negative regulation of translation?
AT5G13020		*90G>A		20	38	39	12	0.419878	
AT5G13050		-3740G>A		9	26	32	11	0.487043	
AT5G13260		-2932_-2931delAT		24	8	27	0	0.25	
		-2589_-2588delAT		9	13	14	3	0.414439	
AT5G13470		*4686C>G		22	45	48	14	0.445835	
AT5G13480		905G>A	Ser302Asn	11	22	30	14	0.348485	
AT5G15050	AtGlcAT14B	744G>A	Trp248*	15	30	41	14	0.412121	glucuronosyltransferase, see Dilokpmiol 2014 Plant Signaling and Behavior
AT5G15060	Lateral organ boundaries (LOB) family protein	343G>A	Val115Ile	11	27	31	8	0.505398	LOB domain is associated with transcription factors
AT5G17710		*68G>A		13	45	35	13	0.505029	
AT5G59620		n.-2330G>T		3	5	14	1	0.558333	

Table 3.6. Outputs from SIMPLE following genomic sequencing of *sup72*, showing possible causative mutations that co-segregate with suppression phenotype.

REFERENCES

1. Liu, J., et al., *Connecting research and teaching introductory cell and molecular biology using an Arabidopsis mutant screen.* Biochem. Mol. Biol. Educ., 2021. **49**(6): p. 926-934.

2. Koo, A.J., J.B. Ohlrogge, and M. Pollard, *On the export of fatty acids from the chloroplast.* J. Biol. Chem., 2004. **279**(16): p. 16101-10.

3. Li, N., et al., *FAX1, a novel membrane protein mediating plastid fatty acid export.* PLoS Biol., 2015. **13**(2): p. e1002053.

4. Tian, Y., et al., *FAX2 mediates fatty acid export from plastids in developing Arabidopsis seeds.* Plant Cell Physiol., 2019. **60**(10): p. 2231-2242.

5. Li, N., et al., *Two plastid fatty acid exporters contribute to seed oil accumulation in Arabidopsis.* Plant Physiol., 2020. **182**(4): p. 1910-1919.

6. Bugaeva, W., et al., *Plastid fatty acid export (FAX) proteins in Arabidopsis thaliana-the role of FAX1 and FAX3 in growth and development.* bioRxiv, 2023. DOI: https://doi.org/10.1101/2023.02.09.527856

7. Cook, R., J. Lupette, and C. Benning, *The role of chloroplast membrane lipid metabolism in plant environmental responses.* Cells, 2021. **10**(3): p. 706.

8. Ruan, J., et al., *Jasmonic acid signaling pathway in plants.* Int. J. Mol. Sci., 2019. **20**(10): p. 2479.

9. Guan, L., et al., *JASSY, a chloroplast outer membrane protein required for jasmonate biosynthesis.* Proc. Natl. Acad. Sci. U.S.A., 2019. **116**(21): p. 10568-10575.

10. Ellinger, D., et al., *DONGLE and DEFECTIVE IN ANTHER DEHISCENCE1 lipases are not essential for wound- and pathogen-induced jasmonate biosynthesis: redundant lipases contribute to jasmonate formation.* Plant Physiol., 2010. **153**(1): p. 114-27.

11. Wang, K., et al., *A Plastid Phosphatidylglycerol Lipase Contributes to the Export of Acyl Groups from Plastids for Seed Oil Biosynthesis.* Plant Cell, 2017. **29**(7): p. 1678-1696.

12. Wang, K., et al., *Two Abscisic Acid-Responsive Plastid Lipase Genes Involved in Jasmonic Acid Biosynthesis in Arabidopsis thaliana.* Plant Cell, 2018. **30**(5): p. 1006-1022.

13. Wachsman, G., et al., *A SIMPLE pipeline for mapping point mutations.* Plant Physiol., 2017. **174**(3): p. 1307-1313.

14. Stone, S.L., et al., *KEEP ON GOING, a RING E3 ligase essential for Arabidopsis growth and development, is involved in abscisic acid signaling.* Plant Cell, 2006. **18**(12): p. 3415-3428.

15. Pauwels, L., et al., *The ring e3 ligase keep on going modulates jasmonate zim-domain12 stability.* Plant Physiol., 2015. **169**(2): p. 1405-1417.

16. Wawrzynska, A., et al., *Powdery Mildew Resistance Conferred by Loss of the ENHANCED DISEASE RESISTANCE1 Protein Kinase Is Suppressed by a Missense Mutation in KEEP ON GOING, a Regulator of Abscisic Acid Signaling* Plant Physiol., 2008. **148**(3): p. 1510-1522.

17. Guo, Q., et al., *JAZ repressors of metabolic defense promote growth and reproductive fitness in Arabidopsis.* Proc. Natl. Acad. Sci. U.S.A., 2018. **115**(45): p. E10768-E10777.

18. Liu, H. and S.L. Stone, *Abscisic acid increases Arabidopsis ABI5 transcription factor levels by promoting KEG E3 ligase self-ubiquitination and proteasomal degradation.* Plant Cell, 2010. **22**(8): p. 2630-2641.

19. Liu, H. and S.L. Stone, *Cytoplasmic degradation of the Arabidopsis transcription factor abscisic acid insensitive 5 is mediated by the RING-type E3 ligase KEEP ON GOING.* J. Biol. Chem., 2013. **288**(28): p. 20267-20279.

20. Gu, Y. and R.W. Innes, *The KEEP ON GOING protein of Arabidopsis recruits the ENHANCED DISEASE RESISTANCE1 protein to trans-Golgi network/early endosome vesicles.* Plant Physiol., 2011. **155**(4): p. 1827-1838.

21. Ng, S., et al., *Cyclin-dependent kinase E1 (CDKE1) provides a cellular switch in plants between growth and stress responses.* J. Biol. Chem., 2013. **288**(5): p. 3449-3459.

CHAPTER 4:

Analysis, conclusions, and perspectives

Introduction

A better understanding of key stages in plant lipid biosynthesis was sought by focusing on two fundamental yet incompletely elucidated processes in Arabidopsis: phosphatidic acid (PA) metabolism and fatty acid (FA) export in the chloroplast. A deeper study of chloroplast lipid phosphate phosphatases (LPPs) revealed that LPPγ and LPPε1 are involved in the processing of ER-derived PA, and that the enzyme responsible for plastid-derived PA dephosphorylation remains unknown. Meanwhile, a suppressor screen in the *PLIP3*-OX background targeted mutants with a decreased capacity for converting the plastid-derived FA derivative 12-oxo-phytodienoic acid (OPDA) to jasmonic acid (JA) in the cytosol, with the goal of attaining mutants deficient in OPDA export from chloroplasts. While such mutants have yet to be identified, mutations in *KEG* and *CDK8* resulted in phenotypic suppression of *PLIP3*-OX, which should provide further insight into the gene products' roles in the JA-responsive transcriptomic network.

Chloroplast LPPs and PA

Localizations and redundancies of LPPγ*,* LPPε1*,* LPPε2*, and* LPPα2

As discussed in chapter 2, in the context of published works [1-3], our chloroplast import data, complementation tests, fatty acid radiolabeling data, and redundancy between LPPγ and LPPε1 all indicate localization of LPPγ and LPPε1 to the chloroplast outer envelope and LPPε2 localization to the inner envelope or thylakoids. Weak import of LPPε1 was observed in the import assay presented in chapter 2, which may point to dual-localization of LPPε1. Similarly, closer observation of Figure 11A in Nguyen 2023 shows a faint band of Venus-tagged LPPε1 at lower molecular weight, which is digested by trypsin and not thermolysin [2]. This may be the small portion of LPPε1-Ven that is fully processed and located at the inner envelope, with the Venus reporter exposed to trypsin. If LPPε1 is indeed also present at the inner envelope, it may have functional redundancy with LPPε2, which would be distinct from its redundant activity with LPPγ.

Interestingly, LPPε1 has also been shown to act redundantly with the ER-localized LPPα2, a phenomenon that was rationalized by associating LPPε1 activity in the chloroplast outer envelope with sites of lipid exchange with the ER [2]. This model was supported by confocal imaging data showing fluorescent-tagged LPPε1 signals emanating from subdomains of the outer envelope in

close proximity to the ER [2]. However, it should be noted that LPPγ was still present in the unviable *lppε1 lppα2* mutant, and so was not able to compensate for the absence of LPPε1. LPPε1 activity at the outer envelope is therefore only partially redundant with that of LPPγ, likely as a result of differential distribution of these enzymes, with just LPPε1 substantially present at contact sites with the ER.

Metabolic roles of LPPγ *and* LPPε1*, and implications for the ER pathway of galactolipid metabolism*

While it has been demonstrated that redundant PA phosphatase (PAP) activity of LPPγ and LPPε1 contributes to the ER pathway of galactolipid biosynthesis, it was also noted that the decreased flux through the pathway in *lppγ lppε1* is relatively mild: it is not sufficient to affect the acyl compositions of major galactolipids, and was only directly discernable in pulse-chase ^{14}C-labeling experiments of fatty acids. The decreased viability of *lppγ lppε1 ats1-1* also supports involvement of LPPγ and LPPε1 in the ER pathway, as the stymied supply of lipids from the plastid pathway compounds the negative effects of a disrupted ER pathway [4-6].

The modest metabolic phenotype of *lppγ lppε1* indicates that alternative sources of ER-derived DAG exist. Soluble PA phosphatases PAH1 and PAH2 are known to be involved in the ER pathway, and their presence in the cytosol could provide them access to PA at the chloroplast outer envelope [7]. The *pah1 pah2* double mutant has a comparable lipid phenotype to *lppγ lppε1* with respect to galactolipid acyl composition and ER pathway fluxes, although plant development is not stunted. A different study reported PAH1 and PAH2 localization to the ER, which would implicate DAG as a mobile lipid between the ER and outer envelope, possibly in addition to PA [8]. However, it is possible that overexpression led to mis-localization of PAH1 and PAH2 in this study, as the phenomenon of over-produced outer envelope proteins accumulating in the ER has been shown for TGD4 [5, 9]. In either case, in *lppγ lppε1*, PAH1 and PAH2 continue to provide ER-derived DAG substrates for galactolipid biosynthesis from PA located at either the ER or cytosolic leaflet of the outer envelope. Pursuit of a quadruple *lppγ lppε1 pah1 pah2* mutant could be informative in determining whether additional DAG-producing enzymes exist in the ER pathway.

If LPPγ, LPPε1, PAH1, and PAH2 are indeed together the main sources of DAG in the ER pathway, it would follow that the TGD complex imports DAG, rather than PA, into the inner envelope. Consequently, PA dephosphorylation at the inner envelope would be exclusive to the plastid pathway. This could explain why the *rbl10* mutant is deficient in PA dephosphorylation in the plastid pathway, despite retaining high PAP activity in mixed envelopes isolated from chloroplasts [10].

If the four aforementioned PAPs are not the primary sources of DAG, and PA is the imported lipid species, it would mean that an unidentified, RBL10-independent enzyme dephosphorylates ER-derived PA at the inner envelope. As previously hypothesized in Lavell 2019, this PAP could be active at the intermembrane-facing leaflet of the inner envelope, and RBL10 may directly or indirectly facilitate plastid PA flipping to this leaflet for subsequent dephosphorylation [10]. Alternatively, there could be a separate RBL10-dependent PAP that acts on PA at the stromal-facing leaflet.

Regarding the TGD complex, if PA is imported, binding of PA by TGD2 and TGD4 could be explained simply as substrate binding to subunits of the import complex. A different explanation for PA binding would be required in the case of a DAG substrate, which introduces the possibility of allosteric regulation by PA.

Regulatory roles of LPPγ*,* LPPε1*, and chloroplast PA*

The lack of growth inhibition in *pah1 pah2*, despite its similar lipid phenotype to *lppγ lppε1*, supports the hypothesis in which LPPγ and LPPε1 draw from a distinct PA pool, which is at the inner leaflet of the chloroplast outer envelope membrane. TGD4 is present in this membrane, and binds PA at its cytosolic-facing N-terminal domain [9, 11]. We hypothesized that if TGD4 is responsible for PA transfer across the outer envelope, then crossing of *tgd4-1* to *lppγ lppε1* would suppress growth inhibition caused by PA at the inner leaflet. However, the *lppγ lppε1 tgd4-1* triple mutants remained small, indicating that either PA import is not sufficiently hindered in *tgd4-1*, that TGD4 binds PA only as part of the transfer from the ER to the outer leaflet, or that PA binding is regulatory and not a substrate interaction. As an allosteric regulator, one would expect PA binding to activate TGD4, as PA is known to accumulate outside of the plastid in mutants deficient

in TGD4, as well as ER pathway proteins TGD1, PAH1, and PAH2 [4, 7, 9]. Crossing of *lppγ lppε1* to the more severe mutant alleles *tgd4-2* or *tgd4-3*, and checking for phenotypic suppression, may provide confirmation on whether TGD4 supplies PA to the inner leaflet of the outer envelope.

PA is also known to be bound to TGD2 at its C-terminal domain, which is thought to extend into the intermembrane space while the N terminus is anchored at the chloroplast inner envelope [12, 13]. The PA bound near the C-terminus is presumably at the inner leaflet of the outer envelope membrane, belonging to the same PA pool utilized by LPPγ and LPPε1. If DAG is the substrate of TGD2, and PA binds allosterically, PA may have a regulatory role as speculated for binding to TGD4. The presumed increase in this PA pool in *lppγ lppε1* may affect the function of the TGD complex. Any such effect is unlikely to be the reason for growth inhibition in *lppγ lppε1*, as severe disruption of the complex in *tgd1-1* does not result in the phenotype, nor does crossing *tgd1-1* to *lppγ lppε1* suppress it. The growth inhibition caused by excess PA at the inner leaflet of the outer envelope membrane is therefore distinct from its association with the TGD complex.

The pathways or mechanisms by which PA affects growth from the intermembrane-facing leaflet of the chloroplast outer envelope are not known, despite being shown both in *lppγ lppε1* mutants and in transgenic lines where DAG kinase is targeted to the intermembrane space [3]. Salicylic acid signaling does not appear to be involved, and *lppγ lppε1* plants do not resemble the JA-induced morphologies of *PLIP*-OX lines or *dgd1* [14-16]. Hormone profiling of *lppγ lppε1* may prove to be valuable in identifying relevant signaling pathways. Moreover, the suppressor mutant screen applied to *lppγ lppε1* is expected to identify novel factors affecting growth regulation in the double mutant. We may discover mutants in PA trafficking to the inner leaflet of the outer envelope, which could contribute to our understanding of membrane lipid metabolism. Other mutants may uncover components that link the altered membrane composition to broader signaling pathways, or reveal novel regulatory PA-dependent factors that would provide broader insights into plant growth regulation. These discoveries should in turn provide more context for the regulatory roles of LPPγ and LPPε1, which may act as regulators through their modulation of this PA pool.

The role of LPPε2 *is unknown*

It was shown that LPPε2 is located at the chloroplast inner envelope or thylakoids, and that its catalytic activity is that of a PAP equivalent to LPPγ and LPPε1. However, an aberrant phenotype of *lppε2* has not been observed, and the same is true for *lppε1 lppε2*, in which potential redundancy is accounted for. It is unlikely that *LPPε2* would be retained during evolution in absence of a metabolic or physiological purpose, and further study would require testing of more diverse environmental conditions. As chloroplasts are central to substantial portions of both metabolism and signaling, any biotic or abiotic stresses are appropriate as challenges. In fact, unpublished preliminary data from the David Kramer lab has shown a decrease in non-photochemical quenching efficiency in *lppε2* under fluctuating light conditions and elevated temperature, which may provide a direction for future research. While LPPε2 has been detected in leaf chloroplasts [1], it is also possible that its primary function is in other tissues, such as roots, flowers, or seeds. An approach targeting characterization of these tissues in *lppε2* and *lppε1 lppε2* may also prove fruitful.

The PA phosphatase of the plastid pathway is unknown

The plastid pathway is dependent on PAP activity at the chloroplast inner envelope, and appears to be largely dependent on RBL10 [10]. Acyl group radiolabeling on isolated chloroplasts from *lppγ lppε1 lppε2* revealed that none of the three known chloroplast LPPs are involved in the plastid pathway. Because there is some residual plastid pathway-derived MGDG in the *rbl10* mutant, it is possible that the RBL10-dependent PAP activity is actually completely abolished, and weak LPPε2 or LPPε1 activity provides minimal compensation. A cross of *rbl10* to *lppε2* or *lppε1 lppε2* would be useful in determining whether this is the case, and thus whether the primary plastid pathway PAP is partially or entirely dependent on RBL10.

One possibility that had been previously discussed is that RBL10 itself is the plastid pathway PAP. This was discounted because mixed envelopes from *rbl10* retain PAP activity, and it was concluded that substrate access by the PAP was deficient in the mutant rather than the phosphatase itself [10]. However, our results show that chloroplast LPPs, which are all present in *rbl10*, would be expected to remain active and possibly obscure the effects of a missing plastid pathway PAP in a

mixed envelope assay. PAP activity assays on separated envelopes would therefore be more informative, in both various *lpp* mutants, *rbl10*, and crosses between them. These results would clarify if the inner envelope PAP activity is dependent on RBL10, and whether it overlaps with some LPP activity. However, this experiment cannot directly implicate RBL10 as a PAP, and separate PA phosphatase assays on the RBL10 protein itself would be needed to address this question. It should be noted that protease activity has not been demonstrated for Arabidopsis RBL1, RBL10, RBL11, nor RBL12, and only witnessed in RBL2 [17-21]. While this is possibly just due to unique specificities for protein substrates, the case may also be that some plant rhomboid-like enzymes hydrolyze lipids rather than proteins.

Another possibility, though unlikely, is that ATS1 has dual function as an acyltransferase and PA phosphatase. This is hypothesized because the *ats1-1* mutant is more deficient in plastid-derived MGDG than plastid-derived PG, which does not require PA dephosphorylation [22]. As shown in chapter 2, in *ats1-1* more plastid PA is allocated to PG relative to MGDG than in Col-0. Therefore, PAP activity in the plastid pathway is lower in *ats1-1*, in addition to the decreased acyltransferase activity. A simple way to explain this would be that ATS1 is also the lipid phosphatase, which would not be unprecedented: Arabidopsis GPAT4 and GPAT6 have lyso-PA phosphatase activity in addition to their acyltransferase activity in the cytoplasm [23]. Finally, according to a preliminary analysis using InterPro, ATS1 and ATS2 share a similar C-terminal acyltransferase domain, while ATS1 has an additional N-terminal alpha-helical bundle, the purpose of which is not known [24]. This possibility can be addressed by *in vitro* testing of ATS1 for PAP activity, and its dependence on the N-terminal domain. If ATS1 is indeed the plastid pathway PAP, an explanation for the PAP dependence on RBL10 would require further investigation.

***PLIP3*-OX suppressor screen**

Implications for KEG mutant suppression of PLIP3-OX

In chapter 3, the candidacy of a mutation in *KEG* for causing phenotypic suppression of *PLIP3*-OX in *sup72* was discussed, along with possible mechanisms of suppression. KEG is a known repressor in the abscisic acid (ABA) pathway, which targets the transcriptional activator ABI5 for degradation in the absence of ABA [25, 26]. An equivalent role in the repression of the JA response

is also possible, as KEG has been shown to bind and stabilize the JA response repressor JAZ12 [27]. Because KEG-mediated JAZ12 stabilization and ABI5 degradation both depend on cytosolic interactions, it is hypothesized that the mutation in *sup72* leads to increased KEG presence in the cytosol, thereby dampening the JA response. This effect would resemble that of the *keg-4* mutant, in which an increased presence of KEG in the cytosol attenuates ABA sensitivity [28, 29]. It is also possible that instead, the *KEG* mutation in *sup72* directly affects its binding and stabilization of JAZ12. In KEG, both the JAZ12 interaction and the trans-golgi network (TGN) sequestration away from the cytosol are dependent on its C-terminal HERC domain [27-29]. Because the *KEG* H1457Y mutation in *sup72* is in the HERC domain, each of the two mechanisms of *PLIP3*-OX phenotypic suppression is a possibility.

In either case, it is likely that phenotypic suppression of *PLIP3*-OX by the H1457Y mutation in *sup72* is not due to loss of function in KEG, but rather to a change that actually increases its repressive activity. Consequently, a traditional complementation approach in *sup72* with the native *KEG* sequence is not expected to reverse the suppression, or prove causality. In order to prove causality, a more complex approach is necessary, particularly as the role of KEG appears to be dose-dependent. In the most direct approach, a *keg* null mutant would be complemented with the native or H1457Y mutant gene. The transformation needs to be performed on the heterozygote, as *keg* null mutants are lethal shortly after germination [30]. After these complementation lines are obtained, they would be crossed to *PLIP3*-OX to determine phenotypic suppression.

Several approaches could be taken to assess whether it is an increase in the cytosolic presence of KEG, or a change in the KEG-JAZ12 interaction that results in *PLIP3*-OX suppression. Studies on the binding affinities between JAZ12 and native or mutant KEG can be carried out in heterologous systems or using purified proteins. In addition, if the mutation specifically affects the KEG-JAZ12 interaction, and not KEG localization, it would be expected that the ABA pathway would be less compromised in *sup72*. Therefore, ABA sensitivity assays, as well as direct studies of KEG H1457Y localization, would determine the extent to which changes in its location affect its role in the JA signaling pathway. Inversely, the role of KEG can be elucidated with a test of the robustness of the JA response in the *keg-4* mutant, in which KEG is known to mislocalize to the cytosol [29].

A larger question that would require further study is why the KEG interactions with transcriptional regulators in the cytosol is so significant, when these proteins are active in the nucleus. In the case of the activator ABI5, it is possible that efficient KEG-mediated degradation following translation is sufficient to out-compete nuclear import. However, for a repressor like JAZ12, it is unclear why stabilization outside of the nucleus would increase repression within the nucleus, as COI1-mediated degradation of JAZ repressors is generally attributed to the nucleus [31]. It is therefore likely that JAZ12 is also targeted by cytosolic factors for degradation, an interaction which would complicate current models of JA signaling. Such factors could be identified through further study of the JAZ12 interactome, or discovered by additional screening for new *PLIP3*-OX suppressors. As previously reported, JAZ12 is likely essential as a viable null mutant has not been demonstrated, and therefore this avenue for studying the repressor may be valuable [27].

Implications for CDK8 mutant suppression of PLIP3-OX

As described in chapter 3, a nonsense mutation of *CDK8* in *sup11* was determined to suppress the JA-induced phenotype of *PLIP3*-OX. A concurrent suppressor screen in the *jazD* background carried out by the Gregg Howe group yielded an equivalent *jazD* suppression by a *CDK8* mutant. Because *jazD* is deficient in transcriptional repressors of JA-responsive genes [32], it is likely that CDK8 serves as a transcriptional activator in at least some portion of the JA response.

Prior literature on CDK8, also referred to as HEN3, RAO1, or CDKE1, points to a transcription-level regulatory role. The *CDK8* mutant *hen3-1* was characterized by its exacerbation of floral deformities in the *hua1 hua2* double mutant [33]. However, *hen3-1* on its own appears to have normal flowers, pointing to functional overlaps with other factors controlling floral development. JA is also implicated in floral development, specifically in the maturation of male tissues [34-36]. However, there is no direct evidence of a connection between JA-dependent signaling and CDK8 in flowers, as *hen3*-associated floral phenotypes result from incorrect differentiation of floral tissues early in development, rather than incomplete maturation of tissues post-differentiation.

The relationship between CDK8 and mitochondrial retrograde signaling also suggests a broader role for the protein beyond JA signaling, which is likely effective on a transcriptional level due to the exclusive localization of CDK8 to the nucleus [37]. More detailed studies of the *PLIP3*-OX *cdk8*

or *jazD cdk8* plants may provide further insights into the regulatory targets of CDK8, as some elements of the JA response may be less suppressed than others. Overall, the results highlight the complex nature of overlapping stress-responsive transcriptional networks in plants, as well as the tissue-dependent variation in the roles of their components.

Effectiveness of the screening approach

The suppressor screen in the *PLIP3*-OX background was originally intended to target mutants in chloroplast OPDA export, with a visual primary screen designed for high throughput, and a secondary screen that would eliminate mutants not impaired in the conversion of OPDA to JA. Approximately 4000 plants were screened within six months, of which 90 passed the primary screen. The visual screen was therefore effective in providing suppressor mutants for further screening or analysis in an acceptable timeframe.

The secondary screen, based on measurements of JA, OPDA, and 12OH-JA, was intended to enrich for mutants impaired specifically in the conversion of OPDA to JA. Mutants lacking OPDA were excluded as likely OPDA biosynthetic mutants, and mutants retaining high JA were excluded as likely deficient in JA perception or signaling. A small number of mutants also exhibited decreased JA coupled with high levels of 12-OH JA, and these were also rejected as they are likely unimpaired in OPDA processing. Although the secondary screen was efficacious in reducing the number of mutants from 90 to 23, both of the candidate suppressor mutants appear to be impaired in JA signaling. The secondary screen was therefore prone to generating false positives, although it may still be effective in enriching for the desired mutant. One technical explanation is that the data generated from hormone quantification had wide variations in the controls, both between runs and within the same run, so the method is quite noisy. It is also possible that the decrease in JA in these mutants was real, but that it resulted from regulatory feedbacks rather than a direct obstruction of OPDA processing.

Subsequent work by Yosia Mugume in the Benning lab determined that two additional mutants, *sup12* and *sup53*, lost PLIP3 function according to their fatty acid profile. These had been selected for sequencing based on results from primary and secondary screening, and confirmation of the correct transgenic sequence. These results emphasize a critical weakness in the screening

approach: that fatty acid profiles were not measured in the secondary screen to ensure functional expression of *PLIP3*. However, the hormone profiles for *sup12* and *sup53* would be expected to match those of other, desired suppressors, and thus provide some support for the efficacy of the hormone measurement approach.

Integration of the PLIP3-OX screen into coursework

The straightforward nature of the primary screen makes it compatible with introductory-level undergraduate coursework, and it was therefore incorporated into a Course-based Undergraduate Research Experience (CURE) [38]. This collaborative effort increased primary screening by approximately 30%, as screening is primarily limited by chamber space and labor. In addition, it was effective in providing access to a candidate pool of undergraduate students, some of whom were subsequently recruited by the lab and took part in various research projects.

Conclusion

The frameworks, results, and open questions discussed here underscore the complexities of plant metabolism and development, and the extent to which the two are inextricable. An unexpected impairment of plant growth was observed in mutants lacking lipid phosphatases LPPγ and LPPε1, two enzymes that also contribute to basal chloroplast metabolism. Meanwhile, the only known PA phosphatase to exist exclusively at the plastid interior, LPPε2, appears to be uninvolved in the major galactolipid pathway in its compartment, and its role in metabolism or regulation has yet to be elucidated. For the *PLIP3*-OX screen, the link between lipid hydrolysis in the chloroplast and JA signaling was exploited to identify novel factors in FA metabolism, and instead led to discovery of a putative coordination mechanism between the JA and ABA response networks. In conclusion, chloroplast lipid metabolism is integrated with various pathways affecting plant physiology, and these newly discovered interactions present valuable inroads to the study of plant growth, development, and survival.

REFERENCES

1. Nakamura, Y., M. Tsuchiya, and H. Ohta, *Plastidic phosphatidic acid phosphatases identified in a distinct subfamily of lipid phosphate phosphatases with prokaryotic origin.* J. Biol. Chem., 2007. **282**(39): p. 29013-21.

2. Nguyen, V.C. and Y. Nakamura, *Distinctly localized lipid phosphate phosphatases mediate endoplasmic reticulum glycerolipid metabolism in Arabidopsis.* Plant Cell, 2023. **35**(5): p. 1548-1571.

3. Muthan, B., et al., *Probing Arabidopsis chloroplast diacylglycerol pools by selectively targeting bacterial diacylglycerol kinase to suborganellar membranes.* Plant Physiol., 2013. **163**(1): p. 61-74.

4. Xu, C., et al., *Mutation of the TGD1 chloroplast envelope protein affects phosphatidate metabolism in Arabidopsis.* Plant Cell, 2005. **17**(11): p. 3094-110.

5. Xu, C., et al., *Lipid trafficking between the endoplasmic reticulum and the plastid in Arabidopsis requires the extraplastidic TGD4 protein.* Plant Cell, 2008. **20**(8): p. 2190-2204.

6. Fan, J., et al., *Arabidopsis TRIGALACTOSYLDIACYLGLYCEROL5 interacts with TGD1, TGD2, and TGD4 to facilitate lipid transfer from the endoplasmic reticulum to plastids.* Plant Cell, 2015. **27**(10): p. 2941-2955.

7. Nakamura, Y., et al., *Arabidopsis lipins mediate eukaryotic pathway of lipid metabolism and cope critically with phosphate starvation.* Proc. Natl. Acad. Sci. U.S.A., 2009. **106**(49): p. 20978-20983.

8. Eastmond, P.J., et al., *Phosphatidic acid phosphohydrolase 1 and 2 regulate phospholipid synthesis at the endoplasmic reticulum in Arabidopsis.* Plant Cell, 2010. **22**(8): p. 2796-811.

9. Wang, Z., C. Xu, and C. Benning, *TGD4 involved in endoplasmic reticulum-to-chloroplast lipid trafficking is a phosphatidic acid binding protein.* Plant J., 2012. **70**(4): p. 614-623.

10. Lavell, A., et al., *A predicted plastid rhomboid protease affects phosphatidic acid metabolism in Arabidopsis thaliana.* Plant J., 2019. **99**(5): p. 978-987.

11. Wang, Z., N.S. Anderson, and C. Benning, *The phosphatidic acid binding site of the Arabidopsis trigalactosyldiacylglycerol 4 (TGD4) protein required for lipid import into chloroplasts.* J. Biol. Chem., 2013. **288**(7): p. 4763-71.

12. Awai, K., et al., *A phosphatidic acid-binding protein of the chloroplast inner envelope membrane involved in lipid trafficking.* Proc. Natl. Acad. Sci. U.S.A., 2006. **103**(28): p. 10817-10822.

13. Lu, B. and C. Benning, *A 25-amino acid sequence of the Arabidopsis TGD2 protein is sufficient for specific binding of phosphatidic acid.* J. Biol. Chem., 2009. **284**(26): p. 17420-17427.

14. Wang, K., et al., *A Plastid Phosphatidylglycerol Lipase Contributes to the Export of Acyl Groups from Plastids for Seed Oil Biosynthesis.* Plant Cell, 2017. **29**(7): p. 1678-1696.

15. Wang, K., et al., *Two Abscisic Acid-Responsive Plastid Lipase Genes Involved in Jasmonic Acid Biosynthesis in Arabidopsis thaliana.* Plant Cell, 2018. **30**(5): p. 1006-1022.

16. Lin, Y.T., et al., *Reduced Biosynthesis of Digalactosyldiacylglycerol, a Major Chloroplast Membrane Lipid, Leads to Oxylipin Overproduction and Phloem Cap Lignification in Arabidopsis.* Plant Cell, 2016. **28**(1): p. 219-32.

17. Kanaoka, M.M., et al., *An Arabidopsis Rhomboid homolog is an intramembrane protease in plants.* FEBS Lett., 2005. **579**(25): p. 5723-5728.

18. Kmiec-Wisniewska, B., et al., *Plant mitochondrial rhomboid, AtRBL12, has different substrate specificity from its yeast counterpart.* Plant Mol. Biol., 2008. **68**: p. 159-171.

19. Knopf, R.R., et al., *Rhomboid proteins in the chloroplast envelope affect the level of allene oxide synthase in Arabidopsis thaliana.* Plant J., 2012. **72**(4): p. 559-571.

20. Thompson, E.P., S.G. Llewellyn Smith, and B.J. Glover, *An Arabidopsis rhomboid protease has roles in the chloroplast and in flower development.* J. Exp. Bot., 2012. **63**(10): p. 3559-3570.

21. Lavell, A., et al., *Proteins associated with the Arabidopsis thaliana plastid rhomboid-like protein RBL10.* Plant J., 2021. **108**(5): p. 1332-1345.

22. Kunst, L. and C. Somerville, *Altered regulation of lipid biosynthesis in a mutant of Arabidopsis deficient in chloroplast glycerol-3-phosphate acyltransferase activity.* Proc. Natl. Acad. Sci. U.S.A., 1988. **85**(12): p. 4143-4147.

23. Yang, W., et al., *A distinct type of glycerol-3-phosphate acyltransferase with sn-2 preference and phosphatase activity producing 2-monoacylglycerol.* Proc. Natl. Acad. Sci. U.S.A., 2010. **107**(26): p. 12040-12045.

24. Paysan-Lafosse, T., et al., *InterPro in 2022.* Nucleic Acids Research, 2023. **51**(D1): p. D418-D427.

25. Liu, H. and S.L. Stone, *Abscisic acid increases Arabidopsis ABI5 transcription factor levels by promoting KEG E3 ligase self-ubiquitination and proteasomal degradation.* Plant Cell, 2010. **22**(8): p. 2630-2641.

26. Liu, H. and S.L. Stone, *Cytoplasmic degradation of the Arabidopsis transcription factor abscisic acid insensitive 5 is mediated by the RING-type E3 ligase KEEP ON GOING.* J. Biol. Chem., 2013. **288**(28): p. 20267-20279.

27. Pauwels, L., et al., *The ring e3 ligase keep on going modulates jasmonate zim-domain12 stability.* Plant Physiol., 2015. **169**(2): p. 1405-1417.

28. Wawrzynska, A., et al., *Powdery Mildew Resistance Conferred by Loss of the ENHANCED DISEASE RESISTANCE1 Protein Kinase Is Suppressed by a Missense Mutation in KEEP ON GOING, a Regulator of Abscisic Acid Signaling* Plant Physiol., 2008. **148**(3): p. 1510-1522.

29. Gu, Y. and R.W. Innes, *The KEEP ON GOING protein of Arabidopsis recruits the ENHANCED DISEASE RESISTANCE1 protein to trans-Golgi network/early endosome vesicles.* Plant Physiol., 2011. **155**(4): p. 1827-1838.

30. Stone, S.L., et al., *KEEP ON GOING, a RING E3 ligase essential for Arabidopsis growth and development, is involved in abscisic acid signaling.* Plant Cell, 2006. **18**(12): p. 3415-3428.

31. Chini, A., M. Boter, and R. Solano, *Plant oxylipins: COI1/JAZs/MYC2 as the core jasmonic acid-signalling module.* FEBS J., 2009. **276**(17): p. 4682-4692.

32. Guo, Q., et al., *JAZ repressors of metabolic defense promote growth and reproductive fitness in Arabidopsis.* Proc. Natl. Acad. Sci. U.S.A., 2018. **115**(45): p. E10768-E10777.

33. Wang, W. and X. Chen, *HUA ENHANCER3 reveals a role for a cyclin-dependent protein kinase in the specification of floral organ identity in Arabidopsis.* Development, 2004. **131**(13): p. 3147–3156.

34. McConn, M. and J. Browse, *The critical requirement for linolenic acid is pollen development, not photosynthesis, in an Arabidopsis mutant.* Plant Cell, 1996. **8**(3): p. 403-416.

35. Ishiguro, S., et al., *The DEFECTIVE IN ANTHER DEHISCENCE1 gene encodes a novel phospholipase A1 catalyzing the initial step of jasmonic acid biosynthesis, which synchronizes pollen maturation, anther dehiscence, and flower opening in Arabidopsis.* Plant Cell, 2001. **13**(10): p. 2191-2209.

36. Park, J.H., et al., *A knock-out mutation in allene oxide synthase results in male sterility and defective wound signal transduction in Arabidopsis due to a block in jasmonic acid biosynthesis.* Plant J., 2002. **31**(1): p. 1-12.

37. Ng, S., et al., *Cyclin-dependent kinase E1 (CDKE1) provides a cellular switch in plants between growth and stress responses.* J. Biol. Chem., 2013. **288**(5): p. 3449-3459.

38. Liu, J., et al., *Connecting research and teaching introductory cell and molecular biology using an Arabidopsis mutant screen.* Biochem. Mol. Biol. Educ., 2021. **49**(6): p. 926-934.